THE APPROXIMATION PROBLEM IN THE SYNTHESIS OF R-C NETWORKS

12T

A THESIS

Presented to

the Faculty of the Graduate Division

Georgia Institute of Technology

In Partial Fulfillment

of the Requirements for the Degree

Doctor of Philosophy in Electrical Engineering

By

Kendall Ling-chiao Su

June 1954

THE APPROXIMATION PROBLEM IN THE SYNTHESIS OF R-C NETWORKS

Approved:

Date approved by chairman June 4, 1954

ACKNOWLEDGMENT

I wish to express my sincerest appreciation to Dr. B. J. Dasher, not only for the suggestion of the problem and his valuable advice and guidance during the course of this research, but also for his confidence in my ability and constant encouragement which have contributed so much toward the completion of this thesis. I also wish to thank Dr. D. L. Finn, Dr. W. B. Jones, Jr., and Dr. A. H. Bailey for making many suggestions and reading the text.

TABLE OF CONTENTS

Page

LIST OF ILLUSTRATIONS

Figure Page

Figure Page

ABSTRACT

Transfer functions that are realizable by R-C networks are those whose poles lie on the negative real axis and are simple. This is the additional restriction that is imposed on all R-C network functions beside all criteria that govern the physical realizability of network functions of any type. The approximation problem for the synthesis of R-C networks is, therefore, the finding of a rational function that approximates certain prescribed characteristics and at the same time conforms with the restrictions on locations of poles of these functions. The circuitry part of the complete synthesis procedure is considered as a separate problem. The complete synthesis problem is considered as solved once the rational function is found.

A survey of work done in association with the approximation problem is presented. This includes the method due to Guillemin and that due to Matthaei. Guillemin's method consists of a change in scale and a Fourier-series approximation of a modified function. This method is applicable to the synthesis of characteristics of any type. It also serves as a proof that R-C networks are capable of reproducing frequency characteristics of any type.

Matthaei's method enables one to produce equal-ripple frequency characteristics of both the low-pass type and the band-pass type. It makes use of the potential analogy concept and a technique that shifts all poles to the real axis.

The method of potential analogy is discussed in detail. Its potential usefulness in connection with the approximation problem of R-C network synthesis is discussed. The usefulness of the method of conformal transformation is emphasized. Conditions governing the validity of this method, the necessity of the existence of certain kinds of symmetry as well as its limitations are pointed out.

Conformal transformations are used to solve several approximation problems in the synthesis of low-pass R-C networks. In particular, two types of transformations are used---the trigonometric or hyperbolic functions and the elliptic functions.

The transformation $s = \sin \frac{z}{4}$ is used to map the entire complex-frequency plane into strips of width of 4π in another complex plane. All poles are placed uniformly along the real axis in the transformed plane and the function representing these singularities can be written into one single term and the algebra is greatly simplified. The following groups of network functions have been investigated on the basis of this simplification.

(1) Networks containing two poles and one zero with poles spaced π units apart.

(2) Networks containing three poles and one pair of conjugate zeros with poles spaced $\frac{2\pi}{3}$ units apart.

(3) Networks containing four poles and one double zero with poles spaced $\frac{\pi}{2}$ units apart.

(4) Networks containing four poles and one pair of conjugate zeros with poles spaced $\frac{\pi}{2}$ units apart.

In cases (1) and (3), zeros are placed along the real axis. In

cases (2) and (4), loci for the co-ordinates of zeros that give equal-ripple characteristics in the pass band are determined. In all cases network functions are written in closed form. From these functions, expressions for tolerance in the pass band and pass-band angular frequency are derived. These parameters are calculated for different locations of zeros and plotted as curves. They are given in terms of co-ordinates in the complex frequency plane. Thus the positions of singularities in the complex-frequency plane corresponding to a certain tolerance and pass band may be found readily from these curves.

Further simplifications are achieved and more information is obtained when elliptic-function transformations are used. The properties of elliptic functions related to the transformations used are discussed. This type of transformation maps one complete complex plane into finite rectangles in the other complex plane. The dimensions of these rectangular cells depend on the value of the modulus of the elliptic function used. These cells are all identical except for their orientations. The cell that contains the origin is taken as the sample cell and all other cells are merely repetitions of this one. The part of this cell that lies in the first quadrant corresponds to the first quadrant of the original plane. Other quadrants will again be repetitions of this quadrant, because of the quadrantal symmetry used.

An intermediate transformation is used so the point at infinity in the complex-frequency plane can be placed at any point along the edges of the cell. The elliptic function used is $w = \mathrm{sn}\ z$, and the intermediate transformation used is $s = \dfrac{w}{\sqrt{A^2 - w^2}}$, where $A = \dfrac{1}{k\ \mathrm{sn}\ (aK, k)}$.

The first case investigated, with the use of the elliptic-function transformations, is the one containing one row of uniformly spaced zeros and one row of uniformly spaced poles. By this arrangement the equal-ripple property is insured and the network function may be written in closed form. These functions are expressed in terms of sn functions of a different modulus and are different for the case of an even number of poles and the case of an odd number of poles. The complexity of these network functions does not depend on the number of singularities. The number of poles and zeros included by these functions depends only on the relative values of the two moduli.

With the network functions expressed in closed form, expressions for the tolerance inside the pass band and attenuation outside the pass band are derived. With a modulus and a number of poles given, tolerances are computed for various positions of the row of zeros. The steepness of cut-off is manifested by calculating the attenuation at a frequency twice that of the pass band. Attenuation at this frequency associated with each location of the row of zeros is also computed. Tolerances and attenuations so obtained are plotted as design curves.

The selection of the modulus for the elliptic function used in the transformation is discussed by considering the effects of changing the modulus. It is found that the value of the modulus affects the final results only very slightly. Therefore the modulus used should be the one that leads to the most practical conveniences.

The effect of the number of poles on the characteristics is very

similar to that of the modulus. An increase in the number of singularities, however, also increases the relative bandwidth as well as the number of elements.

In another group of networks investigated, two rows of zeros are included. In this case the relative positions of the rows of zeros determines not only the pass-band tolerance but also the characteristic outside the pass band.

The gain of this group of networks has a maximum outside the pass band and the part of the frequency characteristic that lies completely under this maximum is taken as the stop band. Network functions are also expressed in closed form. From this result, expressions for the tolerance and the attenuation outside the pass band are derived. In order to obtain systematic results, locations of rows of zeros are found for several practical values of tolerance. Corresponding to each of these arrangements the characteristic outside the pass band is indicatively represented by the stop band and stop-band attenuation which are obtained after the maximum point outside the pass band is located. From these curves singularities in the transformed plane are all determined for the specified characteristic and their locations in the complex-frequency plane can be found by the inverse transformation.

The last group of networks investigated are those that contain one row of zeros and one row of double-zeros. The behavior of these networks is similar to the previous group. The inclusion of a row of double zeros eliminates the possibility of a half-order zero on the imaginary axis which appears in the previous group and requires two networks connected in tandem by a vacuum tube.

Studies similar to those made on the previous group of networks are also made on this one.

Design curves obtained in this research can all be used readily for practical purposes. Several numerical examples are given as illustrations as well as verifications. Similar curves may be constructed for comparison or consideration whenever desired.

CHAPTER I

INTRODUCTION

In many problems of network synthesis, it is sometimes desirable to furnish certain arbitrarily specified transfer characteristics with networks containing only two types of network elements. For low-frequency application, for instance, networks containing only resistance and capacitance are suitable. This is chiefly because when the frequency range over which a network is designed to operate falls on the extremely low part of the frequency spectrum, the required inductive elements of acceptable quality may be too difficult to obtain.

There are other reasons why the synthesis of R-C networks is of practical importance. An R-C network may cost less to construct than an R-L-C network of similar performance, notwithstanding that the former may require considerably larger number of elements. R-C networks contain only one kind of energy storage element and they are not prone to undesirable oscillations which can take place in networks containing R, L and C.

There is no theoretical limitation as to what type of characteristics R-C networks are able to furnish. The method by Guillemin (1) and Patrick and Thomas (2) of approximating any given characteristic by functions realizable by R-C networks discussed in the next chapter serves as a proof that, except for a constant multiplier, any prescribed amplitude characteristic may be approximated to any desired

degree of accuracy by transfer functions realizable by R-C networks. In other words, it is always possible to synthesize an R-C network to give any desired shape of frequency response.

Almost all R-C networks have approximately as many resistive elements as capacitive elements. Therefore it may be expected that R-C networks possess considerable energy loss. This makes the insertion loss of R-C networks a serious problem and it must be compensated for by adequate amplification. Fialkow and Gerst (3)(4) calculated the minimum insertion loss realizable by R-C networks when their poles and zeros are given.

Transfer functions that are realizable by R-C networks are those whose poles are all simple and lie on the negative real axis of the complex-frequency plane, $s = \sigma + j\omega$, provided that all other requirements for functions that are realizable by general networks are met. Therefore problems in R-C networks are identical to problems in general networks except for this additional restriction.

The complete synthesis procedure for any network may be divided into two steps---the approximation and the realization. The approximation part of the problem involves the finding of a rational function of suitable property whose variation along the imaginary axis approximates the specified frequency characteristic to a predetermined degree of accuracy. It is this approximation part of the R-C network synthesis procedure that this research is devoted to.

The realization part of the synthesis procedure is the actual construction of a network whose transfer function has its poles and zeros coinciding with those of the rational function found in the

approximation part of the procedure. Considerable advancement has been attained in recent years in this field.

A method was demonstrated by Guillemin (5), and Patrick and Thomas (6) by which an R-C admittance function may be realized by a number of parallel-connected ladder networks loaded by a one-ohm resistor. This method was improved by Ordung and others (7) so the number of parallel networks is reduced.

An alternative method is provided by Orchard (8) which is also applicable to a generator with non-zero internal impedance and functions which are not of the minimum-phase type.

A lattice R-C network realization method for voltage-ratio functions has been discussed by Bower and Ordung (9) for both open-circuited and R-C loaded output terminal-pairs.

Fleck (10) offered a method of realizing a transfer ratio by means of one single ladder network.

Another method which leads to canonical sections derived from parallel-T networks was devised by Dasher (11). This method results readily in unbalanced two terminal-pair R-C networks.

Fialkow (12) showed a method for realizing voltage-ratio functions by successively splitting the function and subtracting a proper resistance of capacitance. This method results in a complicated network with a very large number of elements.

This wide variety of methods for realizing networks for a given transfer function justifies our leaving this part of the synthesis procedure as a separate problem. It will be assumed that the synthesis is completed once the approximation part of the procedure is solved.

CHAPTER II

FOURIER SERIES METHOD OF APPROXIMATION

One of the earliest methods dealing with the approximation problem of R-C networks is due to Guillemin (13). This method makes use of a scale transformation and Fourier analysis. It will be summarized here.

Assume that it is desired to find a function T(s) such that $|T(j\omega)|^2$ approximates a certain prescribed characteristic, $|F(j\omega)|^2$, (Fig. 1). First apply the scale transformation

$$\phi = 2 \tan^{-1}\omega \tag{1}$$

This transformation is multiple-valued and the new plot $G(\phi) = |F(j\omega)|^2$ is periodic as shown in Fig. 2.

The function, $G(\phi)$, may be approximated by a Fourier series

$$g(\phi) = a_o + a_1 \cos\phi + a_2 \cos 2\phi + \cdots\cdots + a_n \cos n\phi \tag{2}$$

to any desired degree of accuracy provided n is sufficiently large.

Since $\cos k\phi$ is a polynomial of degree k in $\cos\phi$, where k is any positive integer, $g(\phi)$ is an n-th degree polynomial in $\cos\phi$. Thus, we have

$$g(\phi) = b_o + b_1 \cos\phi + b_2 \cos^2\phi + \cdots\cdots + b_n \cos^n\phi . \tag{3}$$

But from equation (1), we have

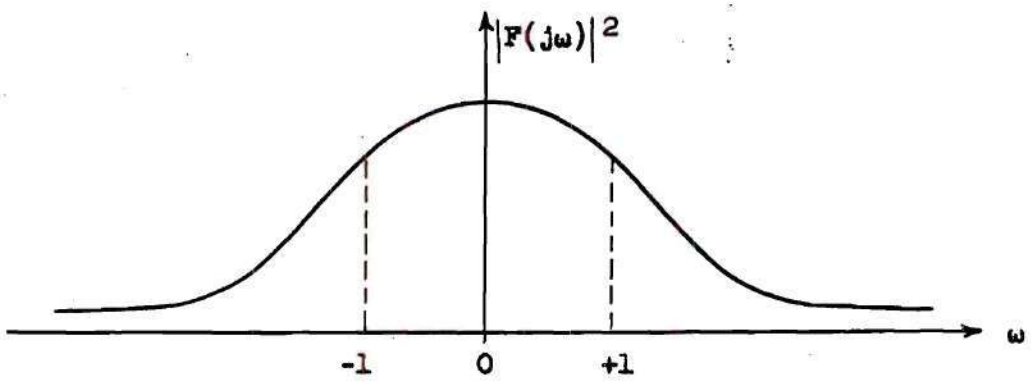

Fig. 1. $|F(j\omega)|^2$ characteristic.

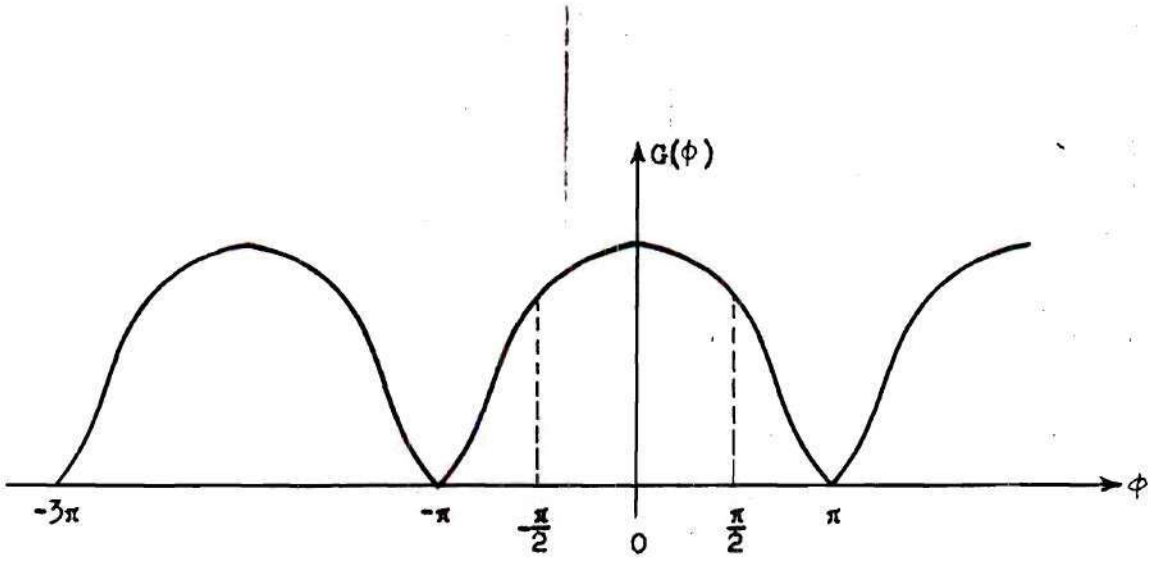

Fig. 2. Plot of G(φ).

$$\cos\phi = \frac{1 - \omega^2}{1 + \omega^2} \cdot \tag{4}$$

So that $g(\phi)$ may be written as

$$g(\phi) = h(\omega^2) = \frac{A_0 + A_1\omega^2 + A_2\omega^4 + \cdots\cdots + A_n\omega^{2n}}{(1 + \omega^2)^n} \cdot \tag{5}$$

Thus we have obtained a function in ω^2 which approximates $|F(j\omega)|^2$ within the same tolerance as $g(\phi)$ approximates $G(\phi)$.

As what would have been the final step of the problem we try to find a function $h_1(s)$ such that $|h_1(j\omega)|^2$ is identical to $h(\omega^2)$. Since the zeros and poles of $h(-s^2)$ occur in symmetrical quadruplets, this step may be accomplished by including all the zeros and poles of $h(-s^2)$ in the left half-plane as the zeros and poles of $h_1(s)$, if a minimum-phase network is desired. But a difficulty arises in that all the poles of $h(-s^2)$ fall on $s = \pm 1$. Since all poles of an R-C transfer function must lie on the negative real axis and must be simple, the resultant $h_1(s)$ will not be realizable by an R-C network.

To remedy this difficulty the following procedure may be used. What is desired here is a function of the form

$$f(\omega^2) = \frac{A_0 + A_1\omega^2 + A_2\omega^4 + \cdots\cdots + A_n\omega^{2n}}{B_0 + B_1\omega^2 + B_2\omega^4 + \cdots\cdots + B_n\omega^{2n}} = \frac{A(\omega^2)}{B(\omega^2)} \tag{6}$$

which approximates $|F(j\omega)|^2$ to the desired accuracy. We may proceed by choosing arbitrarily a function $B(\omega^2)$ so that roots of $B(-s^2) = 0$ are all real and simple. Furthermore, we may write

$$f(\omega^2) = \frac{A(\omega^2)}{B(\omega^2)} = \frac{\dfrac{A(\omega^2)}{(1 + \omega^2)^n}}{\dfrac{B(\omega^2)}{(1 + \omega^2)^n}} = \frac{g_1(\phi)}{g_2(\phi)} = g(\phi) \tag{7}$$

where $g_1(\phi)$ and $g_2(\phi)$ are both n-th degree polynomials in $\cos\phi$. Since $B(\omega^2)$ is known, $g_2(\phi)$ can readily be found by applying equation (4). Then if a function $g_1(\phi)$ is computed to approximate $g_2(\phi)G(\phi)$ in the same way as the function $g(\phi)$ of equation (5) was computed, $f(\omega^2)$ will approximate $|F(j\omega)|^2$ to the same degree of accuracy as $G(\phi)$ does, and the function $f(\omega^2)$ will have the desired properties. The function T(s) may now be formed by including the left half-plane zeros and poles of $f(-s^2)$ and the process is completed.

No rule that governs the selection of positions of roots of the equation $B(\omega^2) = 0$ has yet been developed. As far as the above analysis is concerned their locations are immaterial. It may be considered as absolutely arbitrary for that purpose. Thus the location of the zeros of F(s), which are also the poles of our final network function, must obviously be decided by other practical considerations.

One of the direct consequences of the locations of the poles of T(s), for instance, is the spread of element values of the final network. Obviously if these poles are placed very close together or very far apart, a very wide spread of element values will be needed. Certain optimum distributions of poles must exist between these two extreme situations, although they may not be very critical. Other considerations may be exemplified by matters such as insertion loss, mathematical simplification, etc.

Locating the poles so they have their geometric mean at $s = -1$ has been suggested as an apparently good choice from several points of view. By this distribution, the function $g_2(\phi)$ will be symmetrical about $\phi = \frac{\pi}{2}$, and thus will have only even order terms. This symmetry

of $g_2(\phi)$ about $\phi = \frac{\pi}{2}$ is also a necessary condition for equal-ripple behavior in both the pass band and stop band when a low-pass characteristic is being approximated by this method.

Beside its practical usefulness, this method also has an important merit in that it furnishes a proof that R-C networks are capable of reproducing any shape of frequency characteristics. Since resistances may be considered as coils of extremely low Q, a corollary may be derived from this proof that any given frequency characteristic may be realized by networks containing resistances, capacitances and inductances with any value of Q.

The major disadvantage of this method may be seen from the fact that it is virtually impossible to predict the accuracy of the approximating function. One must start with a choice of the number of poles of T(s), n, as well as the pole positions. From these poles, $B(\omega^2)$, $g_2(\phi)G(\phi)$ and $f(\omega^2)$ may be computed. Whether this $f(\omega^2)$ falls within the acceptable range or not cannot be known until this complete process is finished. On the other hand whether this n is the minimum permissible value of n or not is not known until some other values of n have been tried and compared. Unless the required value of n is small these processes can be very tedious.

CHAPTER III

POTENTIAL ANALOGY

The analogy.—The transfer function of a passive network with lumped elements may generally be expressed in the form

$$T(s) = e^{\alpha + j\beta} = K \frac{(s - A_1)(s - A_2) \ldots . (s - A_n)}{(s - B_1)(s - B_2) \ldots . (s - B_n)} \qquad (8)$$

where A's and B's are, respectively, zeros and poles of T(s). This expression is identical to the expenential of the complex potential, P(s), in a two dimensional electrostatic field with positive unit line charges located at A's and negative unit line charges at B's. Also

$$P(s) = \ln T(s). \qquad (9)$$

Thus there exists a complete analogy between an electrostatic field and a corresponding network function. Those quantities that are analogous to each other may be itemized as follows:

(1) Poles and positive unit line charges.

(2) Zeros and negative unit line charges.

(3) Singularities (poles and zeros) and sources (charges).

(4) Transmission function and complex potential.

(5) Transfer function and exponential of complex potential.

(6) Gain and potential.

(7) Phase and stream function.

Inasmuch as for each quantity in the electrostatic domain there is an analogous quantity in the network-function domain, and vice versa, it is not necessary to introduce two sets of notations. One notation used to denote a certain quantity in one domain can also be used to denote its analogous quantity in the other domain. For instance, the function ($\propto$) may represent either potential or gain depending on what domain it is referred to.

Furthermore, we could actually regard each pair of analogous quantities as exactly the same quantity and use them interchangeably. Throughout this research the quantities within each item listed above will be considered as synonyms.

By this correlation of these two fields the number of problems is reduced to one half of the original. If any property has been investigated in one domain, its analogous property in the other domain is already found. If the analogy between network functions and electrostatic functions fails, the existing problem in one domain may have a meaningless dual problem in the other. This will in no way devaluate our analogy concept because although in these instances we do not gain anything, neither do we lose anything.

The advantage of pointing out this analogy lies mainly in the fact that extensive study has already been done in the theory of electrostatic fields. Thus we may apply all our knowledge and techniques from the field theory to network problems through this analogy. At the present time we would very likely view many network problems from the electrostatic field standpoint, because we have more experience in this field. This situation need not be a permanent one. It is entirely possible

that some day we will be able to manipulate any problem in both domains with equal ease. Then the analogy concept will no longer be of value to us in the same way or to the same extent that it is today. It is also possible that some day we may be able to solve some potential problems by the aid of their network correspondence.

In network problems, we are mainly interested in the finding of a rational function whose magnitude over an axis follows a certain desired pattern. Thus the electrostatic field problems that are of interest are those of determining a set of line charges to produce certain desired potential variations along an axis. Other network problems may include phase characteristics over a part of or over the entire axis. Their analogous problems in the electrostatic field must include the consideration of flux functions. Several useful methods will be discussed later in this chapter.

Restrictions on charge arrangements.—Because of the conditions imposed on the distribution of zeros and poles for network functions, only certain types of charge distribution are directly useful for our purposes, if final network functions are to be physically realizable. These restrictions are:

(1) All charges must be of equal strength or some simple multiple of a unit charge.

(2) Since singularities of physically realizable network functions occur in conjugate pairs, charges must be placed so they are symmetrical about the real axis.

(3) Positive charges must be confined to the left half-plane.

(4) For R-C networks, positive charges must be placed on the negative real axis, and they must all be of equal strength.

(5) If network functions are to be of the minimum-phase type, all negative charges must be confined to the left half-plane.

Arranging charges so they maintain the required symmetry and then modifying this original arrangement to conform with the restrictions listed above while preserving certain characteristics, may simplify the electrostatic field a great deal.

If, for instance, the gain characteristic is the specified quantity, one half of each charge in the left half-plane may be moved to its negative point. This operation does not alter the potential along the imaginary axis. Thus we may at first double the desired potential variation, and arrange all charges in quadrantal symmetry to produce this doubled potential variation, and finally discard all the charges in the right half-plane.

In a similar manner if a unit charge of opposite sign is placed at the negative point of each charge in the left half-plane, the flux function along the imaginary axis will merely be doubled. Thus if a phase characteristic is to be matched a similar simplification may be obtained as when a gain characteristic is to be matched.

Useful methods.--Several methods applicable to solving two-dimensional field problems in electrostatic theory which are also useful in aiding the solution of certain network problems will be described below:

(1) Experimental method.--The calculation of the frequency characteristic of a network function with known locations of poles and zeros is usually a complicated procedure especially when the number of singularities is large. As an alternative one may actually construct the network and measure its frequency response. This is not always a practical method. For instance, if the frequency characteristic needs slight modification by the shifting of certain singularities, the whole procedure must be repeated with exactly the same amount of work as the previous function. Therefore a means of directly measuring the frequency characteristic without either numerical calculation or actual construction of the network is highly desirable.

It would be extremely difficult, if possible at all, to set up a two-dimensional electrostatic field. However, the electroconductive field analog of each electrostatic field problem is very simple to approximate in the laboratory. Since the solutions of these two fields are both the solutions of Laplace's equation their analogy is easy to see.

Thus an electrostatic field may be simulated by a thin layer of a uniform conducting medium. Its sources may be simulated by currents of proper polarities. The strength of these currents must be proportional to the strength of charges. With this arrangement the potential in these two fields will have the same variation throughout the entire s-plane. Their absolute values may also be related so one can be computed from the other.

Two types of conducting media that have been widely used are electrolytes and electroconduction paper. Electrolytic tanks were used

by Hansen and Lundstrom (14), Huggins (15), Boothroyd (16) and others. Electroconduction paper has been adapted in recent years and is made of a special type of paper impregnated with carbon or graphite. This material is considerably easier to handle and its preparation for fields of odd shapes requires much less effort than that of electrolytic tanks. However the accuracy of this method depends largely on the uniformity of the manufacture of the conducting paper and is usually inferior to that of electrolytic tanks.

(2) Distributed charge method.—In order to take advantage of certain analytical results in electrostatic theory, a continuous charge distribution along a certain predetermined contour to give a certain potential variation in the region enclosed by the contour may first be found by any of the analytical methods. Then this distributed charge is approximated by a set of lumped charges of equal strength placed at the center of gravity of the distributed charge it is to represent. An extensive survey of those analytical methods that may be useful for this operation is made by Darlington (17).

(3) Conformal Transformation.—Another powerful method of solving two-dimensional field problems is the conformal transformation. This transformation can be used to reduce the complexity of the problem by changing the geometry of the field and its boundaries to a simpler one. In many instances the field in the new transformed plane has certain symmetry that does not exist in the original plane. Since the transformation preserves the orthogonality of conjugate functions the solution in the transformed plane is identical to that in the original plane provided their sources and boundary conditions correspond to each other.

A well known example of its application in connection with network theory is the low-pass to band-pass transformation of the frequency scale $\omega = \omega_1 - \frac{1}{\omega_1}$. If this scale transformation is extended to be valid over the complete complex frequency plane, or $s = s_1 + \frac{1}{s_1}$, and if poles and zeros are known in s-plane in the low-pass case they are also known for the band-pass case in the s-plane.

This transformation is depicted in Fig. 3. The transformation from the s-plane to the s_1-plane is double-valued. Therefore the s-plane must be a Riemann surface of two sheets on top of each other and joined by the branch cut which is that part of the real axis that is outside a and c. Thus it is seen that the band-pass to low-pass transformation gives simplification only if charges of similar sign are placed so they are geometrically symmetrical about the unit circle. By so doing their s-plane mappings are made to fall on top of each other and only one sheet of the Riemann surface needs to be studied.

Another example is given by the work of Matthaei (18) for the design of R-C band pass filters. The task is accomplished by a hyper-elliptic-function transformation which transforms the entire s-plane into a Riemann surface of two rectangular sheets joined by four branch cuts as shown in Fig. 4. The charges in these two sheets are arranged identically and, therefore, only one sheet needs to be studied. This can only be true when charges in the s-plane are arranged so they are geometrically symmetrical about the ω_o-circle.

The separation of two Riemann sheets, as was done in the two examples mentioned above, is permissible only when the following conditions are satisfied:

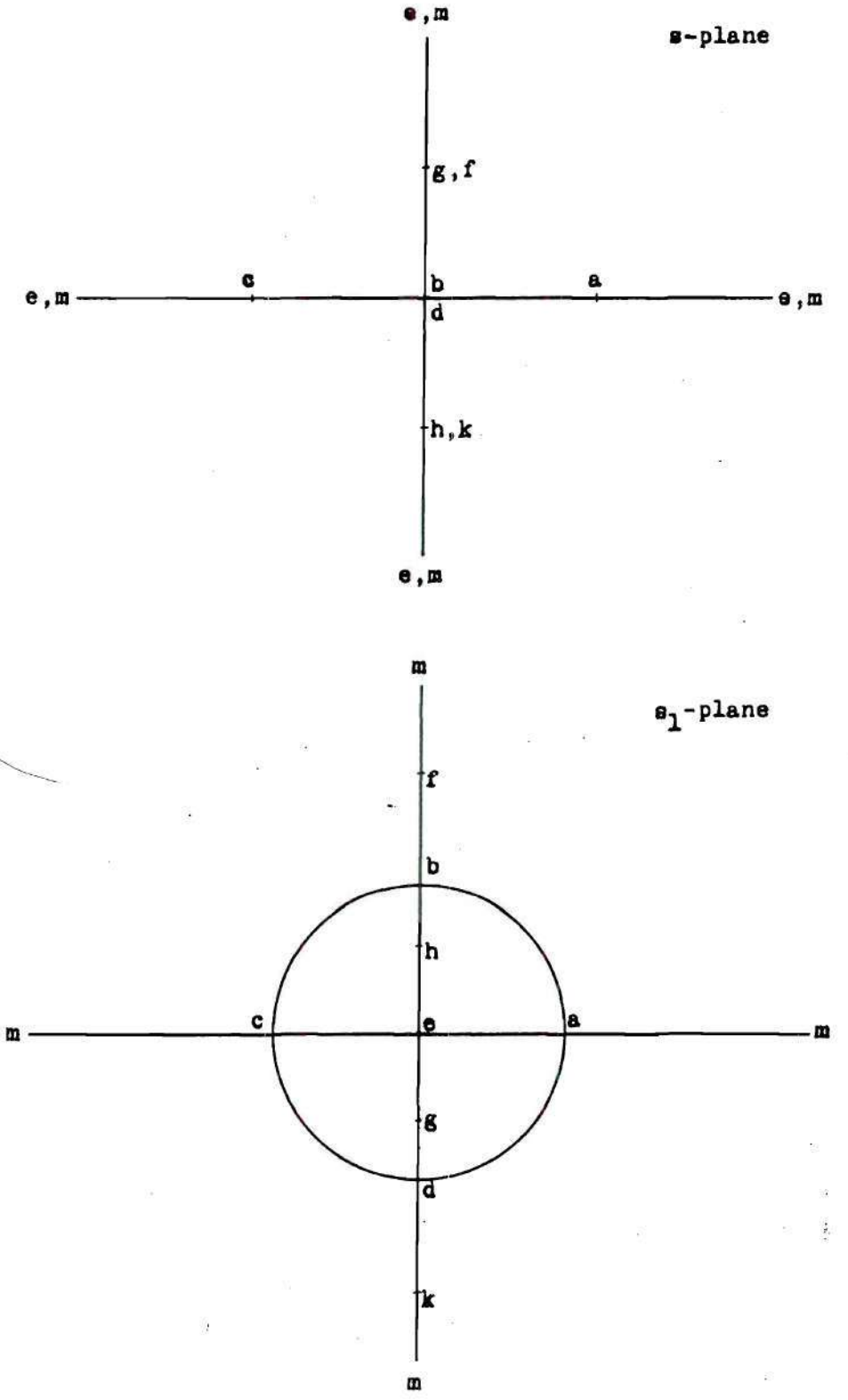

Fig. 3. The transformation $s = s_1 + \frac{1}{s_1}$.

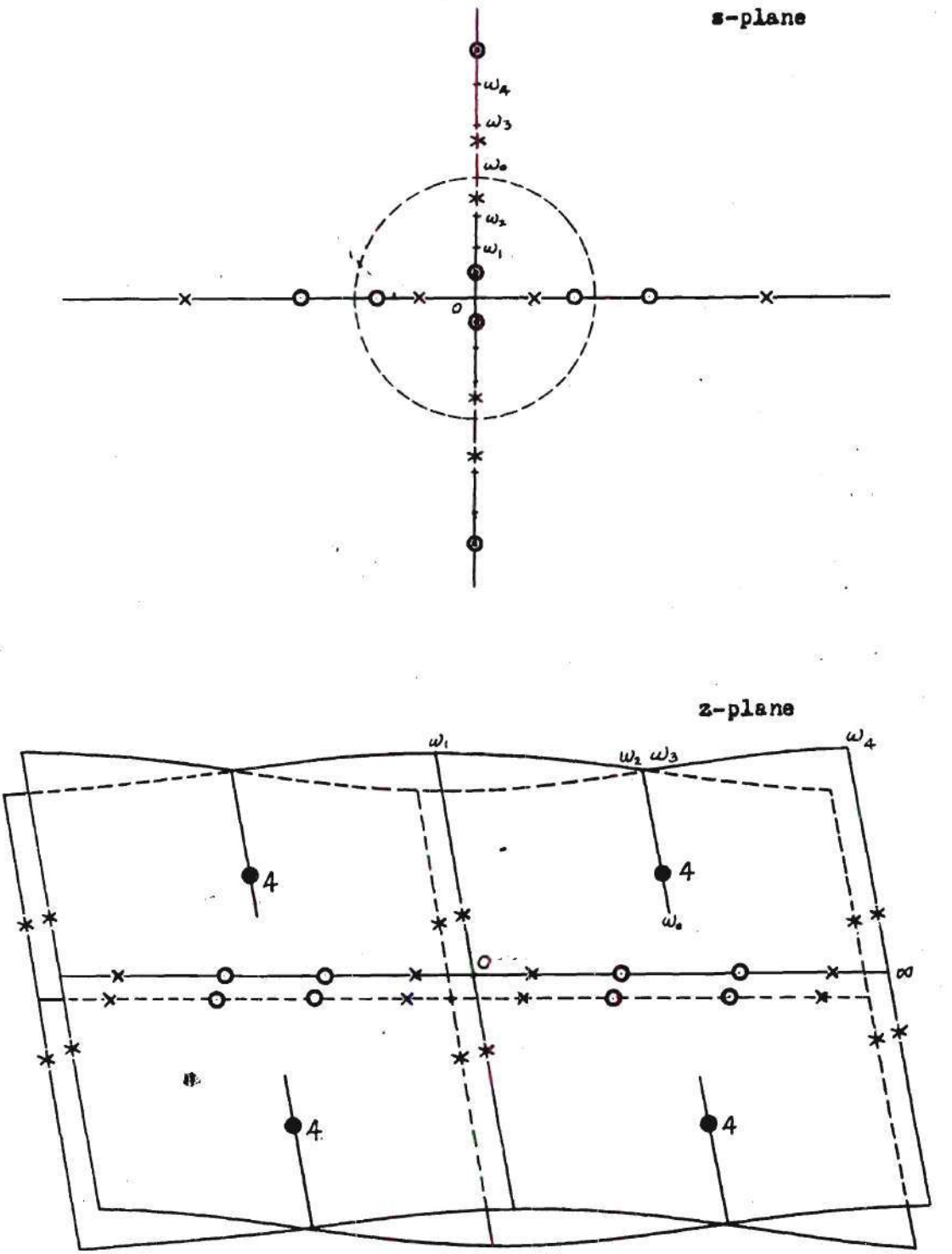

Fig. 4. A hyper-elliptic function transformation.

(1) The behavior of the field in the vicinity of the branch cuts is the same on both sheets.

(2) No flux lines cross the branch cut.

(3) When an axis is folded up against itself each pair of points that are combined must be at the same potential.

These conditions are all satisfied in both examples mentioned above.

An example where these conditions are not fulfilled is the one shown in Fig. 5, in which an attempt was made to design a low-pass R-C filter. Due to the difference in the arrangement of quadrants on the two sheets, charges do not fall on top of each other and all three conditions listed above are violated. Therefore the two sheets cannot be separated. Since a Riemann surface of this type is almost impossible to approximate the transformation is of very little practical value for this problem.

This transformation method has been used to great advantage by many. In setting up an electroconductive analogy of a two-dimensional electrostatic field, such as an analytic tank or an electroconduction sheet, it is not possible to include the complete complex plane. Certain transformations will map the complete plane into a finite region, such as a rectangle or a circle, and make it possible to represent accurately the complete plane by a finite area.

Poles of Butterworth's filter will lie on a straight line if an exponential mapping is used. Tschebytscheff's filters can be simplified to the same extent by a hyperbolic mapping. Fano (19) applied this technique in the reverse direction and obtained filters that

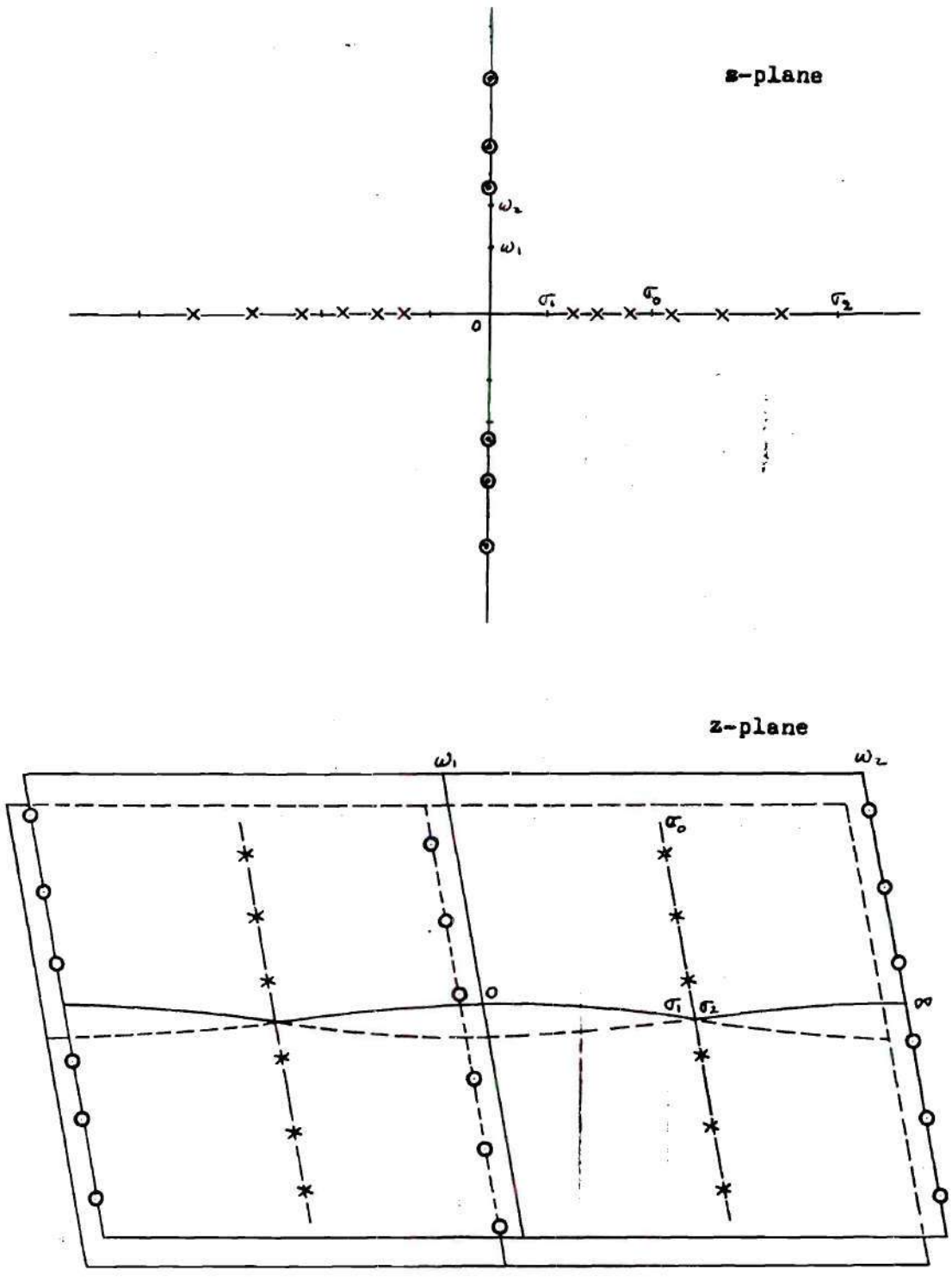

Fig. 5. Another hyper-elliptic function transformation.

display equal-ripple property in both the pass-band and the stop band.

Conformal transformations will be used frequently herein and the detailed properties of each transformation will be discussed wherever it is being used.

CHAPTER IV

POLE SHIFTING METHOD OF PRODUCING LOW-PASS R-C FILTERS

A scheme which makes use of several of the ideas discussed in the last chapter together with a tricky method of pole shifting to obtain equal-ripple characteristic over certain regions was suggested by Matthaei (20).

The preliminary preparation required for this method is the arrangement of charges so they produce equal-ripple potential within certain designated regions. To achieve this goal various methods may be employed as aids. A useful method would be the use of the charged conducting plate which insures the uniformity of potential throughout the region occupied by it. The distributed charge on the conducting plate may finally be approximated by lumped charges.

As an example, suppose it is desired to produce a low-pass frequency characteristic with pass-band designated as from 0 to ω_1 and stop-band from ω_2 on out, and if three poles and three zeros are to be had by the network function, we may place three conducting plates along the $j\omega$-axis as shown in Fig. 6 and put appropriate units of charge on these plates. The charge distribution on these plates may be found. This distribution of charge may be approximated by lumped charges by placing one unit charge of the correct sign at the center of gravity of each region that contains one unit of charge. Thus, the potential in Fig. 6 is approximated by that of Fig. 7, whose charge positions may now be taken as the singularities of a function $T'^2(s)$.

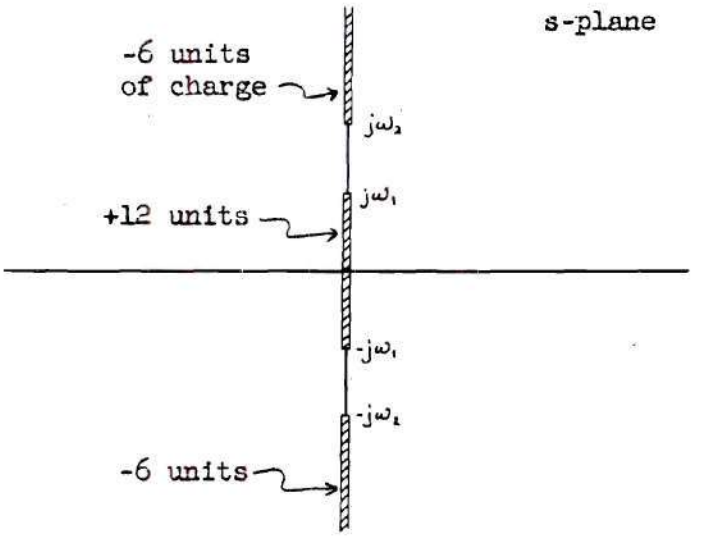

Fig. 6. The arrangement of charged conducting plates.

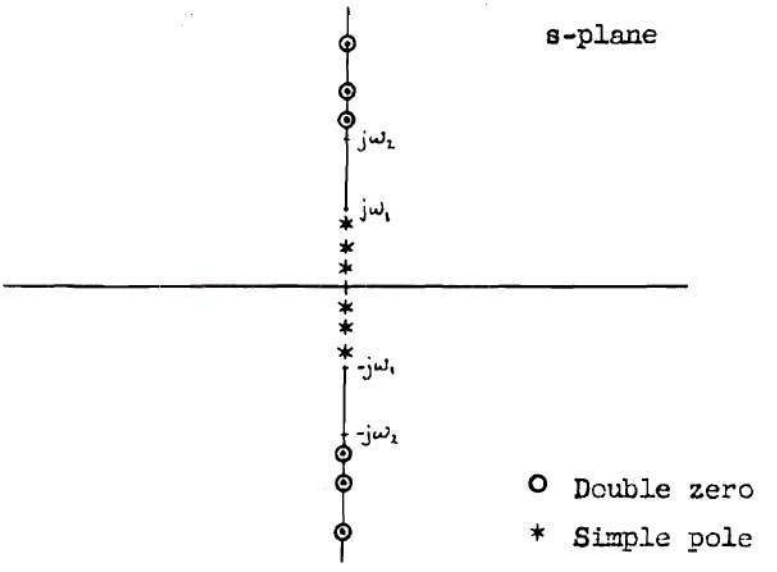

Fig. 7. Lumped-charge approximation of Fig. 6.

Since it is not permissible to leave poles inside the pass band, a new function, T(s), should be taken as our final network function, where

$$T(s)T(-s) = \frac{T'^2(s)}{1 + C\,T'^2(s)} \qquad (10)$$

This transformation from T'(s) to T(s) given by equation (10) involves the following steps:

(1) Take the reciprocal of $T'^2(s)$.

(2) Add a constant C to the reciprocal of $T'^2(s)$.

(3) Take the reciprocal of (2).

The result of this transformation shifts all poles away from the $j\omega$-axis while all zeros remain unaltered. This operation also leaves the positions of maxima and minima within the pass band and stop band unchanged; thus equal-ripple property in both regions is retained. As the final step, the charges in the right half-plane are discarded, and the singularities of T(s) are shown in Fig. 8. The frequency characteristic will have the shape as shown in Fig. 9.

The foregoing results may be approached by a different method. The problem is simplified to a great extent if conformal transformation is used. The transformation that is useful for this particular example is that of a certain elliptic function, which will be discussed later in another chapter. For the present purpose, we need only to suppose that a transformation can be found that maps the entire s-plane onto a rectangle in the z-plane. Then the corresponding problems of those of Figs. 6, 7 and 8 are shown in Figs. 10, 11 and 12.

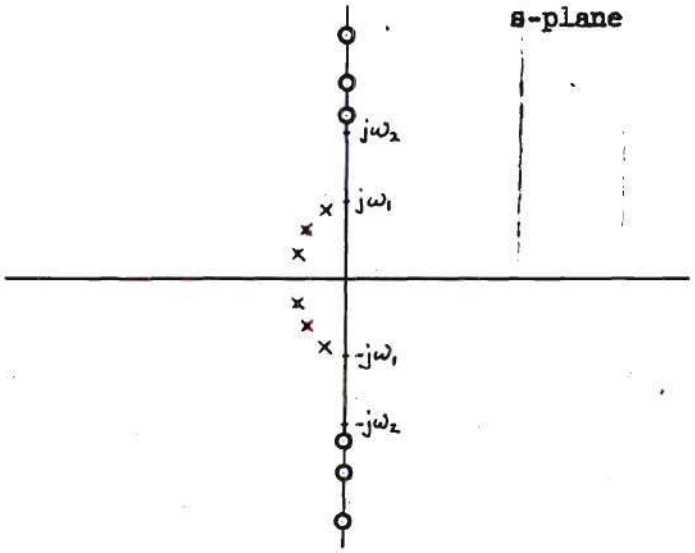

Fig. 8. Poles and zeros of T(s).

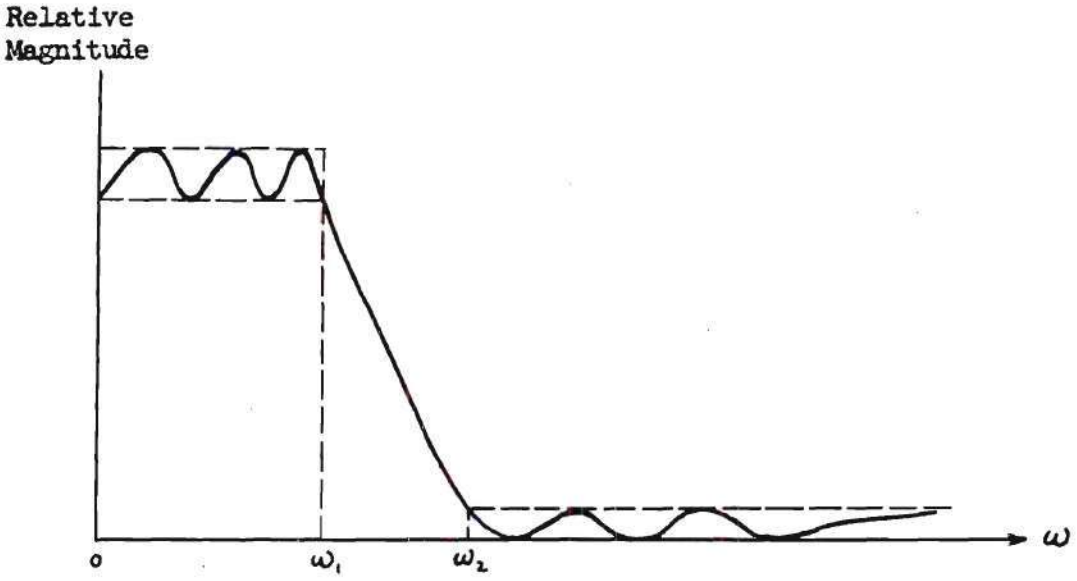

Fig. 9. Frequency characteristic of T(s).

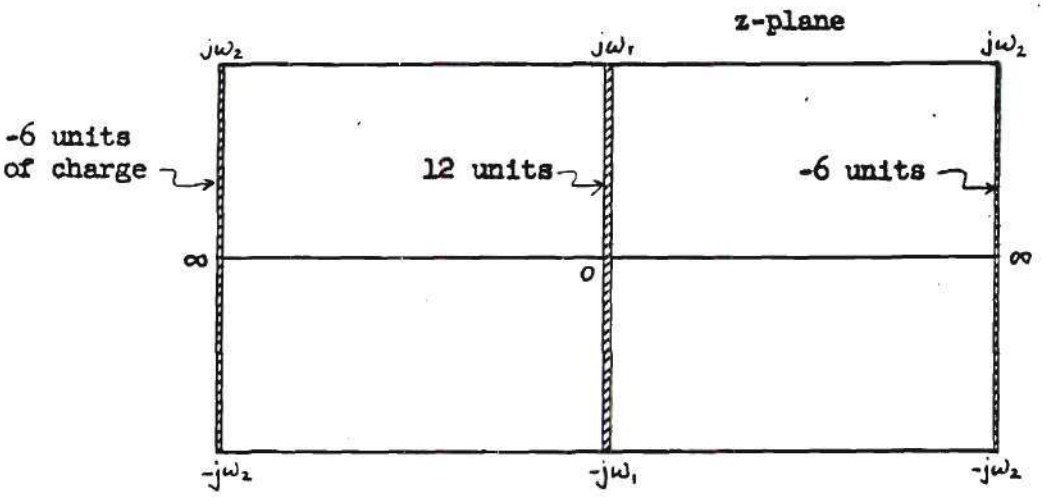

Fig. 10. The z-plane correspondent of Fig. 6.

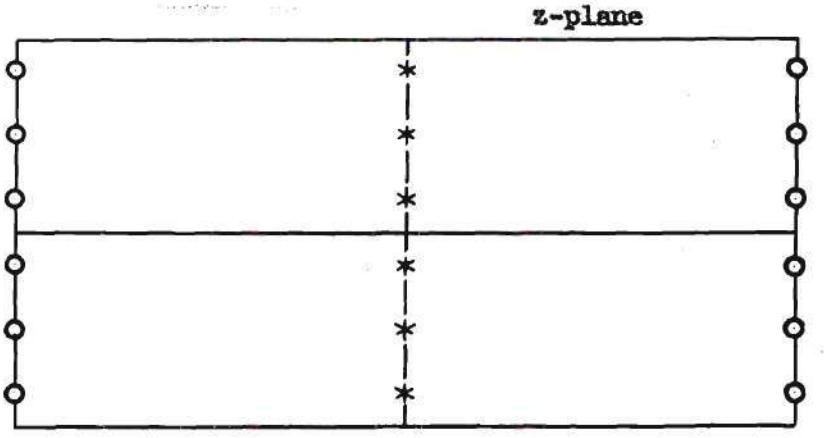

Fig. 11. The z-plane correspondent of Fig. 7.

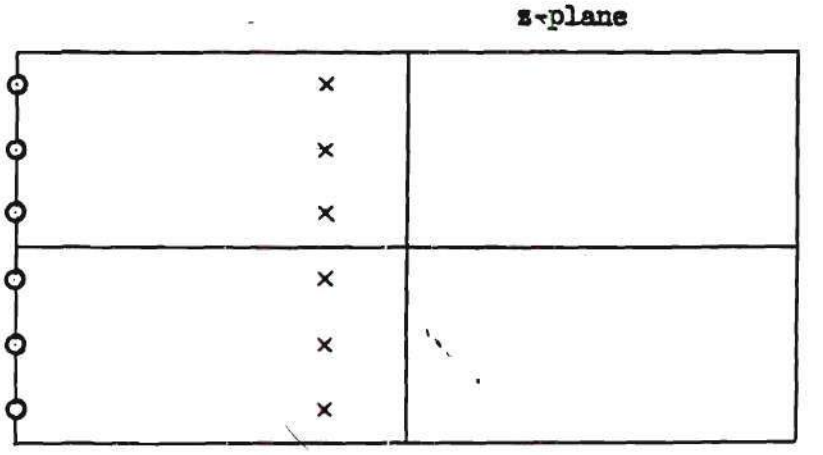

Fig. 12. The z-plane correspondent of Fig. 8.

In the z-plane the conducting plates are parallel to each other and the charge distribution will obviously be uniform. Their lumped charge approximation is simply rows of uniformly spaced charges. Thus poles and zeros of $T'^2(z)$ as well as $T(z)$ will be uniformly spaced. The charge-arrangement part of the problem is greatly simplified. Moreover, one can directly arrive at the arrangement shown in Fig. 12 and be sure of the equal-ripple property in the two frequency ranges without the aid of the conducting-plate middle step.

This example is mentioned here merely for the purpose of illustrating the pole-shifting technique. As can be seen from Fig. 8 the function $T(s)$ is not realizable by any R-C network.

When this method is applied to R-C networks certain additional restrictions must be imposed on the charge arrangement. Most of all, all poles must finally be shifted to the real axis and they must be separate. This can be achieved only if there are as many separate points that are at the same potential as there are poles. If this is the case we may make C equal to the negative of $1/T'^2(s)$ at these points, and these points may be made poles of $T(s)T(-s)$.

For instance, if a certain charge arrangement gives a variation of $T'^2(s)$ along the σ-axis as shown in Fig. 13, it is suitable to be used in connection with our pole shifting technique to change it to a function that is realizable by an R-C network.

Thus, if it is desired to produce a low-pass filter with equal-ripple property in both the pass band and the stop band the charge arrangement as shown in Fig. 7 can no longer be suitable as is evident from Fig. 11 in which it is clear that potential decreases monotonically

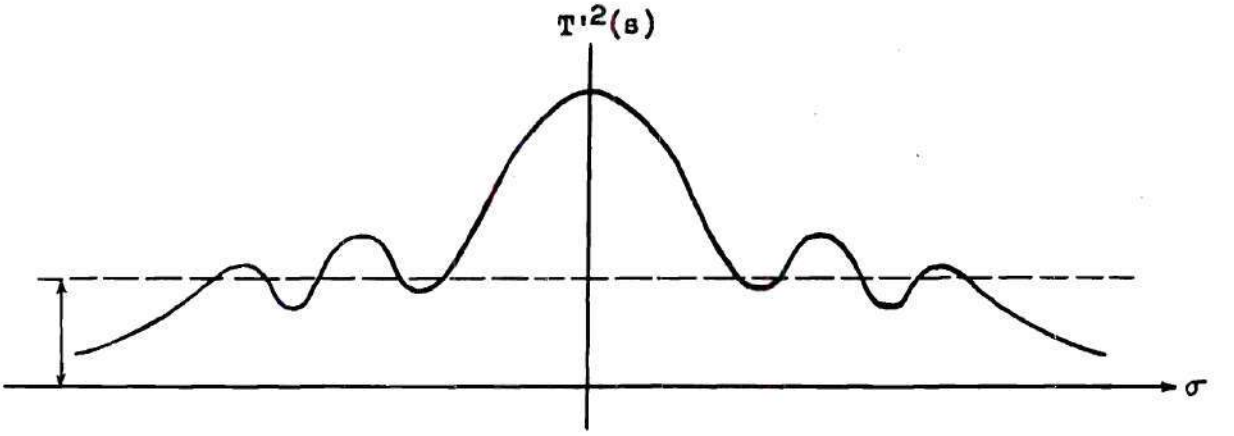

Fig. 13. Variation of $T'^2(s)$ along the σ-axis.

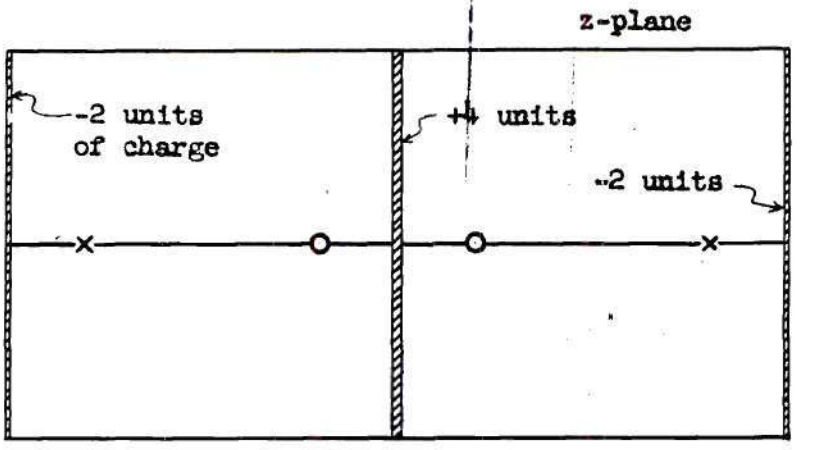

Fig. 14. Charge arrangement with four unit charges placed along the real axis.

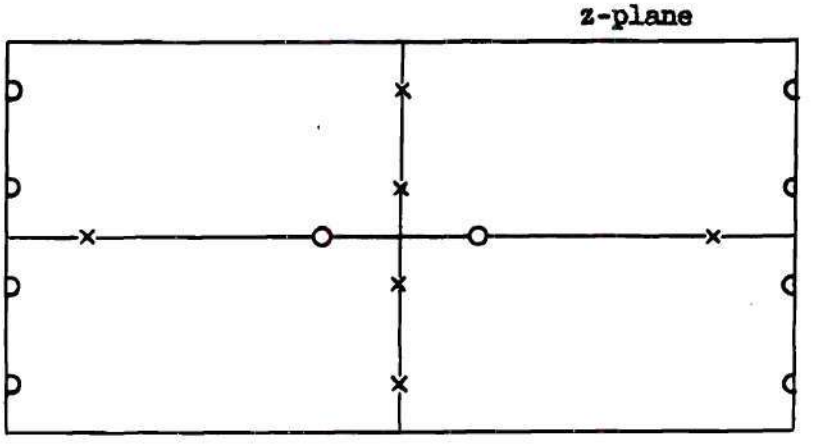

Fig. 15. Lumped-charge approximation of charge arrangement in Fig. 14.

along the real axis as the distance from the origin increases.

Hence if a network function based on a derivation similar to that of Fig. 8 is to be designed so it is realizable by an R-C network, certain modifications must be made. Certainly some charges must be placed near or on the real axis to modify the potential variation along it. For that particular example we may, for instance, start our process by finding the charge distribution on metal sheets with four unit charges placed on the σ-axis as shown in Fig. 14. The negative charges are placed close to the origin so as to lower the potential on the part of the real axis, while the function of the positive charges is just the opposite. After the charges on the metal plates are quantized the charge arrangement has the form as shown in Fig. 15. The potential variation along the σ-axis now has the form shown in Fig. 16. After equation (10) in association with a proper constant C has been applied, the charge distribution will take the form shown in Fig. 17 in the z-plane and Fig. 18 in the s-plane. This arrangement is realizable by two R-C networks connected in tandem with a buffer amplifier and they together will contain six poles.

The essence of this method is well illustrated by the examples just discussed and other problems of a similar nature may be derived accordingly. The success of this method depends largely on the placement of poles and zeros on or near the real axis to produce sufficient saddle points on the real axis. This step is usually a difficult one and a straight forward rule has not yet been devised.

To create a sufficient number of ripples of potential of approximately the same level a minimum number of charges must be used on or

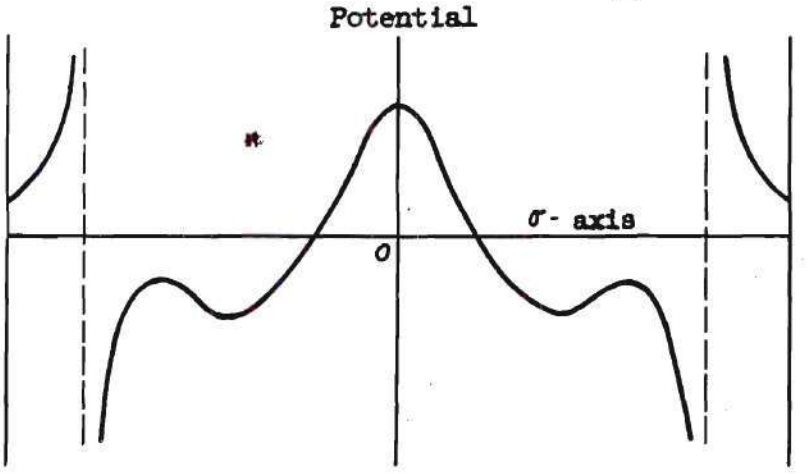

Fig. 16. Potential variation along the σ-axis.

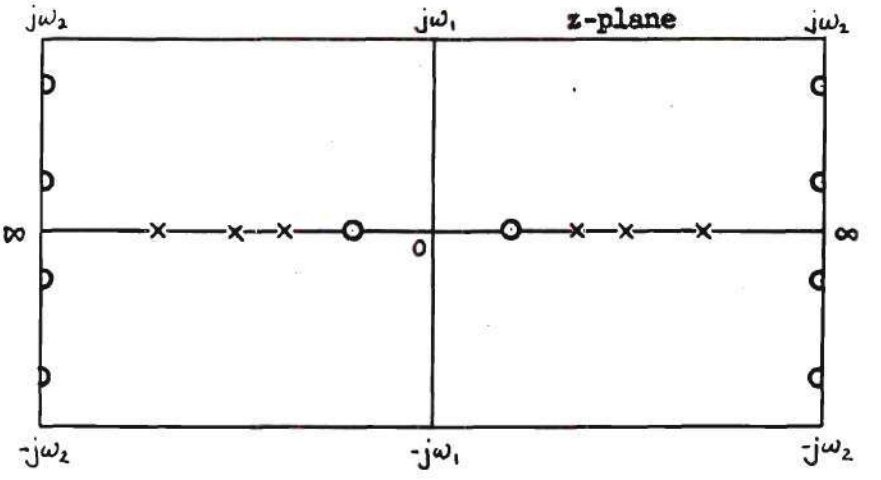

Fig. 17. Singularities in the z-plane.

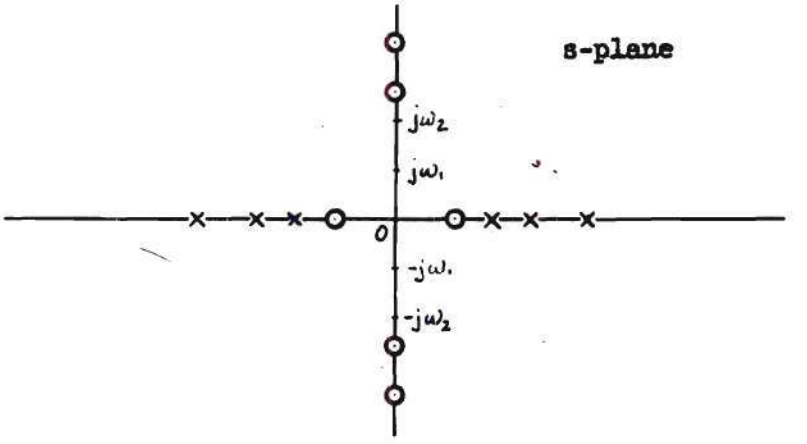

Fig. 18. Singularities in the s-plane.

near the real axis, and certainly no more charges should be used. Matthaei (21) has shown that this number is (Z - 2) where Z is the total number of poles and also the total number of zeros.

Experimental methods can be of great aid to this method. An electrolytic or an electroconduction sheet may be set up to find the charge distribution on the metal sheets in Fig. 14, for instance. The same devices can be used to make preliminary determination of charge positions to give proper potential variation along the real axis, thus eliminating many uncertain guesses required if a numerical cut-and-try method is to be used.

The way results are arrived at by this method is ingenious and direct. However, if the number of poles is large, the calculation may be quite involved and the quantitative results cannot be predicted. Such design quantities as tolerance, sharpness of cut-off and stop-band attenuation can not yet be controlled.

CHAPTER V

DESIGN OF LOW-PASS R-C NETWORKS BY TRIGONOMETRIC AND HYPERBOLIC TRANSFORMATIONS

The Transformation $s = \sin \frac{z}{4}$ and Its Application

The transformation $z = 4 \sin^{-1} s$ maps the s-plane into strips of width 4 in the z-plane. These strips are joined by branch cuts which correspond to that part of the real axis that is outside $s = \pm 1$. The geometry of this transformation is depicted in Fig. 19.

In Fig. 19 (c) is shown the arrangement of quadrants in the z-plane. With the symmetry of charge arrangement to be used, only one strip needs to be illustrated. The others will be repetitions of this one.

In network problems the gain characteristic along the real frequency axis is of primary interest. Therefore we are primarily interested in the potential variation along the y-axis in the z-plane. Since the corresponding points along the ω-axis are arranged in the same sequence on the y-axis, the variations along these two axes in the two planes are of the same shape except for a change in scale.

The usefulness of a conformal transformation depends on its simplification of charge arrangements. Since for R-C networks poles are confined to the real axis, we may place all positive charges in the z-plane only on the real axis and space them uniformly apart. This enables us to represent all positive charges by one single term in the complex potential function. The following groups of networks

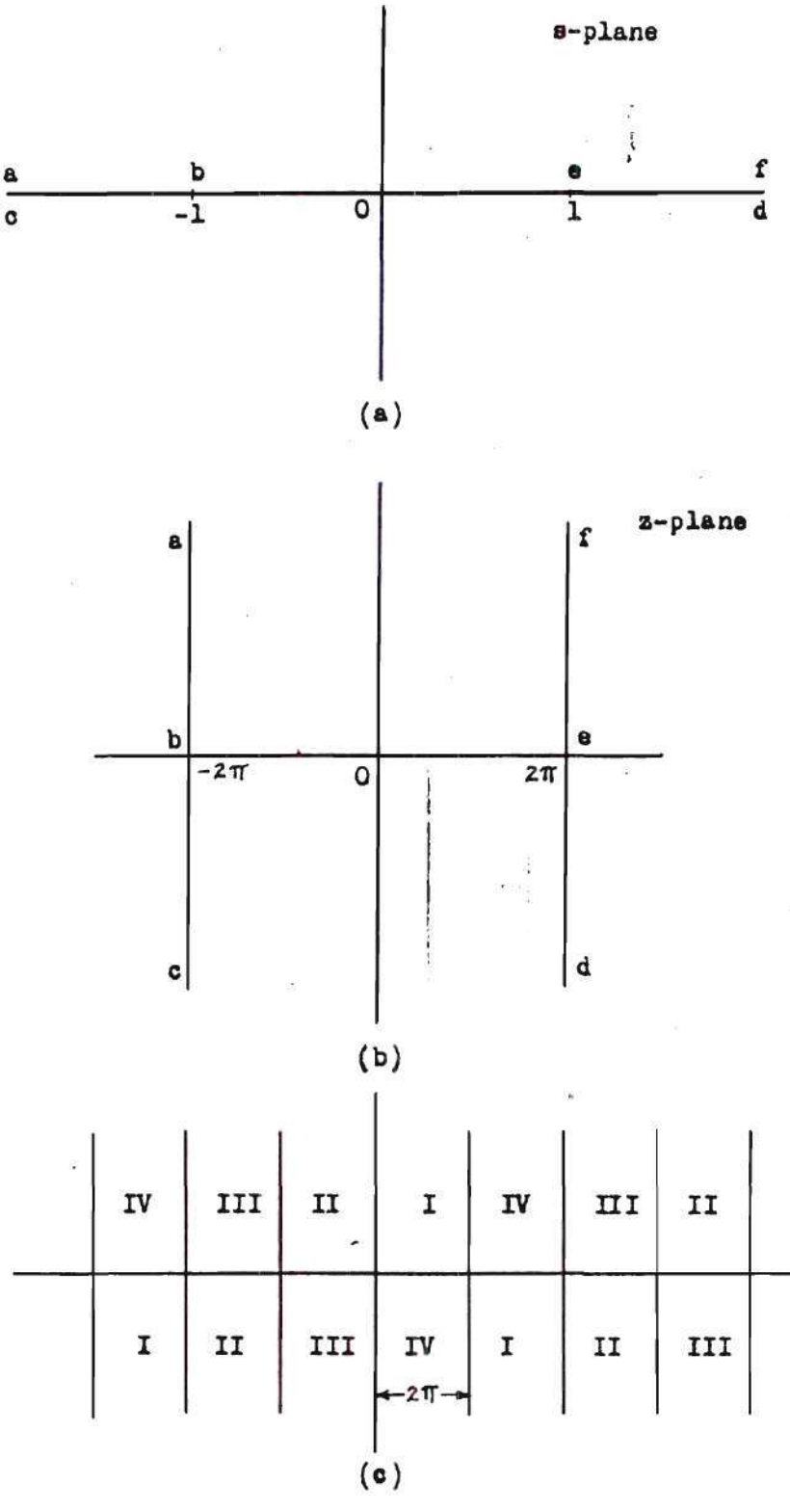

Fig. 19. The transformation $s = \sin \frac{z}{4}$.

are designed on the basis of this simplification.

Networks Containing Two Poles and One Zero

Potential function.—The general charge arrangement for this group of networks is shown in Fig. 20. Positive charges are spaced π units apart and negative charges θ units away from the origin. The function that has these singularities is

$$T(s)T(-s) = \frac{\cos\left(\frac{z}{4} + \frac{a}{2}\right)\cos\left(\frac{z}{4} - \frac{a}{2}\right)}{\cos z}, \tag{11}$$

where

$$a = \frac{1}{2}(2\pi - \theta) \tag{12}$$

or

$$\theta = 2\pi - 2a. \tag{13}$$

It can be seen that $\frac{z}{4} \pm \frac{a}{2} = \pm\frac{\pi}{2}$ when $z = \pm\theta$.

Along the y-axis, $z = jy$, and

$$|T|^2 = \frac{\cosh\frac{y}{2} + \cos a}{\cosh^2\frac{y}{2} - \frac{1}{2}} \tag{14}$$

The variation of $|T|^2$ in equation (14) will have one of the two forms shown in Fig. 21. Curve A, which has a maximum, has a more desirable characteristic as a low-pass filter.

Pass band.—The region corresponding to that between 0 and y_1 in Fig. 21 will be taken as the pass band. In the s-plane the pass band will be denoted by ω_p. Thus

$$\omega_p = \sinh\frac{y_1}{4}. \tag{15}$$

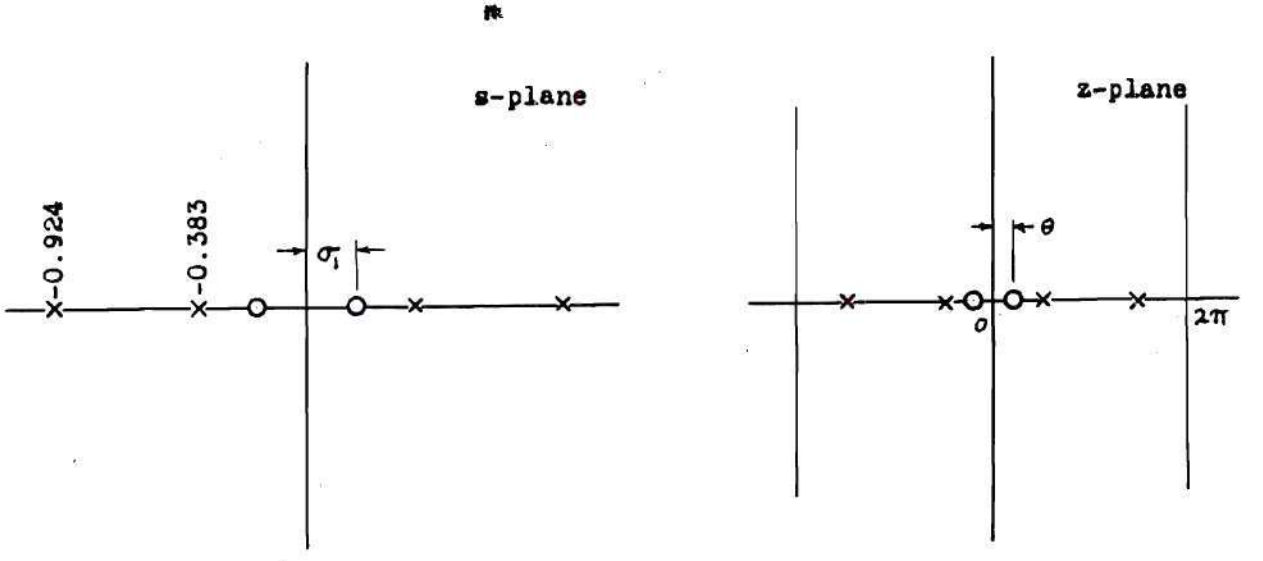

Fig. 20. Charge arrangement for networks containing two poles and one zero.

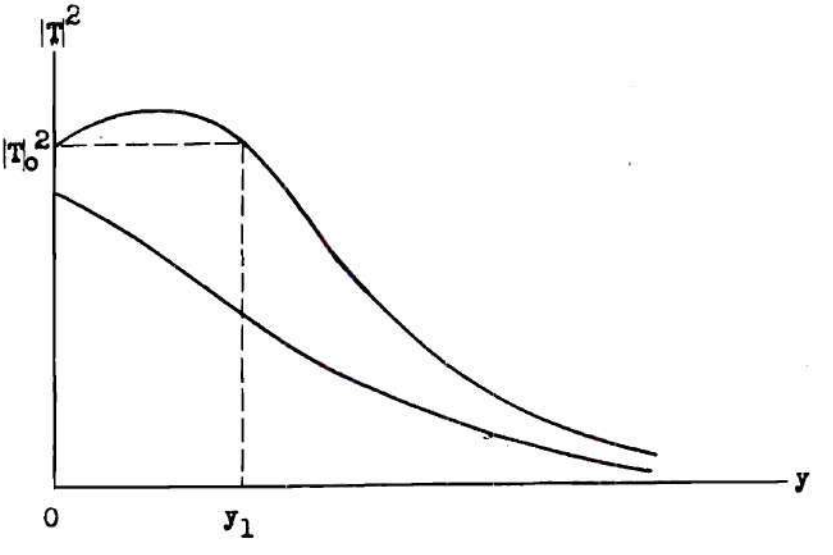

Fig. 21. Variation of $|T|^2$ along the y-axis.

The point y_1 may be found by equating $|T|^2$ at this point and that at the origin, or

$$\frac{\cosh^2 \frac{y_1}{2} - \frac{1}{2}}{\cosh \frac{y_1}{2} + \cos a} = \frac{1}{2(1 + \cos a)} . \tag{16}$$

Equation (16) may be reduced to

$$\left[(1 + \cos a) \cosh \frac{y_1}{2} + (\frac{1}{2} + \cos a) \right] \ (\cosh \frac{y_1}{2} - 1) = 0. \tag{17}$$

Thus

$$\cosh \frac{y_1}{2} = -\frac{2 \cos a + 1}{2(\cos a + 1)} . \tag{18}$$

For equation (18) to have a significant solution

$$- 2 \cos a - 1 \geq 2 \cos a + 2 .$$

This yields

$$\cos a \leq -\frac{3}{4} ,$$

and

$$\theta \leq 82^{\circ}48' . \tag{19}$$

This is the limit of the distance θ within which the $|T|^2$ curve will have the form A shown in Fig. 21.

Tolerance.—The pass band tolerance is defined as the maximum deviation within the pass band. Tolerance will be denoted by ε and expressed in db.

To locate the point where $|T|^2$ is maximum, we may set the derivative of $|T|^2$ with respect to $\cosh \frac{y}{2}$ equal to zero.

$$\frac{d}{d\left(\cosh\frac{y}{2}\right)}\left[\frac{\cosh^2\frac{y}{2}-\frac{1}{2}}{\cosh\frac{y}{2}+\cos a}\right]=0\ . \tag{20}$$

This gives

$$2\left(\cosh\frac{y}{2}+\cos a\right)\cosh\frac{y}{2}-\left(\cosh^2\frac{y}{2}-\frac{1}{2}\right)=0. \tag{21}$$

From this equation, we obtain

$$\cosh\frac{y}{2}=\frac{-2\cos a+\sqrt{4\cos^2 a-2}}{2}\ . \tag{22}$$

Substitute this value of $\cosh\frac{y}{2}$ into equation (14) to get

$$|T|^2_{max}=\frac{1}{-2\cos a+\sqrt{4\cos^2 a-2}}\ . \tag{23}$$

Thus

$$\frac{|T|^2_{max}}{|T|^2_o}=\frac{1}{2(1+\cos a)(-2\cos a+\sqrt{4\cos^2 a-2})} \tag{24}$$

and

$$\text{Tolerance} = \varepsilon = 10\log\left[\frac{|T|^2_{max}}{|T|^2_o}\right]$$

$$=10\log\left[\frac{1}{2(1+\cos a)(-2\cos a+\sqrt{4\cos^2 a-2})}\right]. \tag{25}$$

Here a factor 10 is used as the multiplier of the logarithm instead of 20 because the charges in the right half-plane are already included.

Results and data.—A complete study of this group of R-C networks would be completed if y_1 and tolerance were plotted against all values of θ. In Fig. 22, this is done in terms of parameters in the s-plane.

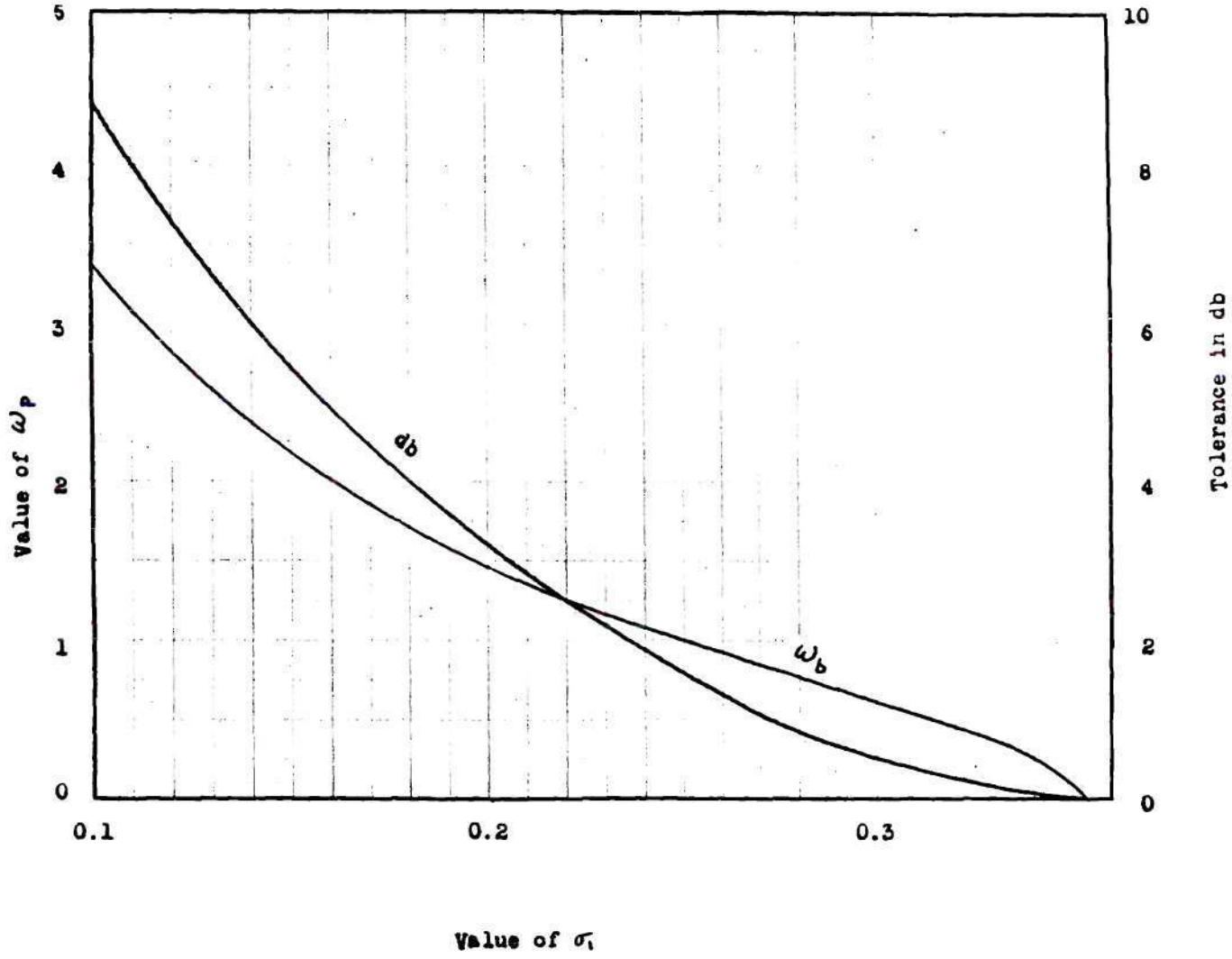

Fig. 22. Tolerance and pass band for networks containing two poles and one zero.

In the s-plane, poles are fixed to be at $s = -0.942$ and $s = -0.383$, and the distance from the zero to the origin is denoted by σ_1 as shown in Fig. 20. Thus these final results are directly usable for design purpose.

Networks Containing Three Poles and One Pair of Conjugate Zeros

Potential function.—The general charge arrangement for this group of networks is shown in Fig. 23. Positive charges are spaced $\frac{2\pi}{3}$ units apart and negative charges are placed θ units from the y-axis and 2b units from the x-axis. The function that has these singularities is

$$T(s)T(-s)=\frac{\cos(\frac{z}{4}+\frac{a}{2}+\frac{jb}{2})\cos(\frac{z}{4}+\frac{a}{2}-\frac{jb}{2})\cos(\frac{z}{4}-\frac{a}{2}+\frac{jb}{2})\cos(\frac{z}{4}-\frac{a}{2}-\frac{jb}{2})}{\cos(\frac{3z}{2})} \quad (26)$$

where a has the same meaning as before. The numerator in expression (26) may be simplified to

$$\frac{1}{4}\left[\cos(\frac{z}{2}+jb)+\cos a\right]\left[\cos(\frac{z}{2}-jb)+\cos a\right]$$

$$=\frac{1}{4}\left\{\cos(\frac{z}{2}+jb)\cos(\frac{z}{2}-jb)+\left[\cos(\frac{z}{2}+jb)+\cos(\frac{z}{2}-jb)\right]\cos a+\cos^2 a\right\}$$

$$=\frac{1}{4}\left\{\cos^2\frac{z}{2}+2\cos\frac{z}{2}\cos a\cosh b+\cos^2 a+\cosh^2 b-1\right\};$$

while the denominator may be written as

$$4\cos^3\frac{z}{2}-3\cos\frac{z}{2}.$$

Thus we have

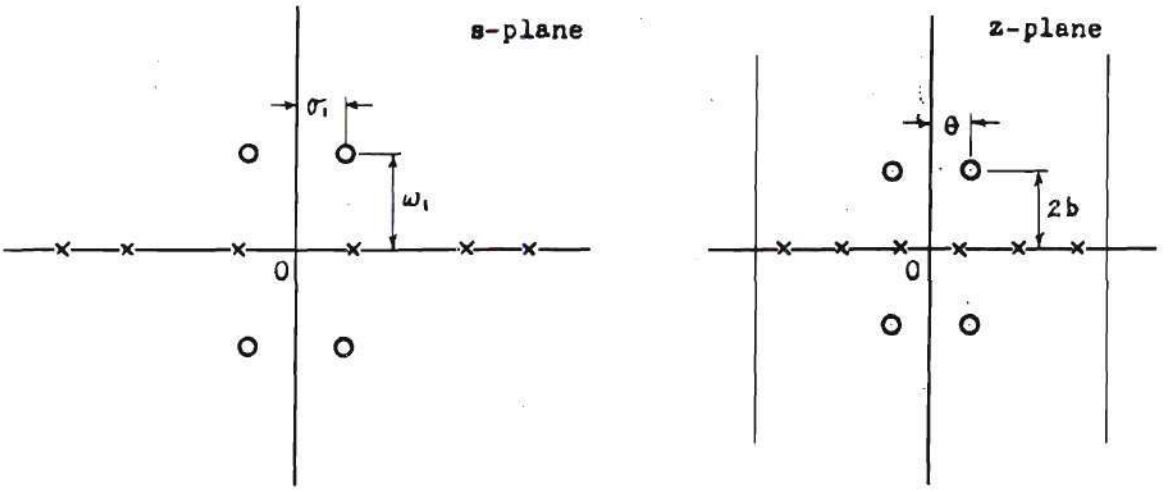

Fig. 23. Charge arrangement for networks containing three poles and one pair of conjugate zeros.

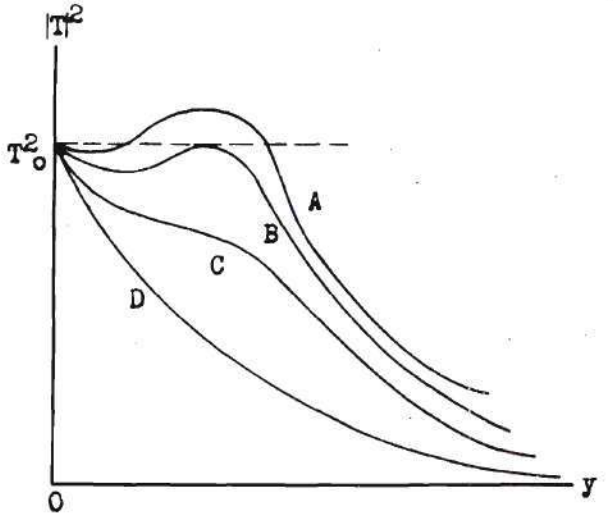

Fig. 24. Variation of $|T|^2$ along the y-axis.

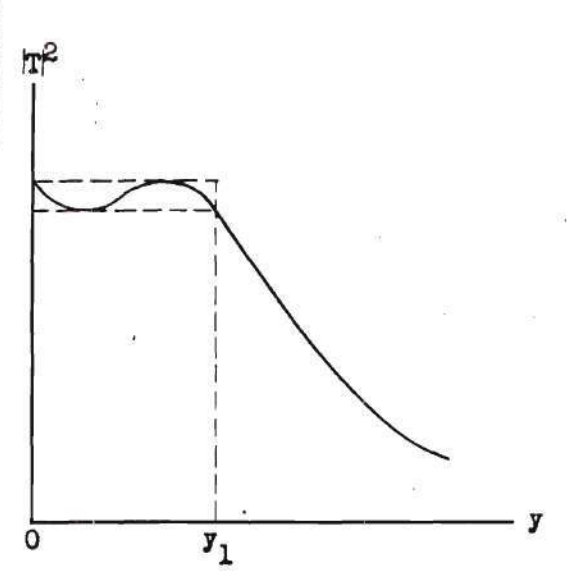

Fig. 25. Curve B of Fig. 24.

$$T(s)T(-s)=\frac{\cos^2\frac{z}{2}+2\cos\frac{z}{2}\cos a\cosh b+\cos^2 a+\cosh^2 b-1}{4\left(4\cos^3\frac{z}{2}-3\cos\frac{z}{2}\right)}. \qquad (27)$$

Along the y-axis, $z = jy$, and

$$|T|^2=\frac{\cosh^2\frac{y}{2}+2\cosh\frac{y}{2}\cos a\cosh b+\cos^2 a+\cosh^2 b-1}{4\left(4\cosh^3\frac{y}{2}-3\cosh\frac{y}{2}\right)}. \qquad (28)$$

Let $u=\cosh\frac{y}{2}$, $f=\cos a$ and $g=\cosh b$; equation (28) becomes

$$|T|^2=\frac{u^2+2fgu+f^2+g^2-1}{4\left(4u^3-3u\right)} \qquad (29)$$

Positions of zeros to yield equal-ripple characteristic.—The variation of $|T|^2$ along the y-axis will have one of the forms shown in Fig. 24. Among them curve B, whose maximum is equal to the value of the function at the origin, displays the equal-ripple property. This curve is reproduced in Fig. 25 and will be treated in more detail.

In order to determine the position of zeros so that $|T|^2$ will vary like curve B, the equation

$$|T|^2-|T|^2_0=0 \qquad (30)$$

must have a real double root. Since when $y=0$, $u=1$, equation (30) becomes

$$\frac{4u^3-3u}{u^2+2fgu+f^2+g^2-1}=\frac{1}{2fg+f^2+g^2} \qquad (31)$$

or

$$(8fg+4f^2+4g^2)u^3-u^2-(8fg+3f^2+3g^2)u+(1-f^2-g^2)=0. \qquad (32)$$

This equation must contain a factor $(u-1)$. After this factor is re-

moved from equation (32), we obtain

$$(8fg + 4f^2 + 4g^2)\, u^2 + (8fg + 4f^2 + 4g^2 - 1)\, u + (f^2 + g^2 - 1) = 0. \qquad (33)$$

If equation (30) has a real double root other then $u = 1$, the discriminant of quadratic equation (33) must vanish. Or

$$(8fg + 4f^2 + 4g^2 - 1)^2 - 4\,(f^2 + g^2 - 1)(8fg + 4f^2 + 4g^2) = 0. \qquad (34)$$

Simplifying equation (34), there is obtained

$$(f + g)^2(32fg + 8) + 1 = 0. \qquad (35)$$

This is the conditional equation for the coordinates of positions of zeros to produce frequency characteristic of the type shown in Fig. 25. The locus of these positions may be plotted by solving equation (35). This locus in the s-plane is plotted in Fig. 26.

Tolerance and pass band.—The definitions of tolerance and pass band are the same as before. They are denoted by ε and y_1 respectively and are indicated in Fig. 25.

Differentiating $|T|^2$ of equation (29) with respect to u and setting the derivative equal to zero, there is obtained

$$(u^2 + 2fg\, u + f^2 + g^2 - 1)(12\, u^2 - 3) - (4\, u^3 - 3u)(2u + 2fg) = 0 \qquad (36)$$

or

$$u^4 + 4fg\, u^3 + (3f^2 + 3g^2 - 2.25)\, u^2 - 0.75(f^2 + g^2 - 1) = 0. \qquad (37)$$

One of the roots of this equation will give the value of y at which the minimum of $|T|^2$ occurs. Thus $|T|^2_{min}$ may be found. Since $|T|^2_{max} = |T|^2_o$, we have

$$\text{Tolerance} = \varepsilon = 10 \log \left[\frac{|T|^2_o}{|T|^2_{min}} \right]. \qquad (38)$$

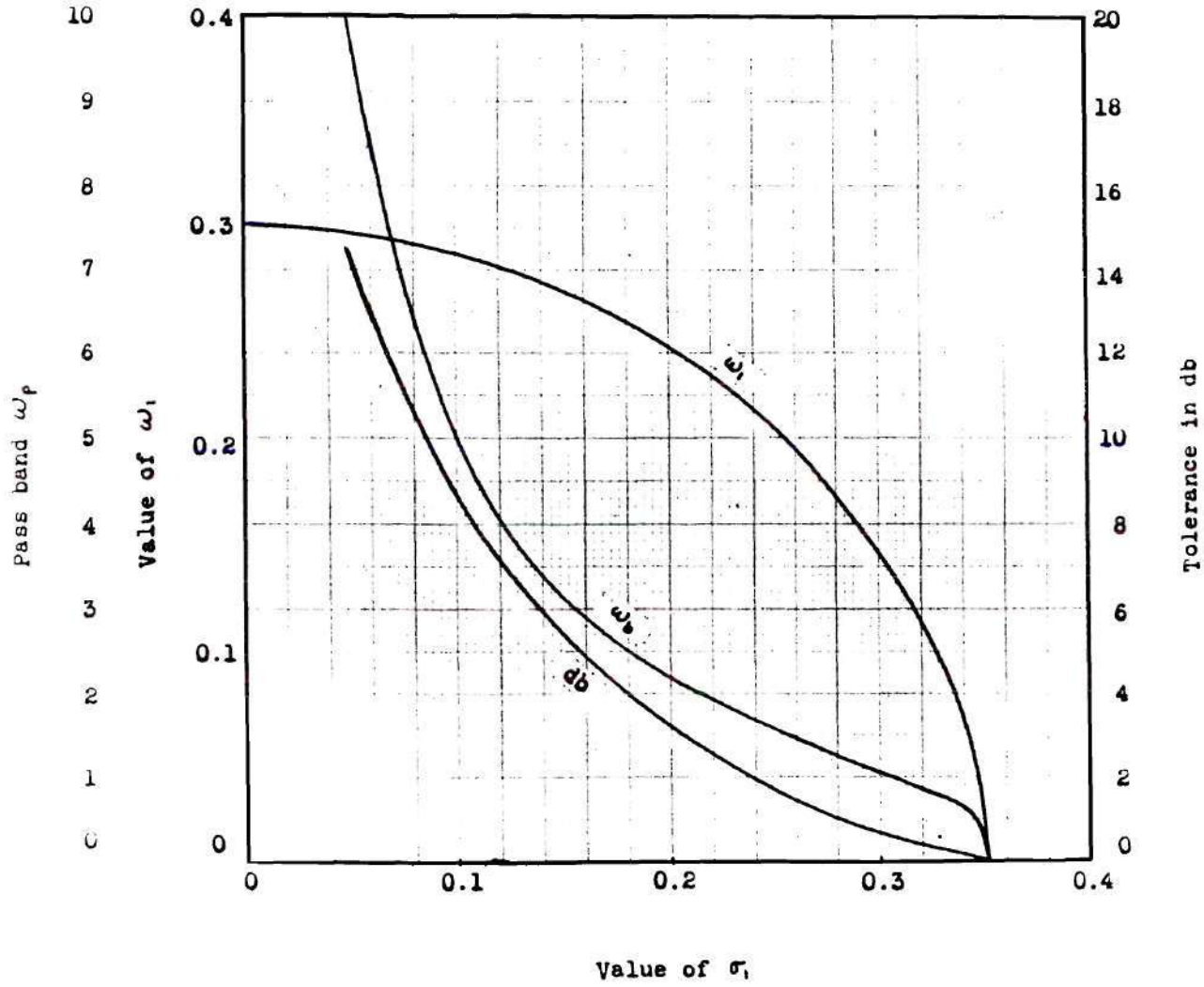

Fig. 26. Locus of zeros, tolerance and pass band for networks containing three poles and one pair of conjugate zeros.

With the value of $|T|^2_{min}$ known the point y_1, the pass band, can be found by locating the point where $|T|^2$ again drops to $|T|^2_{min}$.

Tolerance and pass band in the s-plane, ε and ω_p respectively, are plotted in Fig. 26 for different positions of zeros. The poles of these networks are located at $s = -\sin\frac{\pi}{24}$, $-\sin\frac{\pi}{8}$ and $\sin\frac{5\pi}{24}$ or -0.2588, -0.7071 and -0.9660 in the s-plane.

Networks Containing Four Poles and One Double Zero

Potential function.--Charges for this group of networks are arranged in the manner shown in Fig. 27. The function that has these singularities is

$$T(s)T(-s) = \frac{\cos\frac{z}{2} + \cos a}{\cos 2z} . \tag{39}$$

The potential along the y-axis may be written as

$$|T|^2 = \frac{(u + f)^2}{8u^4 - 8u^2 + 1} \tag{40}$$

by letting $z = jy$ in equation (39). Quantities a, u and f have the same meaning as before.

Pass band.--The variation of $|T|^2$ in equation (40) will have one of the two forms shown in Fig. 21. Curve A, which has a maximum, has a more desirable characteristic as low-pass filter. The region corresponding to that between 0 and y_1 will be taken as the pass band. Let $u_1 = \cosh\frac{y_1}{2}$, we have

$$\frac{(u_1 + f)^2}{8u_1^4 - 8u_1^2 + 1} = (1 + f)^2. \tag{41}$$

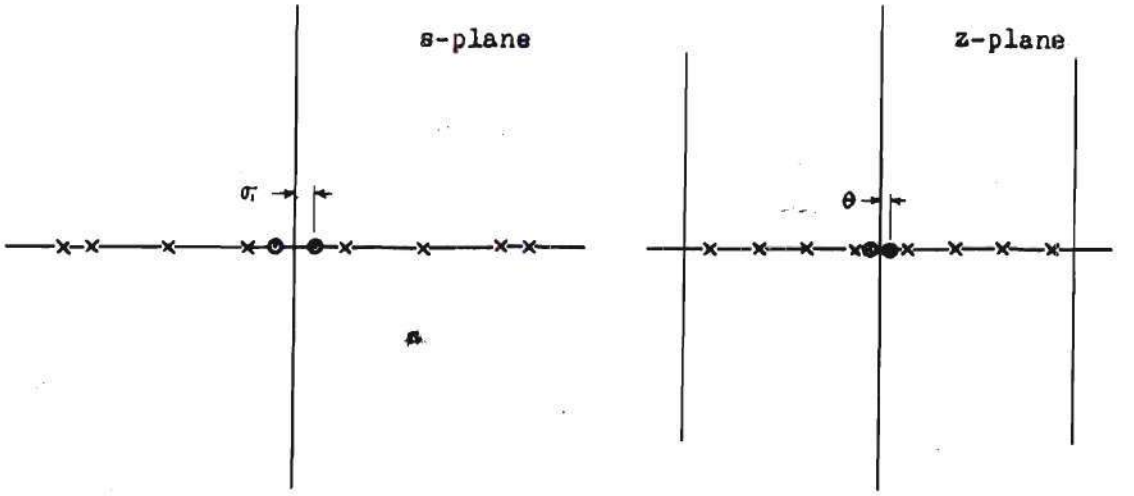

Fig. 27. Charge arrangement for networks containing four poles and one double zero.

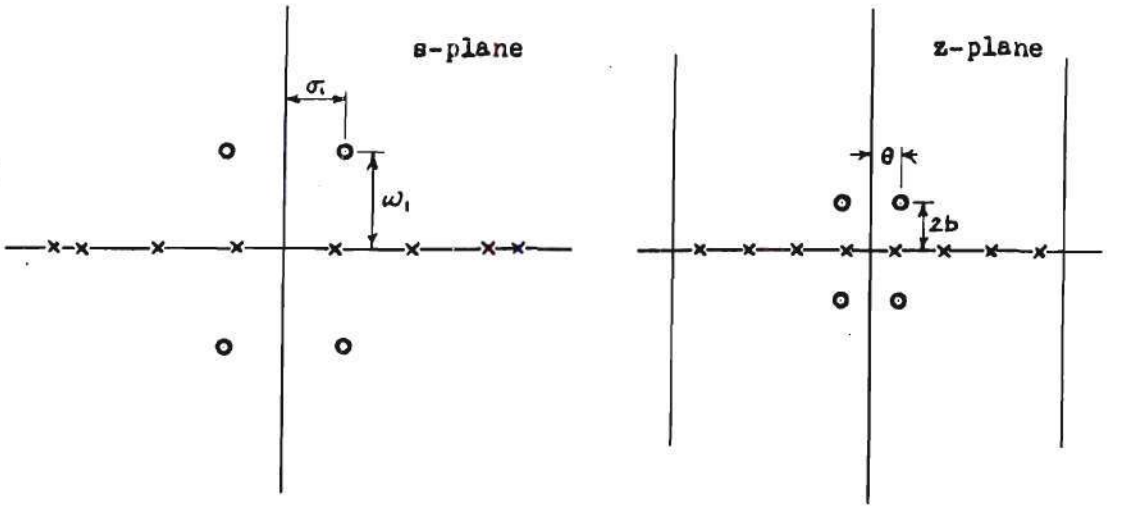

Fig. 28. Charge arrangement for networks containing four poles and one pair of conjugate zeros.

After equation (41) is simplified there is obtained

$$8(f + 1)^2 u_1^4 - \left[8(f + 1)^2 + 1\right] u_1^2 - 2f\, u_1 + (2f + 1) = 0. \quad (42)$$

This equation must contain a factor $(u_1 - 1)$. After this factor is removed, we obtain

$$8(f + 1)^2 u_1^3 + 8(f + 1)^2 u_1^2 - u_1 - (2f + 1) = 0. \quad (43)$$

The root of this equation that is greater than 1 is the point corresponding to y_1.

If equation (43) again has a root $u_1 = 1$, y_1 approaches zero. This is the boundary condition between the two curve shapes indicated in Fig. 21. Let $u_1 = 1$ in equation (43) and we have

$$8(f + 1)^2 + 8(f + 1)^2 - 1 - 2f - 1 = 0 \quad (44)$$

or

$$f = -0.875.$$

This gives

$$a = 180^\circ - 28^\circ 57'$$

and

$$\theta = 57^\circ 54' = 0.3217 \quad . \quad (45)$$

This is the limiting value of the distance θ if the $|T|^2$ curve is to take on the form of curve A in Fig. 21.

Tolerance.--To find the point where maximum potential occurs we set

$$\frac{d}{du}\left[\frac{(u + f)^2}{8u^4 - 8u^2 + 1}\right] \quad (46)$$

equal to zero to obtain

$$(u + f)^2(32\,u^2 - 16\,u) - (8\,u^4 - 8\,u^2 + 1)\,2(u + f) = 0. \qquad (47)$$

After simplification, there is obtained

$$u^4 + 2\,f\,u^3 - f\,u - 0.125 = 0. \qquad (48)$$

Solution of equation (48) for different values of f gives the point at which $|T|^2_{max}$ occurs. Thus,

$$\text{Tolerance} = \varepsilon = 10 \log\left[\frac{|T|^2_{max}}{|T|^2_o}\right]. \qquad (49)$$

Results and data.—Pass band and tolerance values have been calculated for different positions of double-zeros. These results are transformed to the s-plane and plotted in Fig. 29. Poles in the s-plane are located at $-\sin\frac{\pi}{8}$, $-\sin\frac{3\pi}{8}$, $-\sin\frac{5\pi}{8}$ and $-\sin\frac{7\pi}{8}$ which are also equal to −0.1951, −0.5556, −0.8315 and −0.9808 respectively.

Networks Containing Four Poles and One Pair of Conjugate Zeros

Potential function.—Charges for this group of networks are arranged in the manner shown in Fig. 28. The function that has these singularities is

$$T(s)T(-s) = \frac{\cos(\frac{z}{4} + \frac{a}{2} + \frac{jb}{2})\,\cos(\frac{z}{4} + \frac{a}{2} - \frac{jb}{2})\,\cos(\frac{z}{4} - \frac{a}{2} + \frac{jb}{2})\,\cos(\frac{z}{4} - \frac{a}{2} - \frac{jb}{2})}{\cos 2z}, \qquad (50)$$

in which the numerator is identical to that of equation (26) and the denominator is identical to that of equation (39). Thus the potential along the y-axis in the z-plane will be

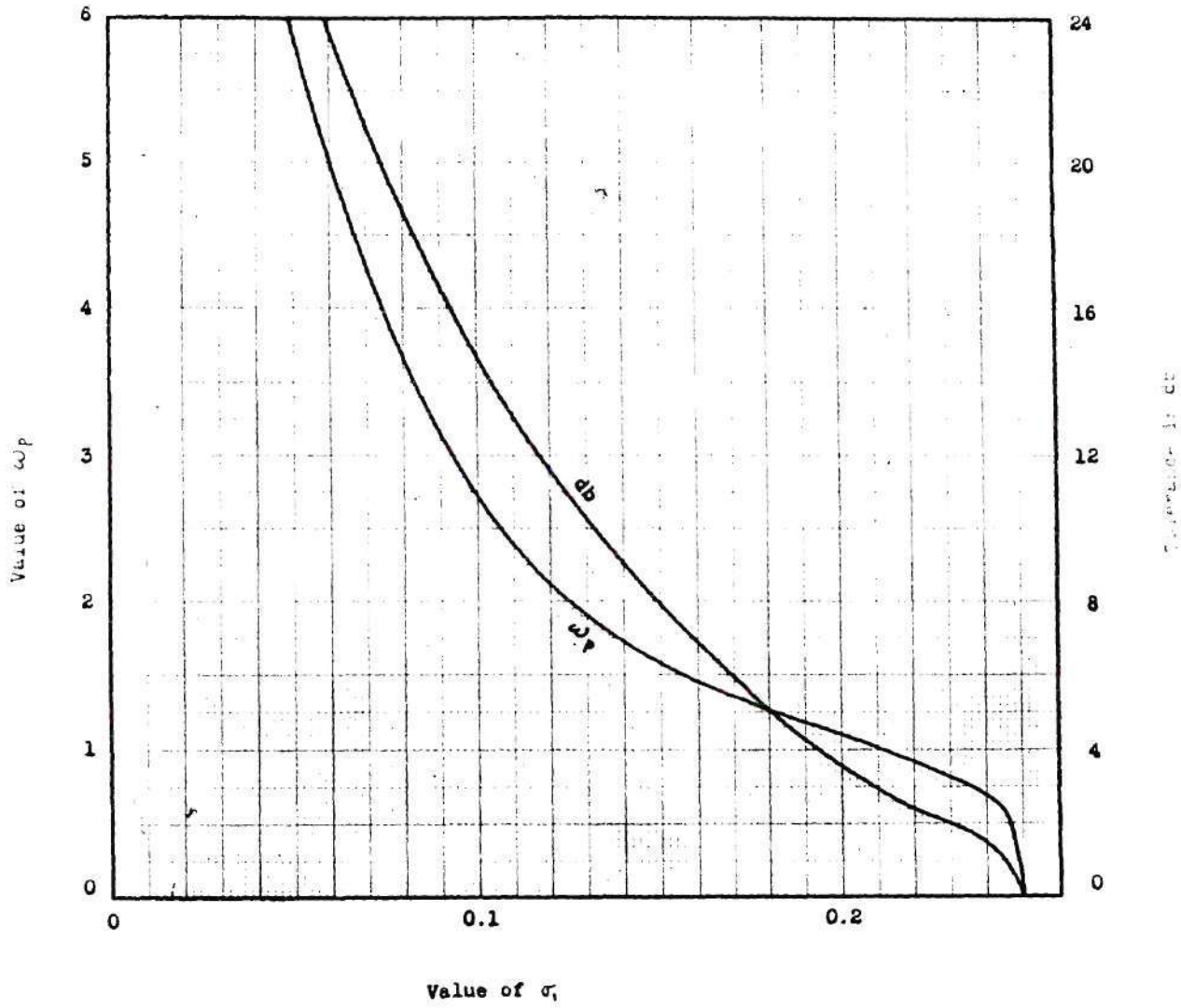

Fig. 29. Tolerance and pass band for networks containing four poles and one double zero.

$$|T|^2 = \frac{u^2 + 2fg\,u + f^2 + g^2 - 1}{4\,(8\,u^4 - 8\,u^2 + 1)} \tag{51}$$

which has the numerator of equation (29) and the denominator of equation (40).

Positions of zeros to yield equal-ripple characteristic.—The variation of potential will have one of the forms shown in Fig. 24. The shape of curve B is the desirable one which is shown in Fig. 25 in more detail. This is realized if the equation

$$|T|^2 - |T|^2_o = 0 \tag{52}$$

has a double-root. Equation (52) is explicitly

$$\frac{u^2 + 2fg\,u + f^2 + g^2 - 1}{8\,u^4 - 8\,u^2 + 1} = (f + g)^2. \tag{53}$$

After simplification, there is obtained

$$8(f + g)^2 u^4 - \left[8(f+g)^2 + 1\right]u^2 - 2fg\,u + 2fg + 1 = 0. \tag{54}$$

After a factor $(u - 1)$ is extracted from this equation, it becomes

$$u^3 + u^2 - \frac{1}{8(f + g)^2}u - \frac{2fg + 1}{8(f + g)^2} = 0 \tag{55}$$

Let $A = 2fg + 1$ and $B = \frac{1}{8(f + g)^2}$ and equation (55) may be rewritten as

$$u^3 + u^2 - B\,u - A\,B = 0. \tag{56}$$

This equation contains a real double-root if its discriminant vanishes, or

$$18\ AB^2 + 4\ AB + B^2 + 4\ B^3 - 27\ A^2B^2 = 0. \tag{57}$$

After simplification we obtain

$$4\ B^2 + (-27\ A^2 + 18\ A + 1)\ B + 4\ A = 0. \tag{58}$$

This is the conditional equation for the co-ordinates of positions of zeros to produce frequency characteristics of the type shown in Fig. 25. The locus of these positions is plotted in Fig. 30.

Tolerance and pass band.—The value of u at which $|T|^2$ is a minimum can be found by setting

$$\frac{d}{du}\left[\frac{8\ u^4 - 8\ u^2 + 1}{u^2 + 2fg\ u + f^2 + g^2 - 1}\right]$$

equal to zero. This process yields

$$(8\ u^4 - 8\ u^2 + 1)(2\ u + 2fg)$$

$$- (u^2 + 2fg\ u + f^2 + g^2 - 1)(32\ u^3 - 16\ u) = 0. \tag{59}$$

Rearranging, we have

$$16\ u^5 + 48\ fg\ u^4 + 32\ (f^2 + g^2 - 1)\ u^3$$

$$- 16\ fg\ u^2 - (16\ f^2 + 16\ g^2 + 18)\ u - 2\ fg = 0. \tag{60}$$

The real root of equation (60) that is greater than unity gives the value of u which corresponds to the minimum of $|T|^2$. Thus $|T|^2_{min}$ can be calculated and tolerance will be given by equation (38)

The edge of the pass band in the z-plane, y_1, may be computed by

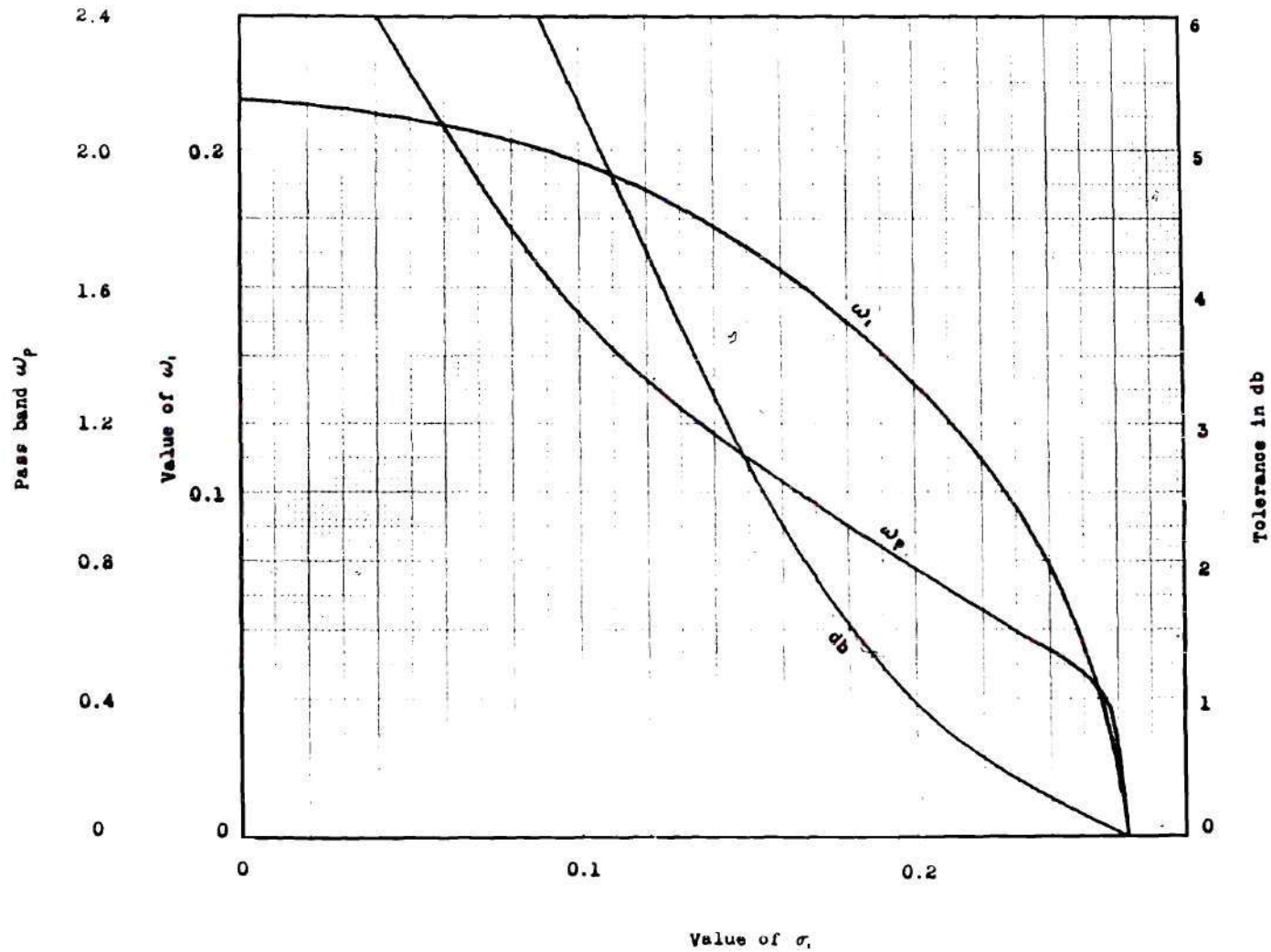

Fig. 30. Locus of zeros, tolerance and pass band for networks containing four poles and one pair of conjugate zeros.

finding the point u_1 where $|T|^2$ again equals $|T|^2_{min}$.

The results for this group of networks are plotted in Fig. 30 and are given in terms of parameters in the s-plane. The positions of their poles are located at $-\sin\frac{\pi}{8}$, $-\sin\frac{3\pi}{8}$, $-\sin\frac{5\pi}{8}$ and $-\sin\frac{7\pi}{8}$ as in the case where four poles and one double-zero were contained in the networks.

CHAPTER VI

DESIGN OF R-C NETWORKS BY THE USE OF ELLIPTIC-FUNCTION TRANSFORMATIONS

Elliptic Functions

Elliptic functions may be defined by the following relationships: If

$$z = \int_0^{\phi} \frac{d\theta}{\sqrt{1 - k^2 \sin^2\theta}}, \tag{61}$$

then $sn\ (z,k) = \sin\phi$, $cn\ (z,k) = \cos\phi$ and $dn\ (z,k) = \sqrt{1 - k^2 \sin^2\phi}$, where z is referred to as the argument and k the modulus of the functions. The modulus k is usually omitted in writing whenever its absence causes no confusion. In such instances elliptic functions are written as sn z, cn z and dn z. These functions are single-valued and doubly periodic.

Their quarter periods are K and jK' given by

$$K = \int_0^{\frac{\pi}{2}} \frac{d\theta}{\sqrt{1 - k^2 \sin^2\theta}} \tag{62}$$

and

$$K' = \int_0^{\frac{\pi}{2}} \frac{d\theta}{\sqrt{1 - k'^2 \sin^2\theta}}, \tag{63}$$

where $k' = \sqrt{1 - k^2}$ is the complementary modulus. Thus,

$$sn\ (z + 4mK + j4nK') = sn\ z, \tag{64}$$

where m and n are any integers. The quantities K and K' are also

known as complete elliptic integrals of the first kind.

When $k = 0$, we have $K = \frac{\pi}{2}$, $K' \to \infty$, so that $sn\,(z,0) = \sin z$, $cn\,(z,0) = \cos z$, $dn\,(z,0) = 1$. When $k = 1$, we have $K \to \infty$, $K' = \frac{\pi}{2}$, so that $sn\,(z,1) = \tanh z$, $cn\,(z,1) = dn\,(z,1) = \operatorname{sech} z$. Thus, when $k = 0$, elliptic functions degenerate into ordinary circular functions, and when $k = 1$, they degenerate into hyperbolic functions.

The ratio of two elliptic functions is denoted by the combination of the first letter of each function, that of the numerator preceding that of the denominator, e.g.

$$cd\ z = \frac{cn\ z}{dn\ z}. \tag{65}$$

The reciprocal of an elliptic function is denoted by interchanging two letters which denote the original function, e.g.

$$ns\ z = \frac{1}{sn\ z}. \tag{66}$$

The following are some formulae useful for calculations herein:

a. Imaginary arguments.

$$sn\,(jy,k) = j\ sc\,(y,\ k') \tag{67}$$

$$cn\,(jy,k) = \quad nc\,(y,\ k') \tag{68}$$

$$dn\,(jy,k) = \quad dc\,(y,\ k') \tag{69}$$

b. Addition theorems.

$$sn\,(u+v) = \frac{sn\ u\ cn\ v\ dn\ v + sn\ v\ cn\ u\ dn\ u}{1 - k^2\ sn^2 u\ sn^2 v} \tag{70}$$

$$\operatorname{cn}(u+v) = \frac{\operatorname{cn} u \operatorname{cn} v - \operatorname{sn} u \operatorname{dn} u \operatorname{sn} v \operatorname{dn} v}{1 - k^2 \operatorname{sn}^2 u \operatorname{sn}^2 v} \tag{71}$$

$$\operatorname{dn}(u+v) = \frac{\operatorname{dn} u \operatorname{dn} v - k^2 \operatorname{sn} u \operatorname{cn} u \operatorname{sn} v \operatorname{cn} v}{1 - k^2 \operatorname{sn}^2 u \operatorname{sn}^2 v} \tag{72}$$

c. Complex argument.

Assume $s_1 = \operatorname{sn}(x,k)$, $c_1 = \operatorname{cn}(x,k)$, $d_1 = \operatorname{dn}(x,k)$,

$s_2 = \operatorname{sn}(y,k')$, $c_2 = \operatorname{cn}(y,k')$, $d_2 = \operatorname{dn}(y,k')$,

then

$$\operatorname{sn} z = \operatorname{sn}(x + jy, k) = \frac{s_1 d_2 + j c_1 d_1 s_2 c_2}{c_2^2 + k^2 s_1^2 s_2^2}, \tag{73}$$

$$\operatorname{cn} z = \operatorname{cn}(x + jy, k) = \frac{c_1 c_2 - j s_1 d_1 s_2 d_2}{c_2^2 + k^2 s_1^2 s_2^2}, \tag{74}$$

$$\operatorname{dn} z = \operatorname{dn}(x + jy, k) = \frac{d_1 c_2 d_2 - j k^2 s_1 c_1 s_2}{c_2^2 + k^2 s_1^2 s_2^2}. \tag{75}$$

d. Special relationships.

$$\operatorname{sn}(-u) = -\operatorname{sn} u \tag{76}$$

$$\operatorname{sn}(u + K) = \operatorname{cd} u \tag{77}$$

$$\operatorname{sn}(u + jK') = \frac{1}{k} \operatorname{ns} u \tag{78}$$

$$\operatorname{sn}(u + K + jK') = \frac{1}{k} \operatorname{dc} u \tag{79}$$

The Transformation $w = \operatorname{sn} z$

The transformation $w = \operatorname{sn} z$ maps a rectangle in the z-plane onto the entire w-plane. Since the sn function is doubly periodic the inverse transformation is multiple-valued. Each point in the w-plane is

mapped into an infinite number of points in the z-plane. Repetition occurs for every 4K along the x-direction and every 2K' along the y-direction. Points spaced 4mK + j2nK' apart, where m and n are any integers, are said to be congruent. Thus congruent points in the z-plane are mapped into the same point in the w-plane.

If the z-plane is divided into rectangles of width 2K and height 2K', the entire z-plane can be considered as the congruent regions of any one single rectangle. These rectangles are termed cells just as in the case of circular and hyperbolic functions where strips of width 2π are termed as their cells. One of these cells, whose vertices are located at K + jK' and its points of quadrantal symmetry, is shown in Fig. 31(a).

The correspondence between the w-plane and a cell in the z-plane is shown in Fig. 31(a) and Fig. 31(b). The manner in which cells in the z-plane are stacked up is illustrated in Fig. 31(c).

Fig. 32 shows how this transformation may be visualized by considering the w-plane as being an elastic sheet. The real axis is partly split and then folded upward and downward, and at the same time the extreme upper and lower parts of the plane as well as the imaginary axis are compressed until finally a rectangle is formed.

The Modified Transformation

The transformation just discussed maps the entire imaginary axis into the line segment aa', Fig. 31, and its congruent regions. Experience has shown that in order to benefit from the transformation method, the imaginary axis should be bent at strategic points. For reasons which

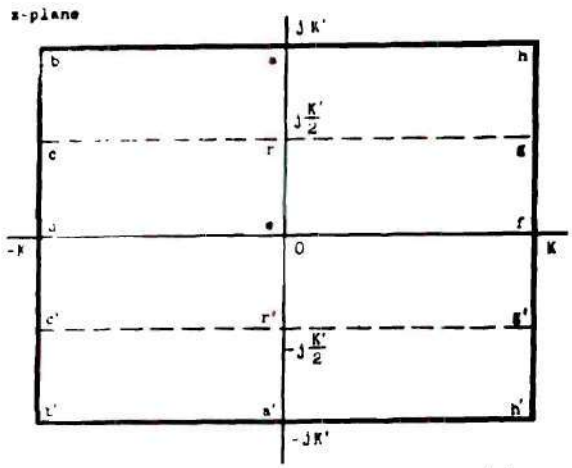

(a)

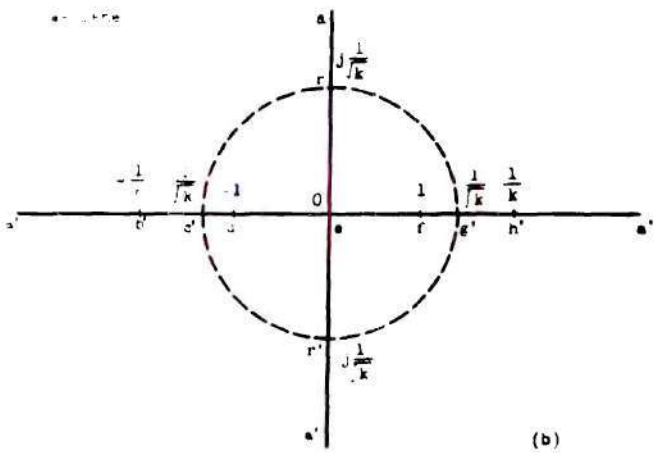

(b)

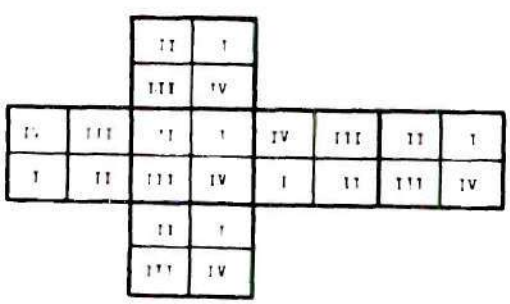

(c)

Fig. 31. The transformation w = sn z.

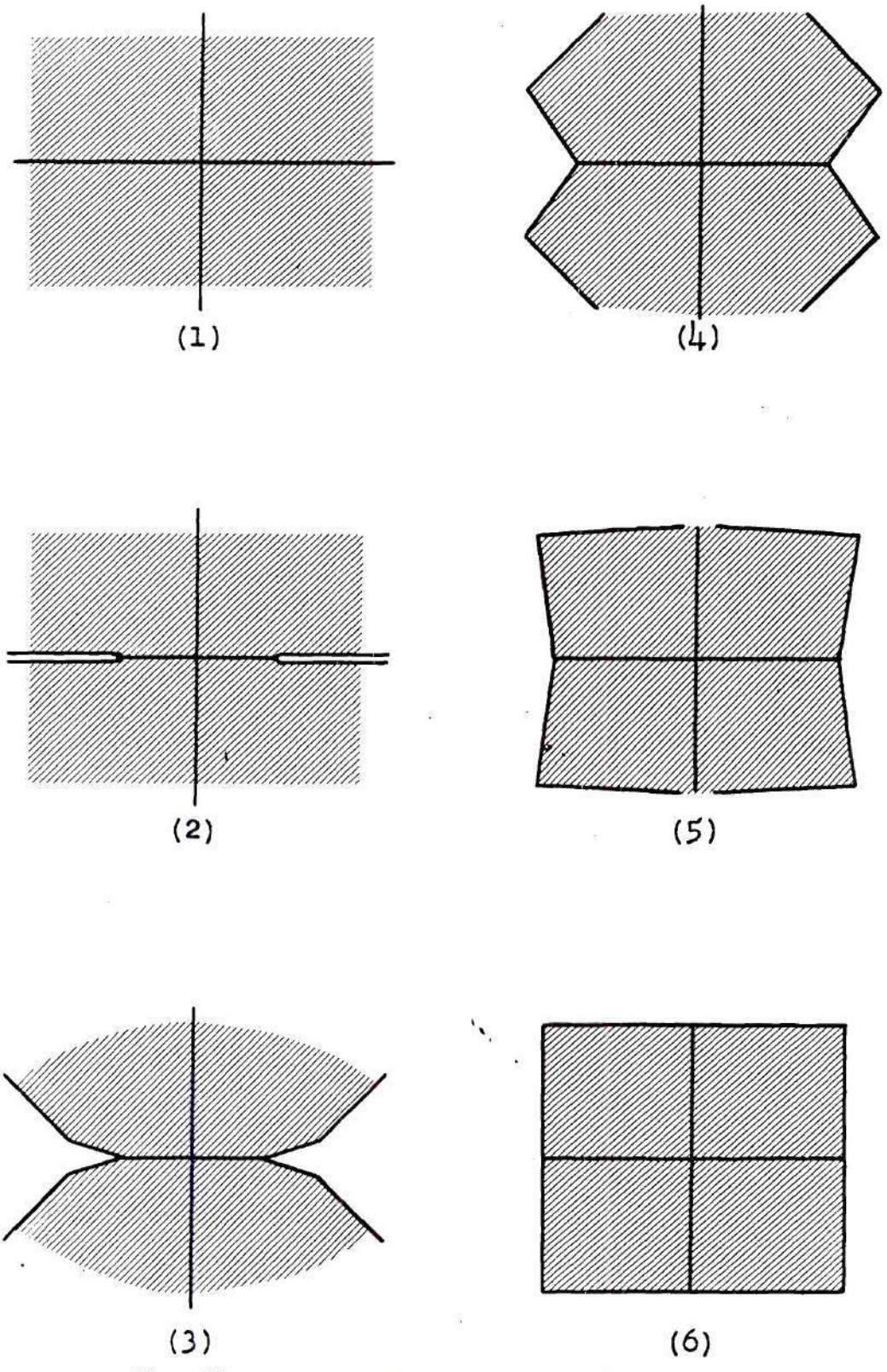

Fig. 32. Compression of the w-plane into a rectangle by the transformation $w = \mathrm{sn}\, z$.

will be apparent later it is desired to place the point at infinity somewhere between a and h, and positioned quadrantally symmetrical to it. This can be achieved by introducing another transformation.

Suppose it is desired to place $s = \infty$ at a point aK from the imaginary axis along a-h. Then this point will be on the u-axis $sn\,(aK + jK') = \frac{1}{k}\,sn\,(aK)$ away from the origin in the w-plane. If the w-plane is mapped into the s-plane by the transformation

$$s = \frac{w}{\sqrt{A^2 - w^2}}, \tag{80}$$

where $A = \frac{1}{k}\,ns\,(aK)$, point $aK + jK'$ in the z-plane is mapped to the point at infinity in the s-plane.

Other properties of this series of transformations are depicted in Fig. 33. The entire imaginary axis is now mapped into the broken lines p-a-e-a'-p' and q-a-e-a'-q'. A diagram similar to that in Fig. 34 can be drawn for this modified transformation. The only difference is that in the present case not only the real axis but also the imaginary axis is partly split and bent. Such a diagram is given in Fig. 34.

Networks Employing One Row of Simple Zeros in the z-plane

Arrangement of charges.—The modified elliptic-function transformation can be used for designing low-pass R-C transfer functions with equal-ripple response inside the pass band. In Fig. 35 is shown a quadrant of one cell in the z-plane. As was shown in Fig. 33, the $j\omega$-axis in the s-plane is mapped into e-a-q, with the part where $0 < \omega < 1$ corresponding to line segment e-a. This portion of the $j\omega$-axis is conveniently chosen to be the pass band.

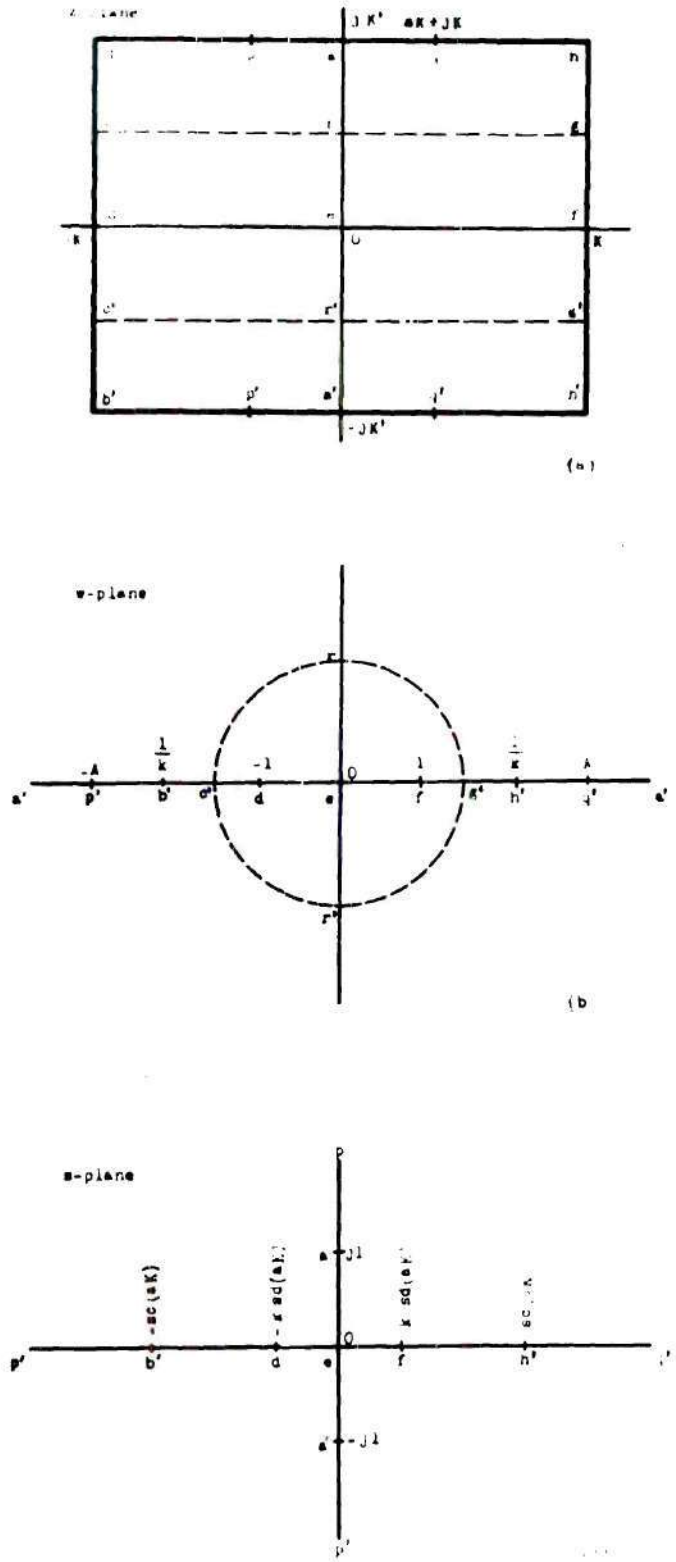

Fig. 33. The modified transformation.

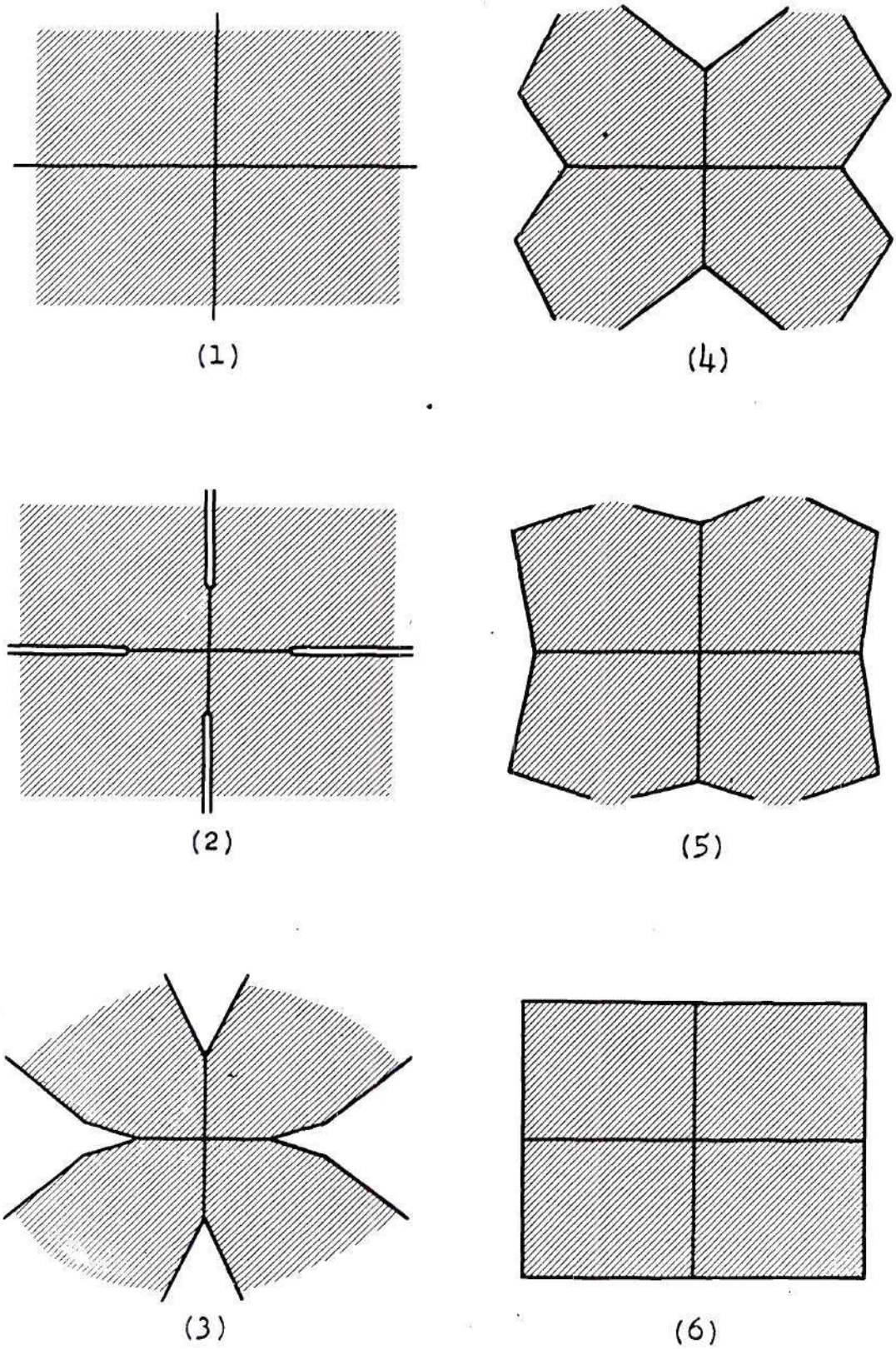

Fig. 34. The compression of the s-plane into a rectangle by the modified transformation.

The σ-axis is mapped into e-f-h-q. This is the only portion in the s-plane where poles are permitted to lie. If we place all the positive charges uniformly along h-f, and place all negative charges unifromly along a line passing through q and parallel to a-e or h-f, the potential variations can thus be obtained. This arrangement is exemplified by that shown in Fig. 36.

The equal-ripple property is more evident when several cells are shown together, as in Fig. 37. Since there are an infinite number of cells in both horizontal and vertical directions the effect due to all charges at a certain point and all its congruent points are identical. Therefore the potential pattern in every cell is identical.

In the s-plane there must be equal numbers of positive and negative charges. Therefore this must also be true within each cell in the z-plane. Due to quadrantal symmetry this must also hold within each quadrant of a cell. In Fig. 36, for instance, two negative charges are completely enclosed by the boundaries. The uppermost negative charge is shared by this cell and the one immediately on top of it. Therefore only one-half of this charge can be considered as lying within this quarter-cell. All five positive charges, however, are shared by this quarter-cell and the one adjacent to it and on its right. Therefore only half of each charge lies within this quadrant. By this consideration, within this quadrant there are two and one-half units of negative charges and the same number of positive charges.

Observations of arrangements similar to Figs. 36 and 37 indicates that negative charges should be spaced twice as far apart among them-

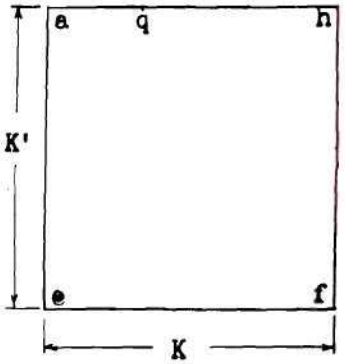

Fig. 35. A quarter of a cell in the z-plane.

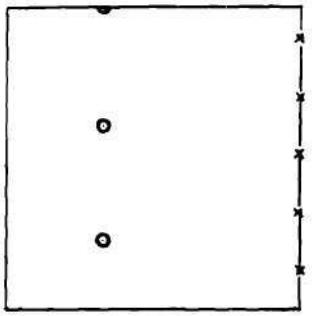

Fig. 36. An arrangement that produces equal ripple potential along the imaginary axis.

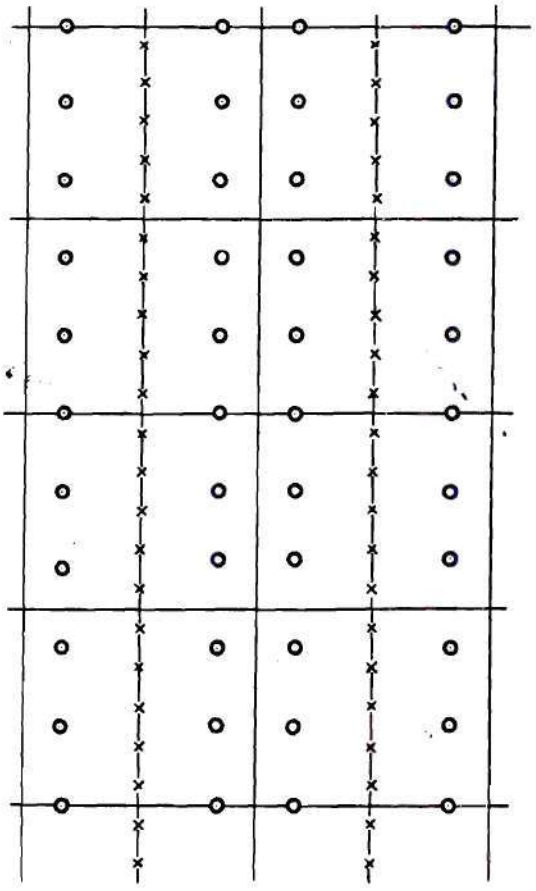

Fig. 37. Charge arrangement in several cells.

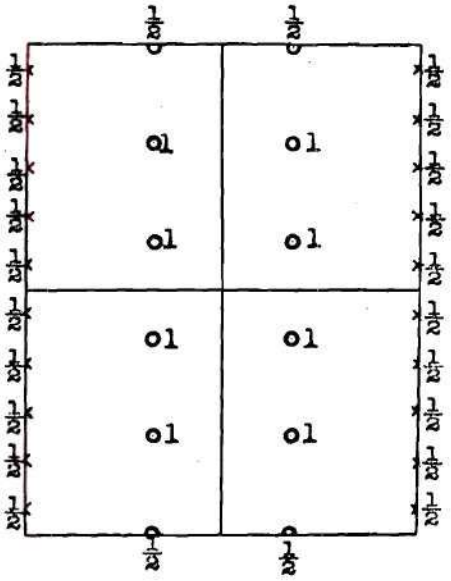

Fig. 38. Charge content in one cell.

selves as positive charges. A more precise diagram of charges contained in one cell is shown in Fig. 38.

When charges are mapped into the s-plane, every half-unit charge will combine with the other half-unit charge located at its conjugate point to form a unit charge. The final charge arrangement thus conforms with the requirement that all charges in the s-plane must be of unit strength. Such combination, however, does not take place for any charge placed at f or d. Also, any charge placed at points like h will be shared by four cells, and thus only one-quarter of a unit charge lies in each cell. So charges placed at h, f or d will result in half-unit charges in the s-plane. Therefore placement of charges at such points is not permissible.

Along a-q, Fig. 35, the potential decreases monotonically as one approaches the negative charge at q. Since a-q corresponds to the region outside the pass-band, the desired general shape of the frequency characteristic is obtained.

Numerical example.—As a numerical example, the following values of parameters are chosen:

$$k = 0.3162, \qquad k^2 = 0.1, \qquad a = 0.5, \qquad n = 3,$$

where n is the number of poles that the final transfer function will contain. Corresponding to these parameters, $K = 1.6124$ and $K' = 2.5781$.

One cell in the z-plane is indicated in Fig. 39, which is drawn approximately to scale. Positive charges are placed at $(K + j\,0.430)$, $(K + j\,1.289)$ and $(K + j\,2.148)$; negative charges are placed at $(0.806 + j\,0.860)$ and $(0.806 + j\,K')$. Only positions of charges in

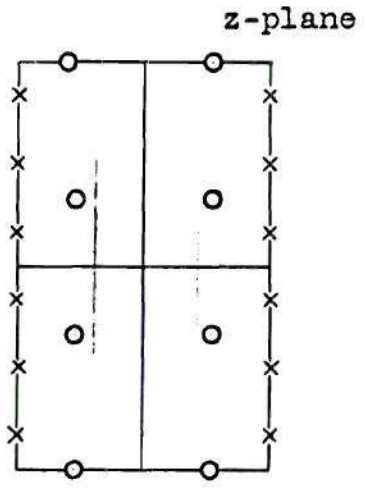

Fig. 39. Charges in one cell of the z-plane.

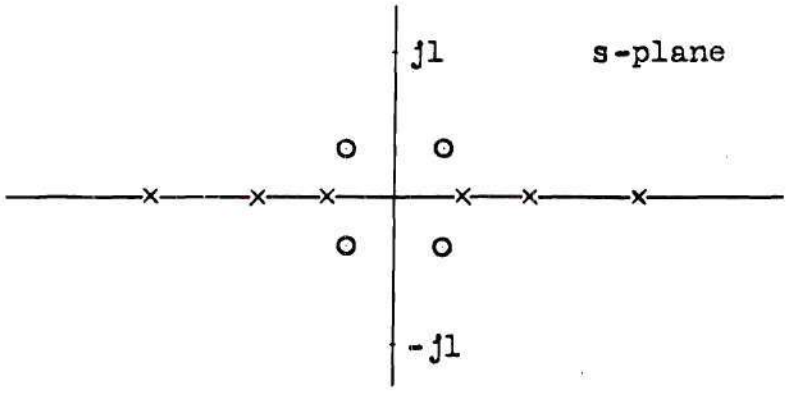

Fig. 40. Charges in the s-plane.

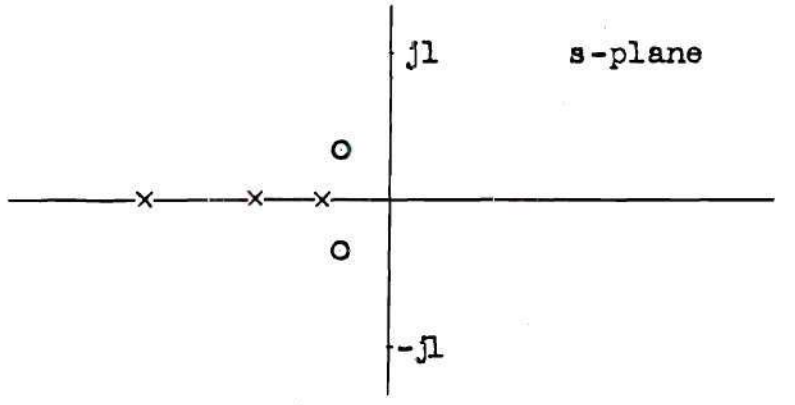

Fig. 41. Singularities of the final network.

the first quadrant are stated here since others can be located by symmetry.

Locations of these charges in the s-plane as well as in the intermediate w-plane are listed below:

	z-plane	w-plane	s-plane
Positive charge	K + j 0.430	1.083	0.252
Positive charge	K + j 1.289	1.780	0.439
Positive charge	K + j 2.148	2.915	0.876
Negative charge	0.806 + j 0.860	1.002 + j 0.639	0.224 + j 0.154
Negative charge	0.806 + j K'	4.425	∞

The transformation from the w-plane to the s-plane is

$$s = \frac{w}{\sqrt{4.425^2 - w^2}} .$$

Charges in the s-plane are shown in Fig. 40. As a final step, we discard all the charges in the right half-plane. The final transfer function should have singularities coinciding with charges in the left half-plane as illustrated in Fig. 41. Hence

$$T(s) = \frac{(s + 0.224 + j0.154)(s + 0.224 - j0.154)}{(s + 0.252)(s + 0.439)(s + 0.876)}$$

$$= \frac{s^2 + 0.448\, s + 0.074}{s^3 + 1.567\, s^2 + 0.716\, s + 0.097} .$$

A plot of $|T|^2$ along the imaginary axis based on the function given above is shown in Fig. 42 which displays the equal-ripple low-pass characteristic.

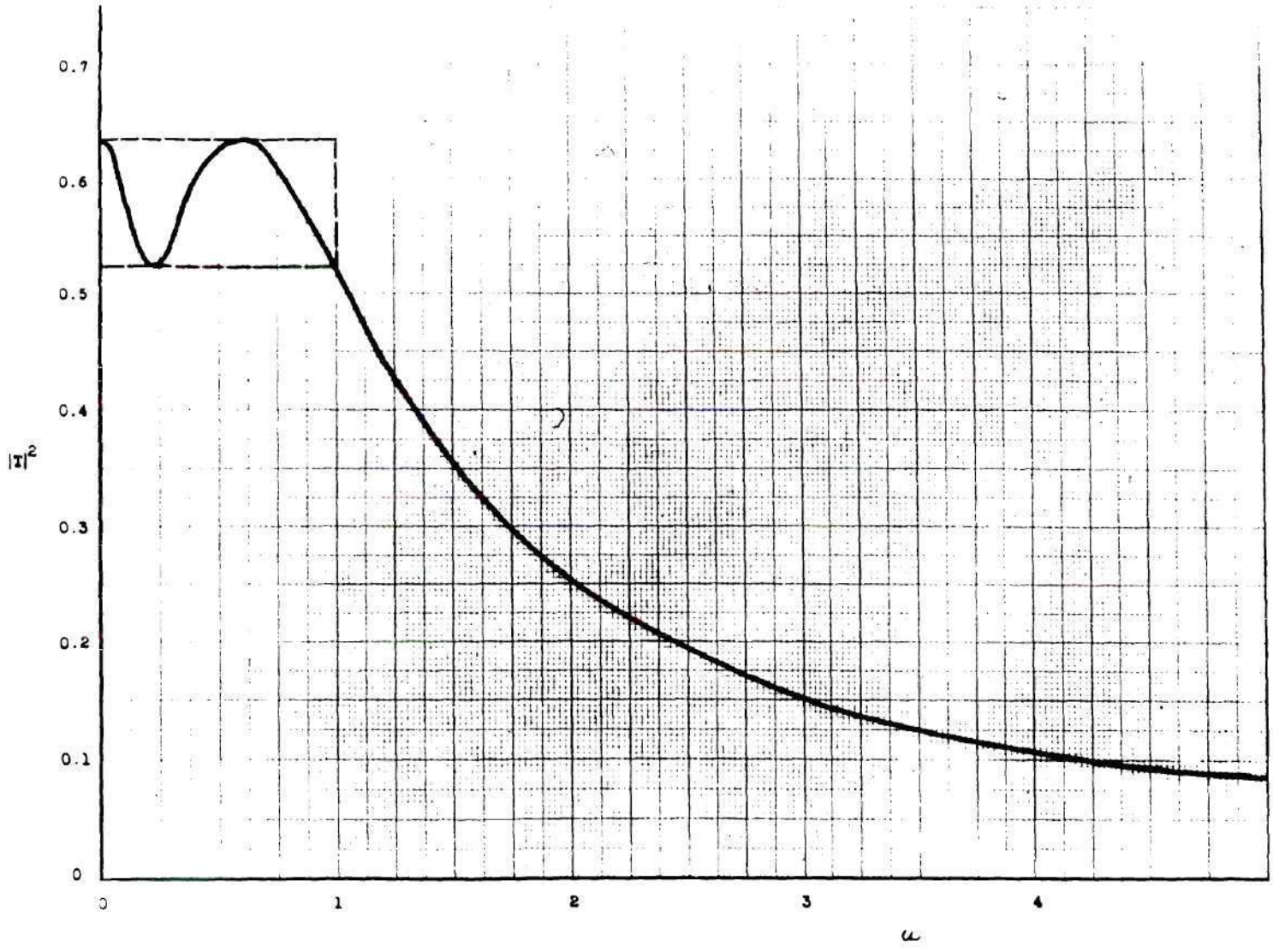

Fig. 42. Frequency characteristic for k = 0.3162, a = 0.5 and n =3.

Functions that have the desired singularities.--The potential due to charge arrangements of the type shown in Fig. 37 can be expressed in closed form. First let n be odd. Consider the function $sn^2(C_1 z, k_1)$ in the $C_1 z$-plane, where C_1 is a constant and k_1 is another modulus, both to be determined later. This function consists of an infinite number of horizontal rows of double zeros and double poles spaced K_1' apart along the $C_1 y$ direction. Zero and pole rows alternate with each other starting with one zero row passing through the origin. Within each row, poles or zeros are spaced $2K_1$ apart. Constant K_1 and K_1' are complete elliptical integrals of moduli k_1 and $k_1' = \sqrt{1 - k_1^2}$ respectively. This singularity arrangement is depicted in Fig. 43.

Zeros of the function $sn^2(C_1 z, k_1)$ can be shifted to any desired positions by adding a proper constant to it. In particular, the function

$$sn^2(C_1 z, k_1) - sn^2(aK_1 + j K_1', k_1) \tag{81}$$

obviously vanishes at $C_1 z = aK_1 + j K_1'$ and all its congruent points. Thus function (81) has the distribution of singularities as shown in Fig. 44. This process of shifting zeros does not affect the positions of poles.

Similarly, the function

$$sn^2(C_1 z, k_1) - sn^2\left(K_1 + j \frac{K_1'}{2}, k_1\right) \tag{82}$$

will have its zeros located at $K_1 + j \frac{K_1'}{2}$ and all its congruent points. Its singularities are depicted in Fig. 45.

Finally if function (82) is divided into function (81), the poles

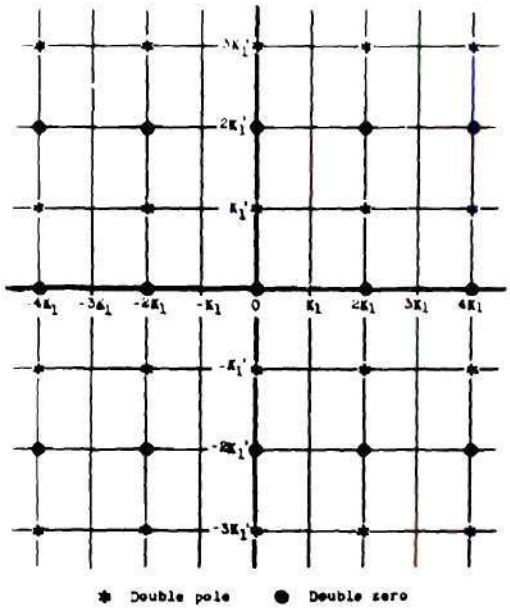

Fig. 43. Zeros and poles of the function $sn^2(C_1 z, k_1)$.

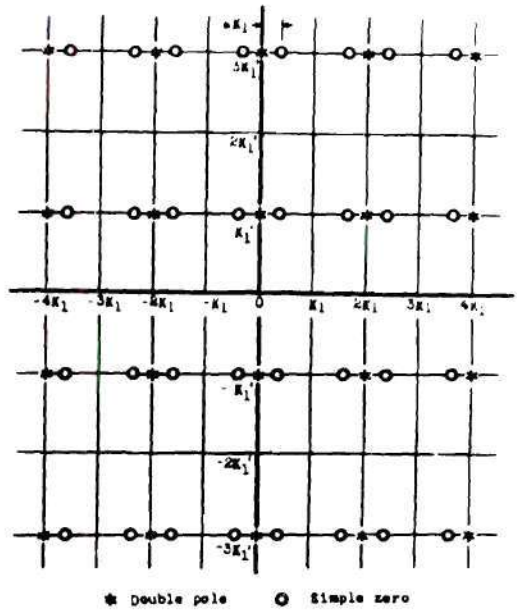

Fig. 44. Zeros and poles of function (81).

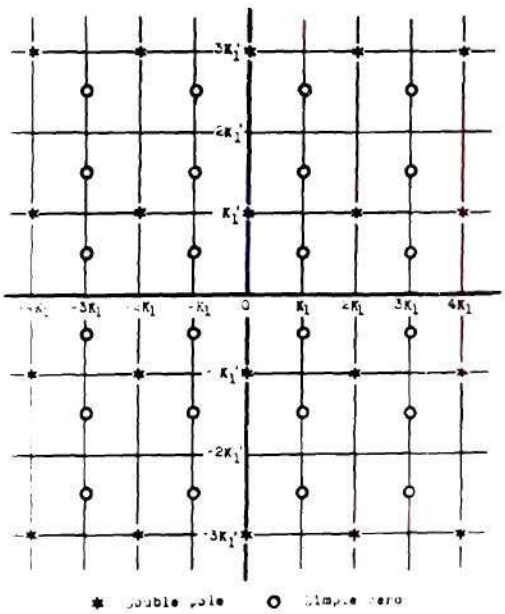

Fig. 45. Zeros and poles of function (82).

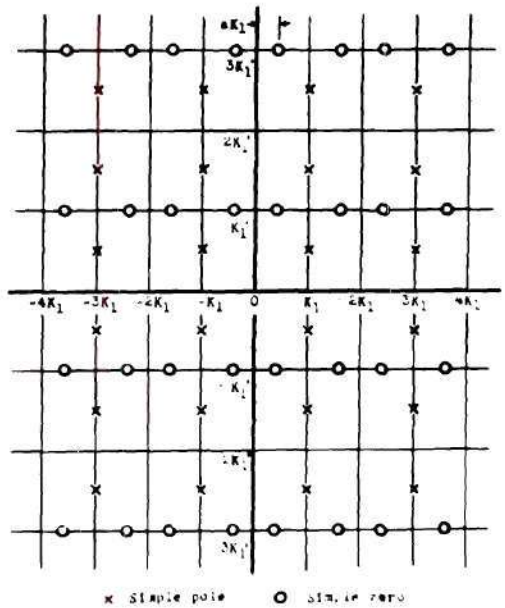

Fig. 46. Zeros and poles of function (84).

of function (82) will cancel with those of function (81), the zeros of function (82) become poles of this new function, and the zeros of function (81) are also zeros of this new function. Thus the function

$$\frac{sn^2(C_1 z,\ k_1) - sn^2(aK_1 + j\,K_1',\ k_1)}{sn^2(C_1 z,\ k_1) - sn^2(K_1 + j\,\frac{K_1'}{2},\ k_1)} \tag{83}$$

will have singularities as shown in Fig. 46. It is clear that this arrangement is similar to that in Fig. 37. Expression (83) may be reduced to

$$T\left[s(z)\right] T\left[-s(z)\right] = \frac{sn^2(C_1 z,\ k_1) - \frac{1}{k_1^2}\, ns^2(aK_1,\ k_1)}{sn^2(C_1 z,\ k_1) - \frac{1}{k_1}} . \tag{84}$$

In order to make equation (84) capable of representing the charge distribution in the z-plane k_1 must be so adjusted that the dimension of n cells of modulus k_1 in the $C_1 z$-plane is proportional to one cell of modulus k in the z-plane, and C_1 be so adjusted that those two cells are identical. Thus

$$\frac{nK_1'}{K_1} = \frac{K'}{K}, \tag{85}$$

and

$$\frac{K_1}{C_1} = K.$$

This adjustment of k_1 and C_1 is illustrated by Fig. 47.

For a given k (and thus K and K') and n, the new modulus k_1 can be found by its nome q_1, which in turn is given by

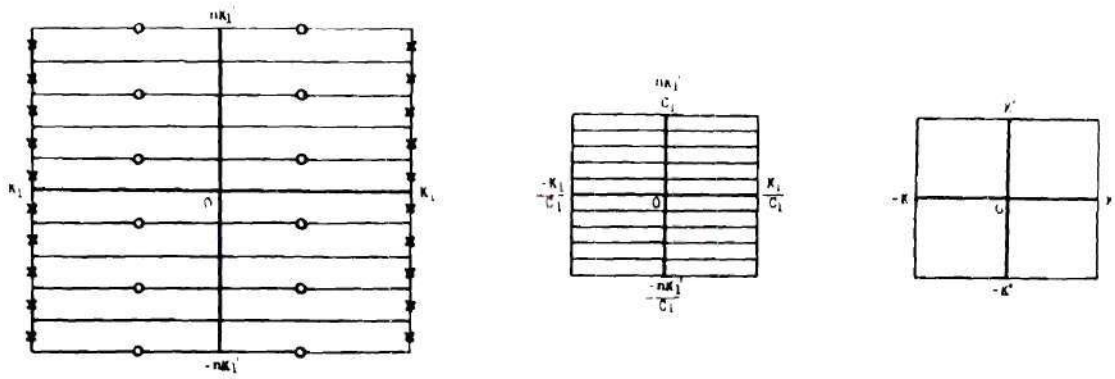

Fig. 47. A number of cells of modulus k_1 reduced to coincide with a single cell of modulus k.

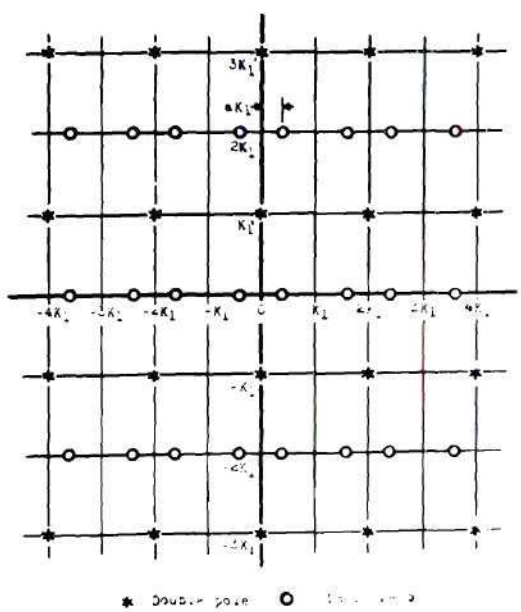

Fig. 48. Zeros and poles of function (88).

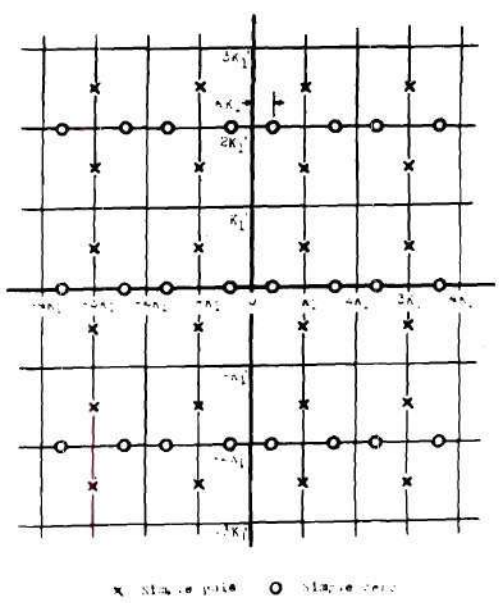

Fig. 49. Zeros and poles of function (90).

$$q_1 = e^{-\frac{K_1'}{K_1}} = e^{-\frac{K'}{nK}} \tag{87}$$

Knowing q_1, k_1 may be either calculated by infinite series or found from a table.

When n is even, it is necessary to place one zero on the real axis. Therefore the function representing it is slightly different. Expression (82) need not be changed since whether n is even or odd poles are all equally spaced about the real axis and no poles may be placed on it. Expression (81), however, must be modified to read

$$sn^2(C_1 z, k_1) - sn^2(aK_1, k_1). \tag{88}$$

This places one zero on the real axis. The singularities of function (88) are shown in Fig. 48. When function (82) is divided into function (88), the new function

$$\frac{sn^2(C_1 z, k_1) - sn^2(aK_1, k_1)}{sn^2(C_1 z, k_1) - sn^2(K_1 + j\frac{K_1'}{2}, k_1)} \tag{89}$$

will have singularities as shown in Fig. 49. Function (89) may be simplified to read

$$T[s(z)]\,T[-s(z)] = \frac{sn^2(C_1 z, k_1) - sn^2(aK_1, k_1)}{sn^2(C_1 z, k_1) - \frac{1}{k_1}} \cdot \tag{90}$$

Tolerance and attenuation outside the pass band.—Consider the case when n is odd. In equation (84), the first term in both the numerator and the denominator, $sn^2(C_1 z, k_1)$, is negative along the imaginary

axis, and is increasing numerically from zero to infinity as $C_1 z$ is increased from zero to jK_1'. The second term in the numerator is always greater than the second term in the denominator, or

$$\frac{1}{k_1^2 \ sn^2(aK_1)} > \frac{1}{k_1}, \tag{91}$$

since $sn(aK_1) \leq 1$. Therefore $|T|^2$ is monotonically decreasing along the imaginary axis as $C_1 z$ is increased from zero to jK_1'. The potential along the remainder of the axis will merely be the repetitions of this variation.

It follows that maxima occur at every point $2mK_1'$ from the origin, where m is any integer, and minima occur at every point midway between two maxima. Therefore the maximum potential along the imaginary axis is

$$|T|^2_{max} = |T|^2_o = \frac{1}{k_1 \ sn^2(aK_1)} \tag{92}$$

and the minimum is

$$|T|^2_{min} = |T|^2_{jK'} = 1. \tag{93}$$

Hence,

$$\text{Tolerance} = \varepsilon = 20 \log\left[\frac{|T|_{max}}{|T|_{min}}\right] = 10 \log\left[\frac{1}{k_1 sn^2(aK_1)}\right]. \tag{94}$$

When n is even, the charge arrangement is in essence the same as when n is odd. The only difference is that in one case charges are shifted in the vertical direction by an amount equal to K_1' from the other. Therefore for even n the minimum points are located at the origin and points

$2mK_1'$ away from it, while maximum points are located at points like jK_1'. From equation (90) we have

$$|T|^2_{max} = |T|^2_{jK'} = 1 \tag{95}$$

and

$$|T|^2_{min} = |T|^2_{o} = k_1 \, sn^2(aK_1, k_1). \tag{96}$$

Hence

$$\text{Tolerance} = \varepsilon = 20 \log\left[\frac{|T|_{max}}{|T|_{min}}\right] = 10 \log\left[\frac{1}{k_1 \, sn^2(aK_1', k_1)}\right] \tag{97}$$

which is the same as equation (94).

If it is desired to find the attenuation at a certain point outside the pass band, it is first necessary to locate its corresponding point in the z-plane. Let the frequency in question be ω_2. Then

$$j\omega_2 = \frac{w_2}{\sqrt{\frac{1}{k^2 \, sn^2(aK, k)} - w_2^2}} .$$

Square both sides and put $w_2 = sn \, z_2$, to obtain

$$-\omega_2^2 = \frac{sn^2(z_2)}{\frac{1}{k^2 \, sn^2(aK, k)} - sn^2(z_2)}$$

and solve for $sn(z_2)$. Thus,

$$sn^2(z_2) = \frac{\omega_2^2}{(\omega_2^2 - 1) \, k^2 \, sn^2(aK, k)} \tag{98}$$

Let $z_2 = j \, K' + bK$; then

$$\text{sn}\ (z_2) = \text{sn}\ (jK' + bK) = \frac{1}{k}\,\text{ns}\ (bK).$$

Substitute this expression for $\text{sn}(z_2)$ into equation (98):

$$\text{sn}\ (bK) = \frac{\sqrt{\omega_2^2 - 1}}{\omega_2}\ \text{sn}\ (aK). \tag{99}$$

From this equation b can be found. Substitution of $C_1 z_2 = bK_1 + jK_1'$ into equation (84) or (90) gives the attenuation at ω_2.

As an illustrative example let it be desired to find the magnitude of $|T|^2$ at $\omega_2 = 2$ for the numerical example of Fig. 41, in which

$$k^2 = 0.1, \qquad a = 0.5, \qquad n = 3, \qquad K = 1.6124, \qquad K' = 2.5781.$$

It is found that

$$q_1 = e^{-\frac{K'}{nK}} = 0.1873$$

and

$$k_1 = 0.9782.$$

Since

$$\text{sn}\left(\frac{K}{2}\right) = \frac{1}{\sqrt{1 + k'}},$$

we have

$$\text{sn}\ (aK) = \text{sn}\ (0.5K) = \frac{1}{\sqrt{1 + 0.9487}} = 0.7162.$$

Thus

$$\text{sn}\ (bK) = 0.6202,$$

and

$$b = \frac{37.62^\circ}{90^\circ} = 0.418$$

from a table.

So

$$sn^2(C_1 z_2, k_1) = \frac{1}{k_1^2\, sn^2(bK_1, k_1)} = 1.4399.$$

In equation (84)

$$\frac{1}{k_1^2\, sn^2(aK_1, k_1)} = 1.2625$$

and

$$\frac{1}{k_1} = 1.0223.$$

Hence

$$|T|^2_{j2} = \frac{1.4399 - 1.2625}{1.4399 - 1.0223} = \frac{0.1774}{0.4176} = 0.425.$$

From equation (94)

$$|T|^2_{max} = \frac{1}{k_1\ sn^2(aK_1, k_1)} = 1.235.$$

Thus

$$\frac{|T|^2_{j2}}{|T|^2_{max}} = \frac{0.425}{1.235} = 0.344.$$

Also, from the network function

$$T(s) = \frac{s^2 + 0.448\ s + 0.074}{s^3 + 1.567\ s^2 + 0.716\ s + 0.097}$$

we have

$$|T|^2_{j2} = 0.200$$

and

$$|T|^2_{max} = |T|^2_o = 0.582.$$

So

$$\frac{|T|^2_{j2}}{|T|^2_{max}} = \frac{0.200}{0.582} = 0.344$$

which agrees with our previous calculation.

Selection of the modulus k.--At this point a question may be raised: What value of k should be taken for the transformation from the s-plane to the w-plane? This question can best be answered by investigating effects of changing the value of k.

For a given value of k, and thus K and K', except for very low tolerance, there exists a corresponding value of a that gives the specified tolerance inside the pass band. Therefore k is not a controlling factor over the tolerance. If there are two values of k, and the a's in both cases are so adjusted that the tolerances are the same, although their maxima and minima occur at different values of ω in the s-plane, they have the same maximum and minimum values as well as the same band edge. What may be affected by the different values of k is the part of the characteristic that is outside the pass band. But this effect is expected to be very slight. This may be inferred by observing that despite the fact that two rectangles may have different proportions, the variation of potential along that portion of the upper horizontal side of a cell corresponding to p-q in Fig. 33, for two values of k, do not differ from each other materially since the charge arrangements are similar in both cases and any discrepancy will be of only second order.

Fig. 50 gives the attenuation at $\omega = 2$ for different tolerances for $n = 3$ when k is allowed to assume two extreme values. The difference

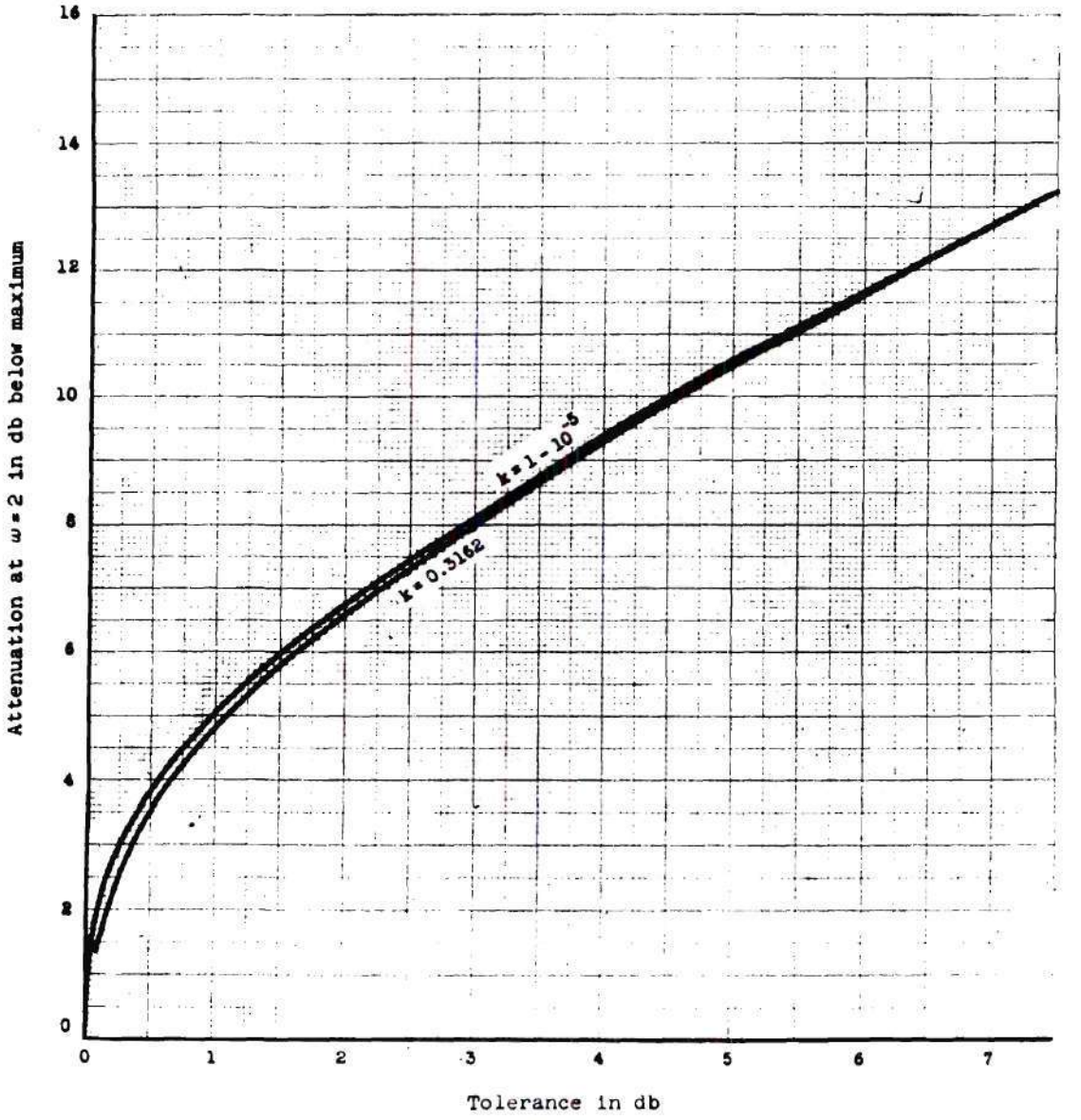

Fig. 50. Attenuation at $\omega = 2$ for different tolerance for $k = 0.3162$ and $k = 1 - 10^{-5}$, $n = 3$.

is so little that the slight improvement in the steepness outside the pass band hardly justifies the use of high value of k which will lead to inconvenient element values.

As was shown in Fig. 33, the region in which we place poles is that part of real axis between k sd(aK) and sc(aK). As k is increased both of these quantities approach unity. The result of this is that all poles will jam into a very narrow region in the neighborhood of s = 1 in the s-plane, which will require elements of extreme sizes in the final network.

When k is very small, k sd(aK) approaches k sin $\frac{a\pi}{2}$ and sc(aK) approaches tan $\frac{a\pi}{2}$. Thus one value may approach zero while the other may become unreasonably large. Poles which lie somewhere between these two points may be scattered very far apart in ratios which also result in inconvenient element sizes.

Thus the choice of the value of k is the one that will scatter the poles in a nearly uniform manner. One can not really pin down a single value of k which is indisputably superior to all others since pole distribution is basically somewhat arbitrary for R-C transfer function. As an example, a value of k^2 equal to 0.1 renders reasonable pole distributions for almost all values of a.

Selection of n.--Increasing n increases the number of cells that are to be included in one rectangle which is to be transformed into the entire s-plane. This reduces the height of each cell, which is also what happens when k is increased. Therefore, so far as the geometry in the C_1z-plane is concerned, the effect of changing n is similar to that of changing k, except that n can only be an integer.

It follows that if two sets of values of n and k are adjusted so they have similarly proportioned cells in the C_1z-plane, the value of a for a particular tolerance will also be the same in both instances. The set with higher value of n (lower k) will have its final rectangle, which is to be transformed into the entire s-plane, relatively, higher than the one with lower n. But for the set with a smaller k, b will be larger for the same ω_2. This means the point in the z-plane which corresponds to $\omega=\omega_2$ lies farther away from the imaginary axis when n is larger. This gives rise to an additional increase in steepness outside the pass band aside from that due to reproportioning the cells in the C_1z-plane by using a higher k alone as was discussed in the previous section. Therefore increasing n improves the steepness outside the pass band to a greater extent, although still slight, than increasing k. The price is paid of a greater number of elements. Fig. 51 is a plot of attenuation at $\omega = 2$ for $n = 3$ and $n = 20$ when $k^2 = 0.1$.

It is clear that the improvement of the low-pass characteristic obtained by increasing n is still so little that it hardly seems worth the price we pay in additional elements. However, there is another consequence due to increasing n, and that is the relative bandwidth. Fig. 52 shows the arrangement of poles for n equal to 1, 3 and 5 while the proportion of cells are maintained to be the same. If these rectangles are drawn so they all have the same width, it is clear that the portion that is to be mapped into the pass-band increases as n is increased, while the portion that is to be mapped into non-pass band region remains unchanged. Thus it is expected that relative band width is increased when n is made larger.

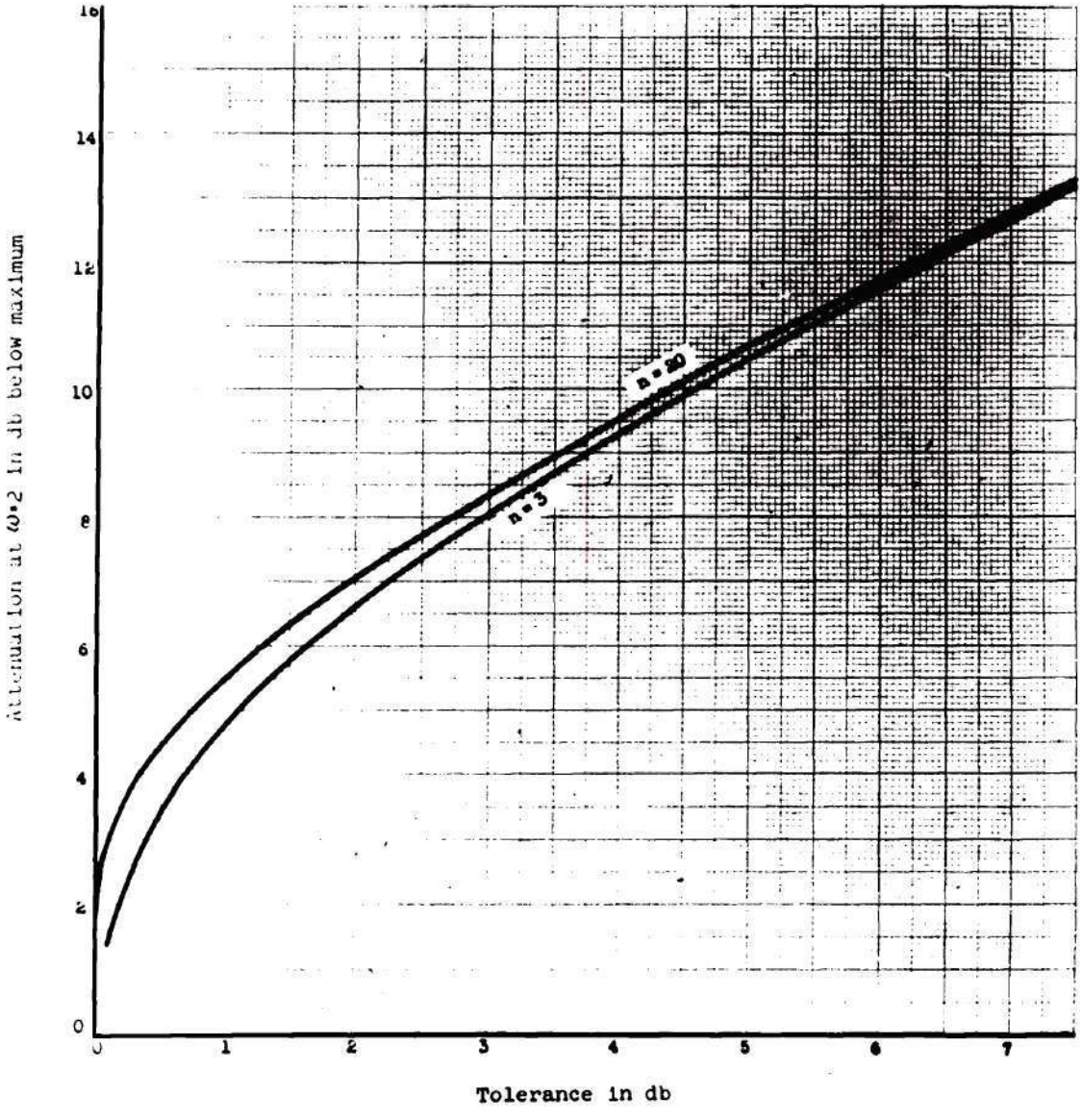

Fig. 51. Attenuation at $\omega = 2$ for different tolerance for $n = 3$ and $n = 20$, $k^2 = 0.1$.

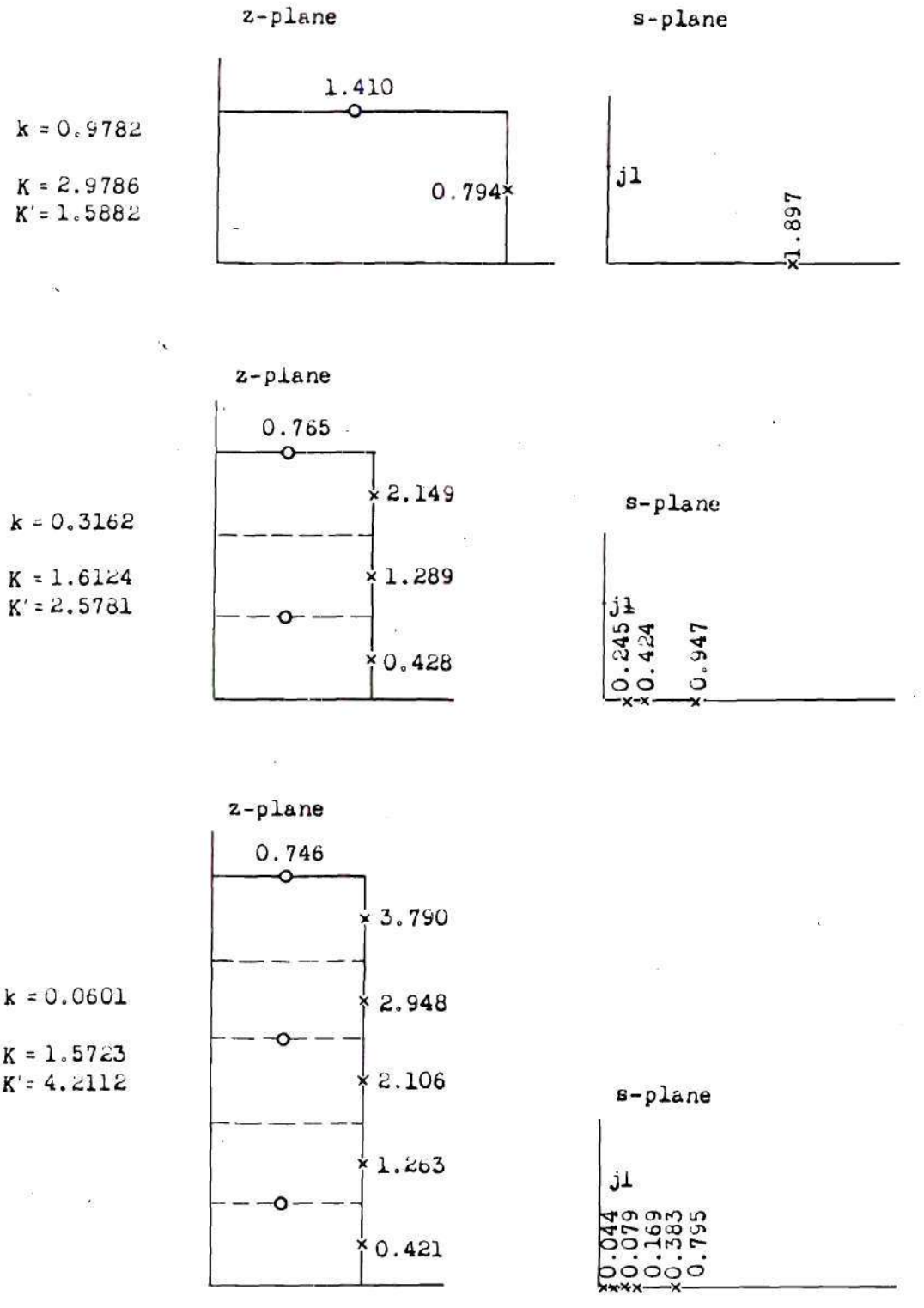

Fig. 52. Effect of the value of n on the distance of poles from the imaginary axis.

Since the bandwidth is normalized to be unity in this treatment, an increase in relative bandwidth is equivalent to a movement of poles toward the imaginary axis. This is illustrated by the example given in Fig. 52.

Networks Employing Two Rows of Zeros in the z-plane

The method used in the last section employs a single row of zeros parallel to the uniformly spaced row of poles in the z-plane. The ability and potentiality of such an arrangement have been studied.

One common method of improving the cut-off characteristic of R-C low pass networks is to place zeros along the real frequency axis. The use of this device and of the elliptic-function transformation yield the following charge arrangements.

Charge arrangement in the z-plane.—In Fig. 53(a) is shown a quarter of a rectangle which is finally to be mapped onto the entire s-plane. The charge arrangement in this figure is of the type used in the last section. This arrangement will be modified such that a zero will eventually be placed on the imaginary axis. The mapping geometry will be kept unchanged. Region a-e will still be the pass band, region h-f the region where poles are allowed to lie and point q the point at infinity.

If it is desired to place a zero along the $j\omega$ -axis in the s-plane, a negative charge must be placed between a and q, say cK from point a. This is shown in Fig. 53(b). Accompanying the addition of this zero it is desirable to bring in also the rest of the complete row of zeros parallel to a-e which includes the zero at $z = cK + jK'$.

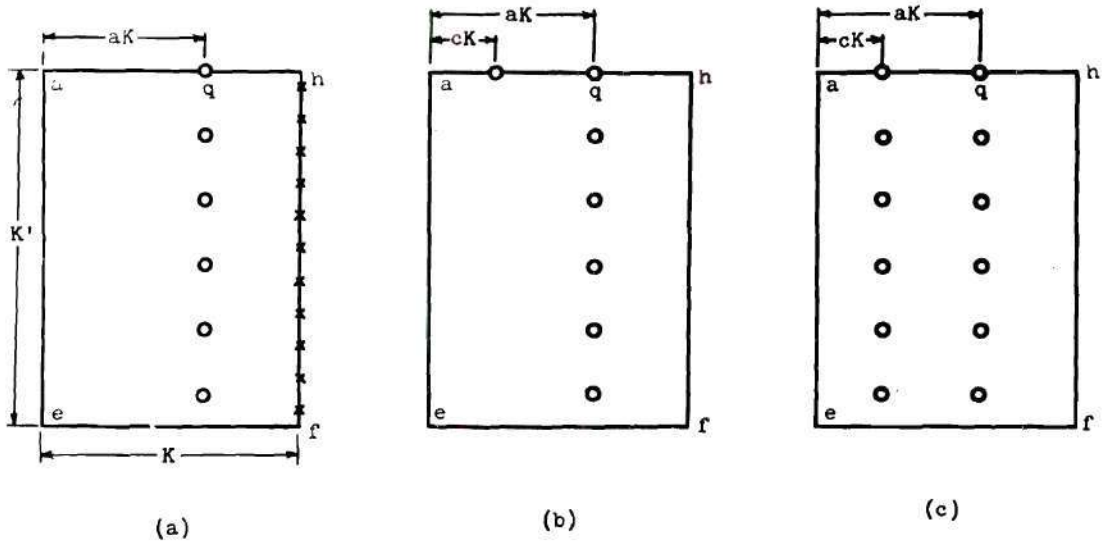

Fig. 53. Charge arrangements in the C_1z-plane.

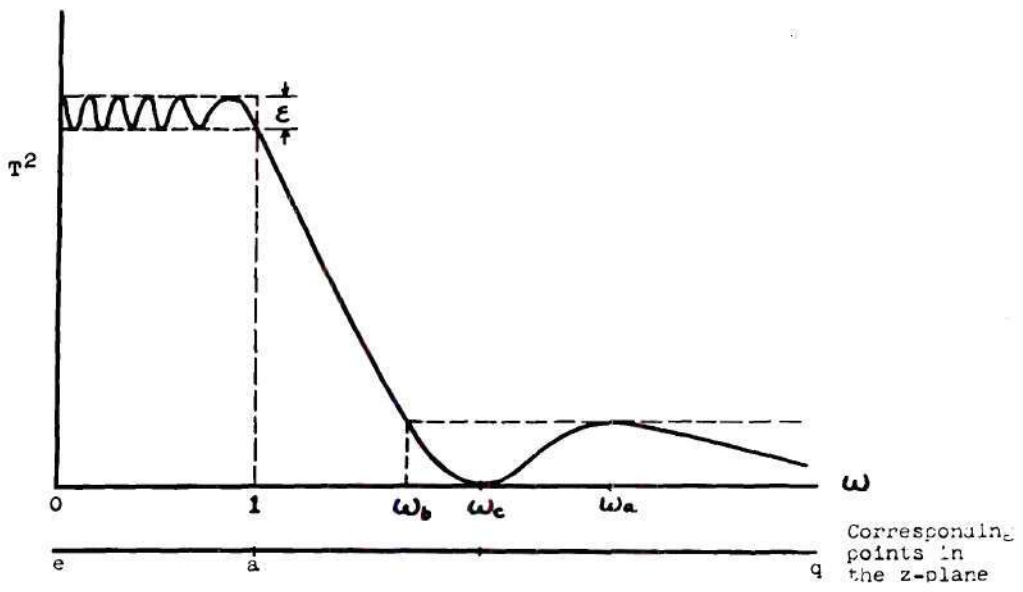

Fig. 54. Typical frequency characteristic employing charge arrangements of the type shown in Fig. 53.

The reasons for bringing in a complete row of zeros are: (1) The addition of a zero alone upsets the equal-ripple characteristic along a-e; (2) The usefulness of the elliptical-function transformation depends mostly on our being able to write the potential function in reasonably simple closed form. As was seen in the last section this, in turn, depends on the possibility of dividing the rectangle into several smaller rectangles with identical charge content.

Thus the desired arrangement should be as illustrated in Fig. 53(c). The frequency characteristic of R-C networks based on this type of charge arrangement will take the general form shown in Fig. 54. As before, pass-band angular frequency is normalized to be unity. Point ω_b, beyond which $|T|^2$ does not exceed a certain magnitude, may be defined as the lower bound of the stop-band. Definitions of other quantities are self-evident from the figure.

Functions with desired singularities.--To write a function that will yield singularities coinciding with charges in Fig. 53(c), for $n/2$ odd, consider the following functions:

$$sn^2(C_1 z, k_1) - sn^2(aK_1 + jK_1', k_1) \tag{100}$$

$$sn^2(C_1 z, k_1) - sn^2(cK_1 + jK_1', k_1) \tag{101}$$

$$sn^2(C_1 z, k_1) - sn^2\left(K_1 + j\frac{K_1'}{4}, k_1\right) \tag{102}$$

$$sn^2(C_1 z, k_1) - sn^2\left(K_1 + j\frac{3K_1'}{4}, k_1\right) \tag{103}$$

Their singularities are depicted in Fig. 55. For each function only a part of the first quadrant is shown.

Thus the function

$$\frac{\left[sn^2(C_1z,k_1)-sn^2(aK_1+jK_1',k_1)\right]\left[sn^2(C_1z,k_1)-sn^2(cK_1+jK_1',k_1)\right]}{\left[sn^2(C_1z,k_1)-sn^2(K_1+j\frac{K_1'}{4},k_1)\right]\left[sn^2(C_1z,k_1)-sn^2(K_1+j\frac{3K_1'}{4},k_1)\right]} \tag{104}$$

will have singularities as shown in Fig. 56.

Finally, if the modulus k_1, whose quarter periods are K_1 and K_1', and C_1 are so adjusted that $n/2$ cells of modulus k_1 are included in one cell of modulus k which is to be mapped onto the entire s-plane, or

$$\frac{nK_1'}{2K_1}=\frac{K'}{K} \quad \text{and} \quad \frac{K_1}{C_1}=K, \tag{105}$$

function (104) will be the sought-for expression.

Pass-band tolerance and stop-band attenuation.--Function (104) may be written as

$$T(s)T(-s) = \frac{sn^2(C_1z,\,k_1)-\dfrac{1}{k_1^2sn^2(aK_1,\,k_1)}}{sn^2(C_1z,\,k_1)-\dfrac{1}{dn^2(\frac{K_1'}{4},\,k_1')}} \times \frac{sn^2(C_1z,\,k_1)-\dfrac{1}{k_1^2sn^2(aK_1,\,k_1)}}{sn^2(C_1z,\,k_1)-\dfrac{1}{dn^2(\frac{3K_1'}{4},\,k')}} \tag{106}$$

The maximum of this function along the $j\omega$-axis occurs when $s=0$, where $sn(C_1z,\,k_1)=0$. Hence,

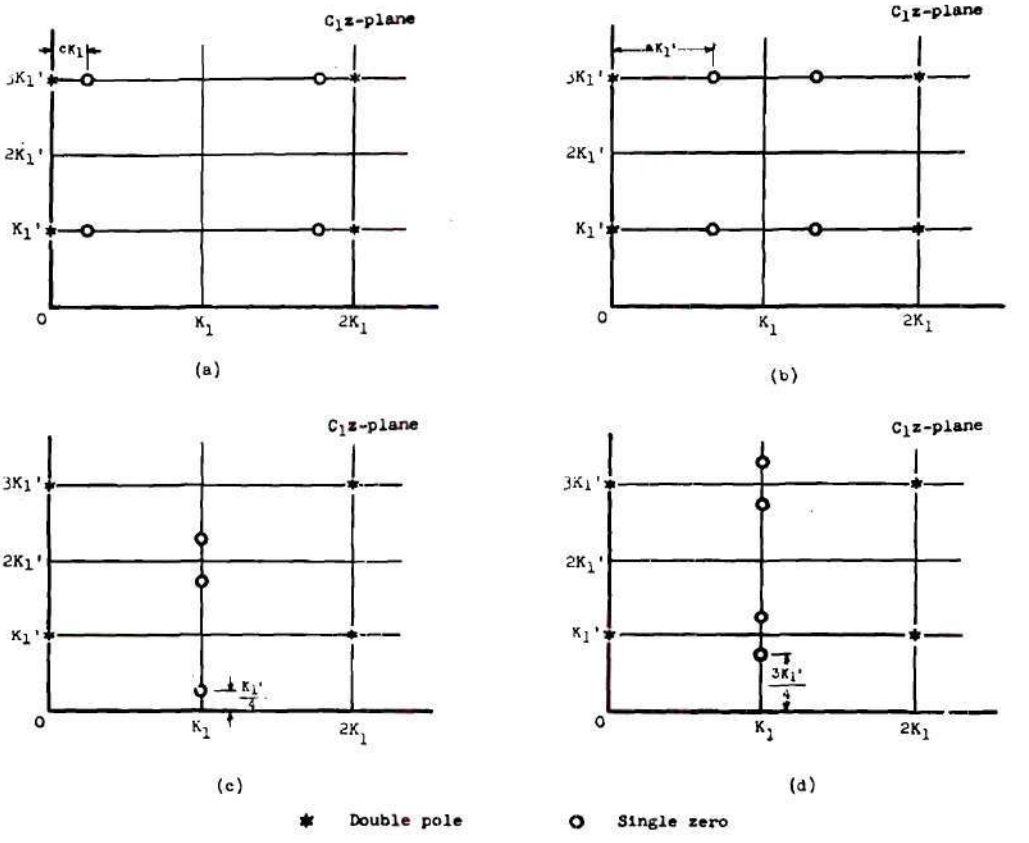

Fig. 55. Zeros and poles of functions (100) to (103).

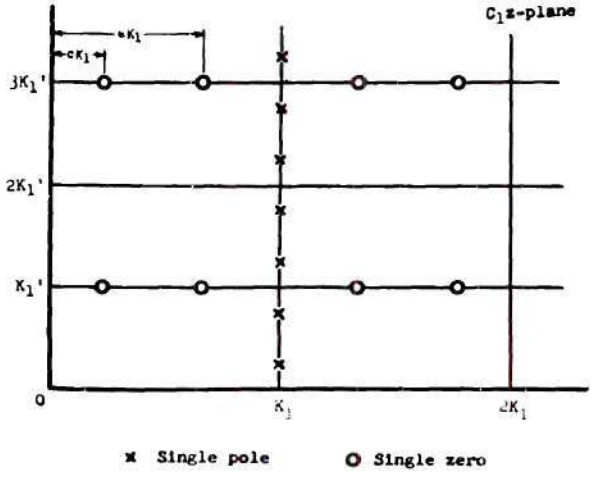

Fig. 56. Zeros and poles of function (104).

$$|T|^2_{max} = \frac{dn^2(\frac{K_1'}{4}, k_1')\ dn^2(\frac{3K_1'}{4}, k_1')}{k_1^4\ sn^2(aK_1, k_1)\ sn^2(cK_1, k_1)}. \tag{107}$$

Its minimum occurs when $C_1 z = jmK_1'$, where m is any odd integer, at which $sn^2(C_1 z, k_1) = \infty$. Hence

$$|T|^2_{min} = 1. \tag{108}$$

Thus

$$\text{Tolerance} = \varepsilon = 20 \log \frac{|T|_{max}}{|T|_{min}}$$

$$= 10 \log \left[\frac{dn^2(\frac{K_1'}{4}, k_1')\ dn^2(\frac{3K_1'}{4}, k_1')}{k_1^4\ sn^2(aK_1, k_1)\ sn^2(cK_1, k_1)} \right] \tag{109}$$

for odd $n/2$.

A similar analysis for even $n/2$ gives

$$T(s)T(-s) = \frac{sn^2(C_1 z, k_1) - sn^2(aK_1, k_1)}{sn^2(C_1 z, k_1) - \frac{1}{dn^2(\frac{K_1'}{4}, k')}}$$

$$\times \frac{sn^2(C_1 z, k_1) - sn^2(cK_1, k_1)}{sn^2(C_1 z, k_1) - \frac{1}{dn^2(\frac{3K_1'}{4}, k_1')}} \tag{110}$$

and

$$\text{Tolerance} = \varepsilon$$

$$= 10 \log \left[\frac{1}{sn^2(aK_1, k_1)\ sn^2(cK_1, k_1)\ dn^2(\frac{K_1'}{4}, k_1')\ dn^2(\frac{3K_1'}{4}, k_1')} \right]. \tag{111}$$

Now if it is desired to calculate the attenuation at any particular point, ω_x, outside the pass band, let the corresponding point in the C_1z-plane of this point be xK_1 from point a, Fig. 53, along a-q. Substitute $C_1z = xK_1 + jK_1'$ into equation (106),

$$T(s)T(-s) = \frac{\dfrac{1}{k_1^2\,sn^2(xK_1,\,k_1)} - \dfrac{1}{k_1^2\,sn^2(aK_1,\,k_1)}}{\dfrac{1}{k_1^2\,sn^2(xK_1,\,k_1)} - \dfrac{1}{dn^2(\frac{K_1'}{4},\,k_1')}}$$

$$\times \frac{\dfrac{1}{k_1^2\,sn^2(xK_1,\,k_1)} - \dfrac{1}{k_1^2 sn^2(cK_1,\,k_1)}}{\dfrac{1}{k_1^2\,sn^2(xK_1,\,k_1)} - \dfrac{1}{dn^2(\frac{3K_1'}{4},\,k_1')}}$$

$$= \frac{dn^2(\frac{K_1'}{4},\,k_1')\,dn^2(\frac{3K_1'}{4},\,k_1')}{k_1^4\,sn^2(aK_1,\,k_1)\,sn^2(cK_1,\,k_1)}$$

$$\times \frac{sn^2(xK_1,\,k_1) - sn^2(aK_1,\,k_1)}{sn^2(xK_1,\,k_1) - \frac{1}{k_1^2}\,dn^2(\frac{K_1'}{4},\,k_1')}$$

$$\times \frac{sn^2(xK_1,\,k_1) - sn^2(cK_1,\,k_1)}{sn^2(xK_1,\,k_1) - \frac{1}{k_1^2}\,dn^2(\frac{3K_1'}{4},\,k_1')}\,.$$

Hence

$$\frac{|T|^2_x}{|T|^2_{max}} = \frac{\left[sn^2(xK_1,k_1) - sn^2(aK_1,k_1)\right]\left[sn^2(xK_1,k_1) - sn^2(cK_1,k_1)\right]}{\left[sn^2(xK_1,k_1) - \frac{1}{k_1^2}dn^2(\frac{K_1'}{4},k_1')\right]\left[sn^2(xK_1,k_1) - \frac{1}{k_1^2}dn^2(\frac{3K_1'}{4},k_1')\right]}\,. \quad (112)$$

With quantities a and c given, function (112) is the ratio of two quadratics in $sn^2(xK_1,k_1)$. This makes the investigation of the behavior of the portion of the response characteristic outside the pass band very simple. In particular, ω_a can be located by differentiating (112) with respect to $sn^2(xK_1,k_1)$. After setting the derivative equal to zero and solving for $sn^2(xK_1,k_1)$, the argument xK_1 is the distance from point a to the point that corresponds to $s = j\omega_a$ in the s-plane. By the same token ω_b can be located by equating (112) to maximum found at ω_a and solving for $sn^2(xK_1,k_1)$. The argument xK_1 now gives the distance from a to the point that corresponds to the point $s=j\omega_b$ in the s-plane.

Design data and considerations.--By the same reasoning given in the end of the last section it may be inferred that, by the use of this type of charge arrangement, the number of poles, n, has only very slight effect on the cut-off characteristic. This is specially true when n is not small. Therefore an investigation of a particular set of n positive and n negative charges will give a good indication of the quality of this type network.

For a fixed pass-band tolerance the two rows of zeros may assume different relative positions, provided they satisfy certain conditions. From equation (109), for any value of a that lies within a certain limit, there exists a corresponding value of c which will give the same tolerance. However, the stop band attenuation and ω_b will be different for each set of different values of a and c.

Therefore, for certain pass-band tolerances some precalculated data about their stop-band attenuation and ω_b will be very informative. Figs. 57, 58, 59 and 60 are plots of stop-band attenuation, ω_c and c for

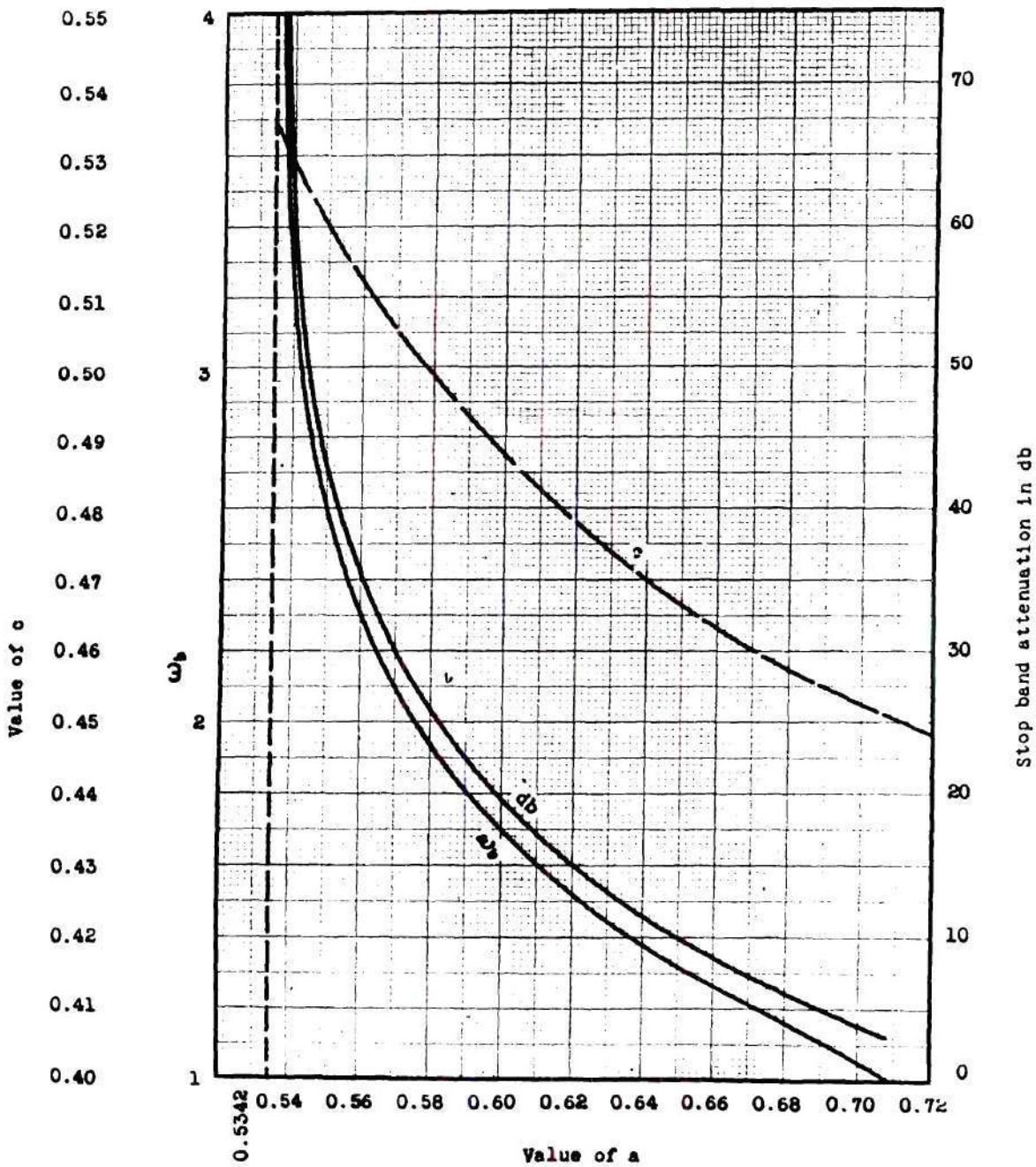

Fig. 57. Stop-band attenuation and ω_b for pass-band tolerance of 3 db, n = 6 and $k^2 = 0.1$.

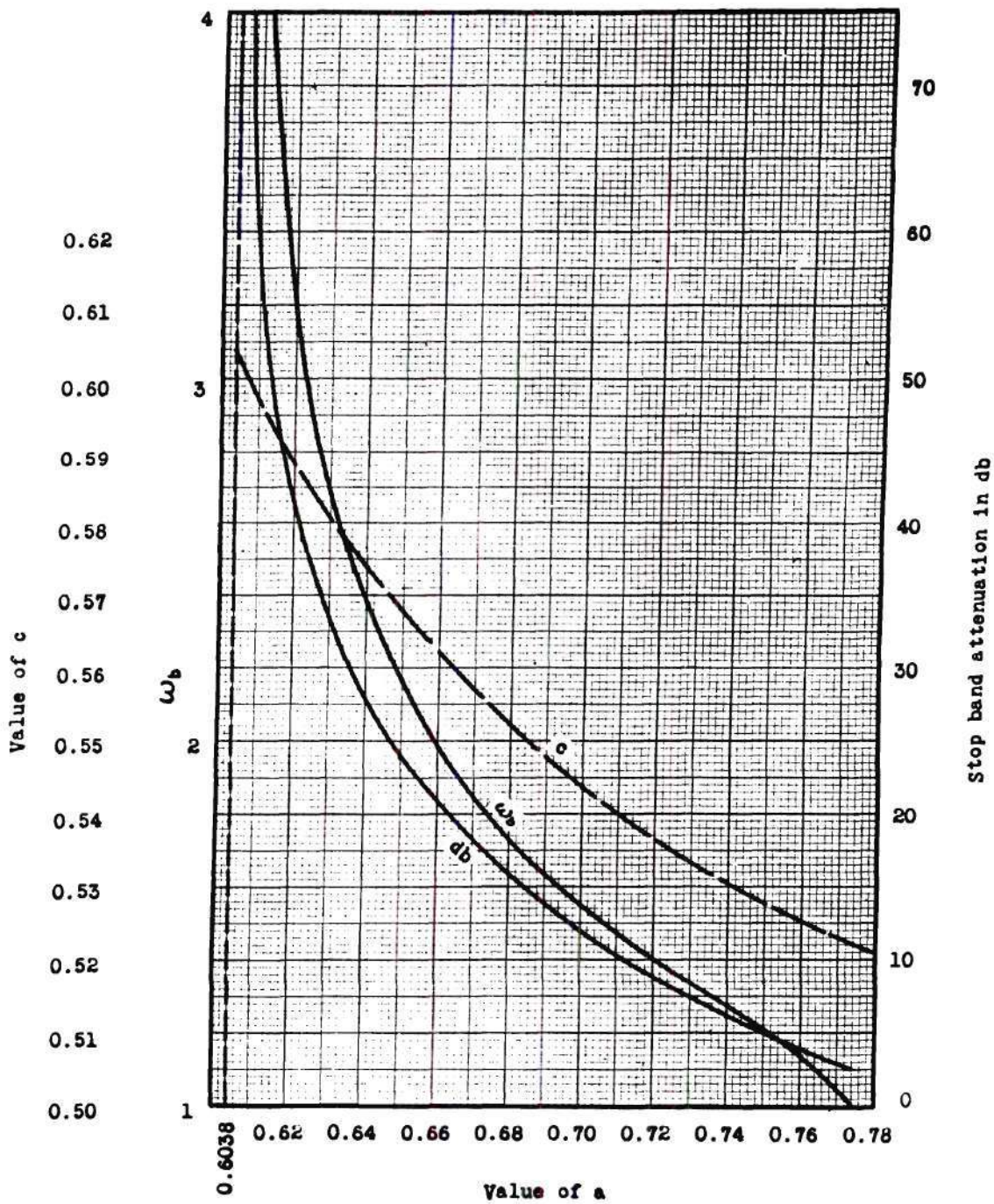

Fig. 58. Stop-band attenuation and ω_b for pass-band tolerance of 2 db, n = 6 and $k^2 = 0.1$.

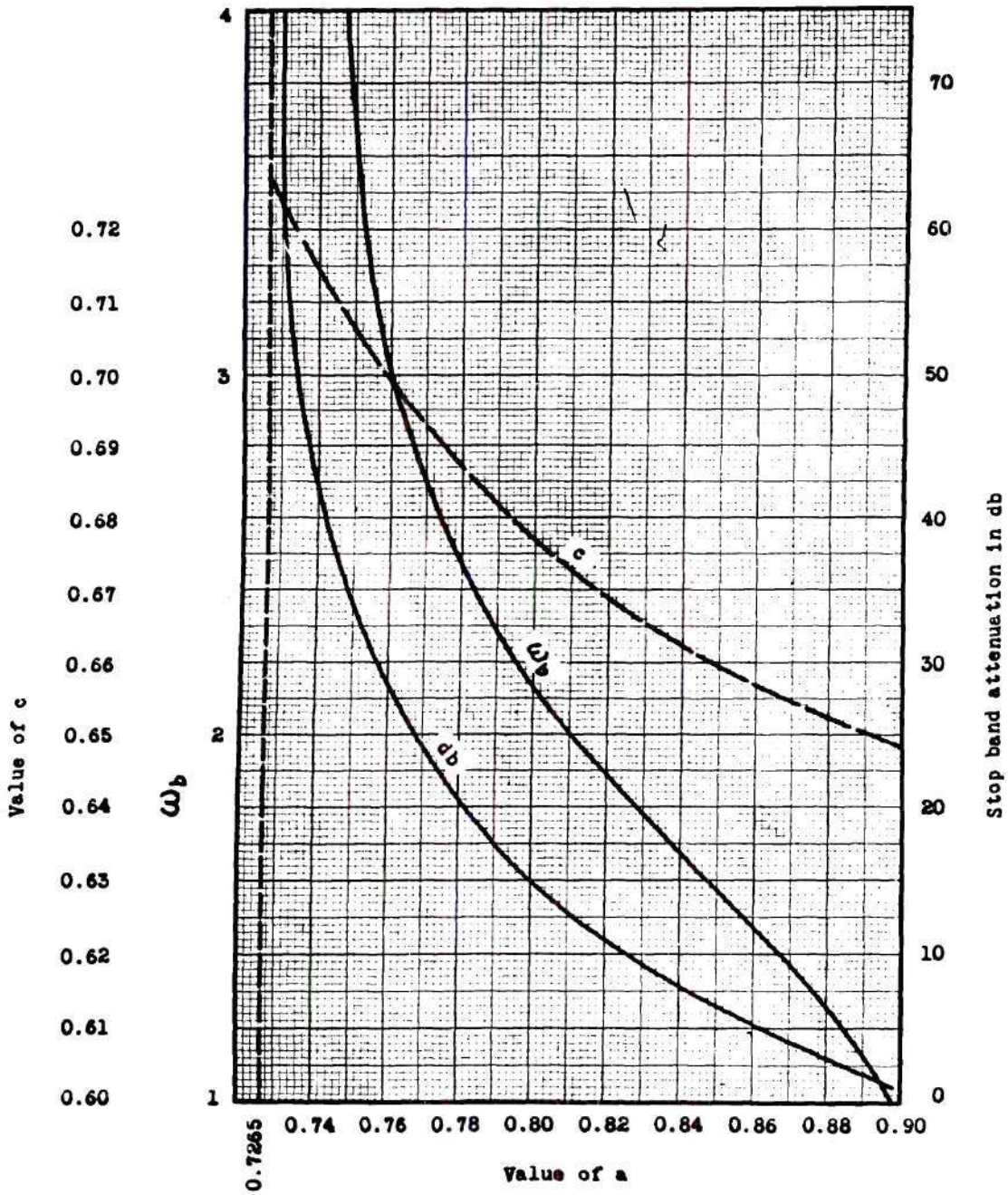

Fig. 59. Stop-band attenuation and ω_b for pass-band tolerance of 1 db, n= 6 and $k^2 = 0.1$.

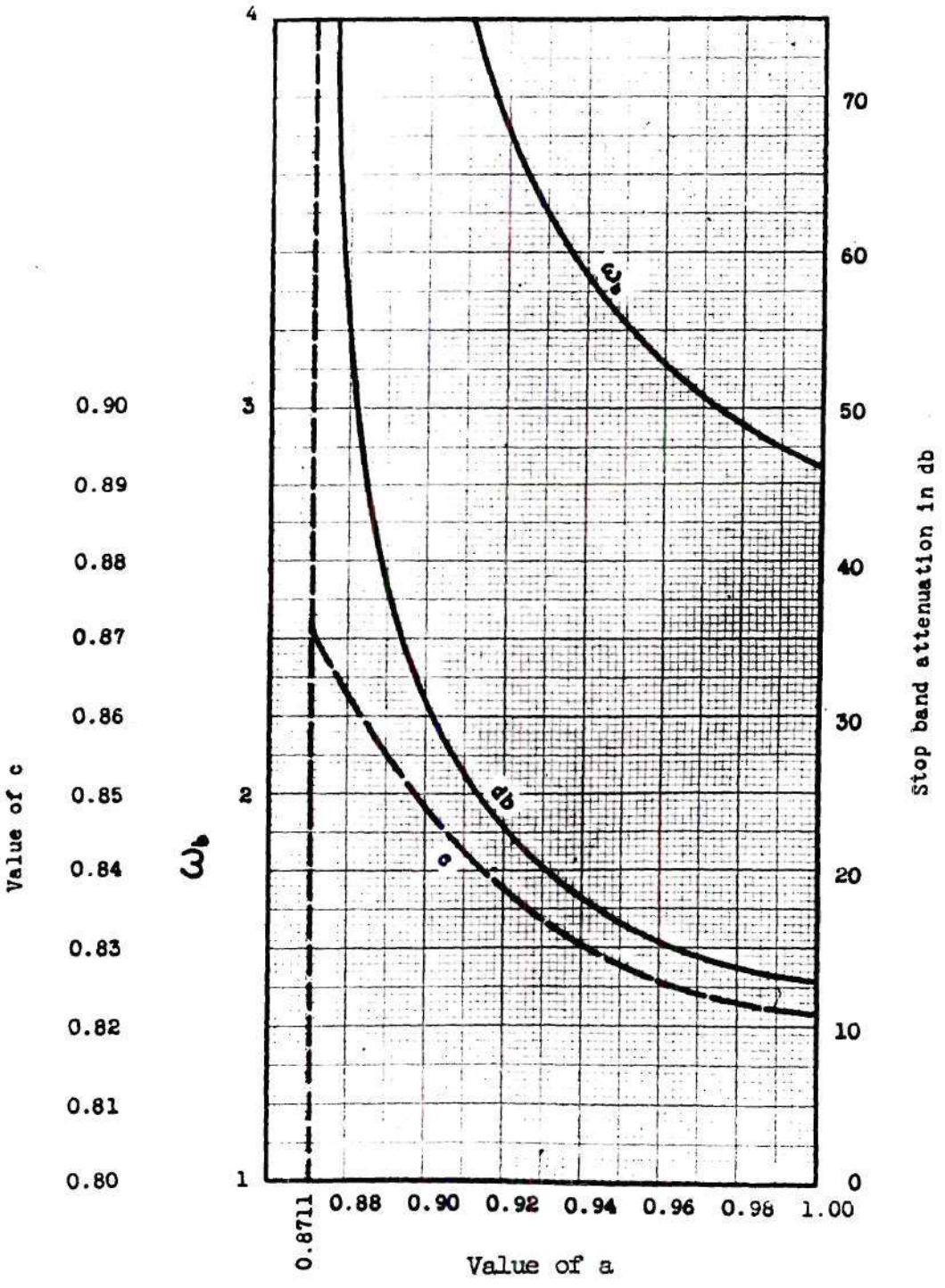

Fig. 60. Stop-band attenuation and ω_b for pass-band tolerance of 1/2 db, n= 6, and k^2 = 0.1.

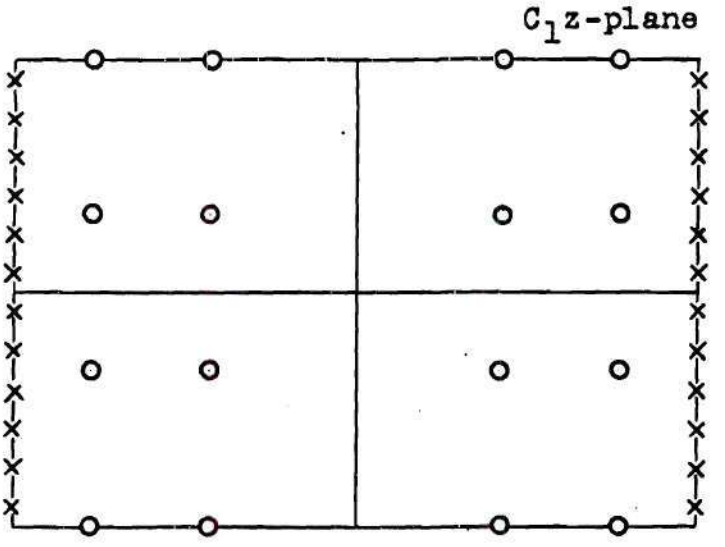

Fig. 61. Charges in the C_1z-plane.

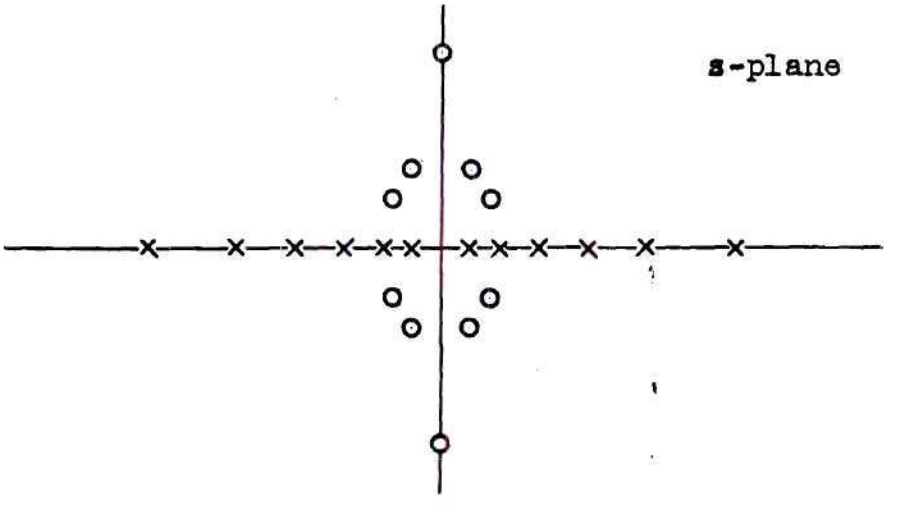

Fig. 62. Charges in the s-plane.

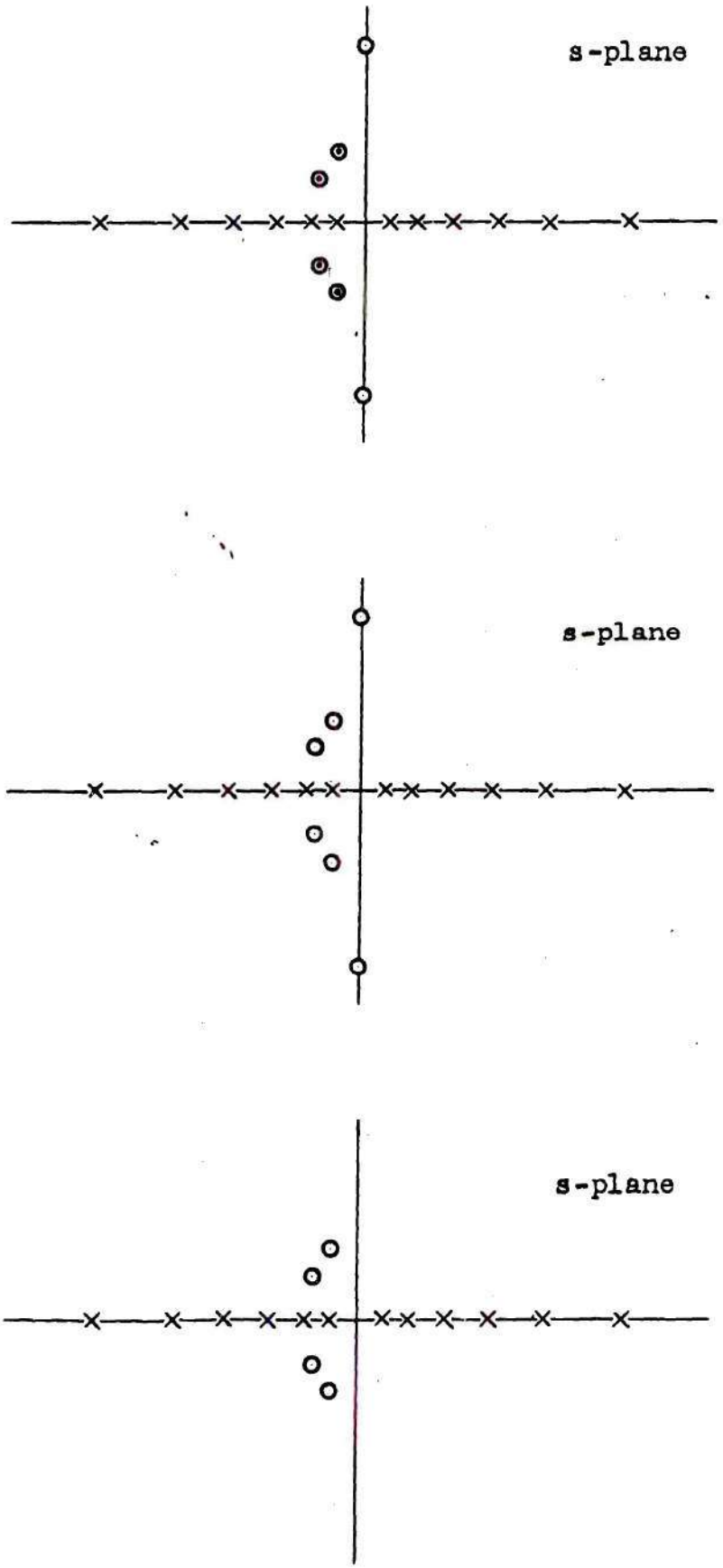

Fig. 63. Charges in the left half-plane are doubled and regrouped into two sets of charges.

different values of a for tolerances of 3db, 2db, 1db and ½db. In any case n is taken as 6 and k^2 as 0.1. Sample computations for these curves are given in Appendix I.

The curves in Figs. 57 to 60 are plotted for the type of charge arrangement as shown in Fig. 61. Corresponding zeros and poles of these charge sets in the s-plane are shown in Fig. 62. In the process of realizing this network, the right half-plane singularities are discarded. This leaves two half-unit charges on the $j\omega$-axis. Since this is not physically realizable it is necessary to double all charges (Fig. 63(a)) and two networks must be constructed, connected in tandem and isolated by a vacuum tube. One takes in the two single zeros on the $j\omega$-axis and one half of each double-singularity (Fig. 63(b)) and the other takes in the other half of each singularity only (Fig. 63(c)). Thus tolerances and attenuations of final networks must be twice those given by equations 109, 111 and 112. This has already been taken into account in the curves in Figs. 57 to 60. In other words, these curves give combined tolerances and attenuations of both stages.

Networks Employing One Row of Simple-Zeros and One Row of Double Zeros

The difficulty caused by half-unit charges on the imaginary-axis may be overcome by a different method than doubling the charges in the left half-plane, namely, by doubling the charges in the row closer to the pass band before charges are mapped onto the s-plane, as shown in Fig. 64. This leaves two unit charges on the imaginary axis after right half-plane charges have been discarded. This is shown in Fig. 65. Some conjugate pairs of double zeros will be left in the left half-plane.

But this is not objectionable. Accompanying this process, the number of poles must be increased accordingly.

The reasons for doubling the complete row of negative charges rather than just the one on the $j\omega$-axis alone are precisely the same as those for bringing in a new row of negative charges in Fig. 53. It is evident that now n must be a multiple of 3. And the singularities required in each cell in this case are 1.5 times those in the previous one. But since it is necessary to construct two networks in tandem when half-unit charges are left on the $j\omega$-axis, we actually eliminate 25 per cent of the poles when this new scheme is used.

Functions with desired singularities.—Following the procedure by which equation (104) was arrived at, the function that possesses singularities coinciding with charges shown in Fig. 64 may be written as

$$T(s)T(-s) = \frac{sn^2(C_1 z, k_1) - sn^2(aK_1 + jK_1', k_1)}{sn^2(C_1 z, k_1) - sn^2(K_1 + j\frac{K_1'}{6}, k_1)}$$

$$\times \frac{\left[sn^2(C_1 z, k_1) - sn^2(cK_1 + jK_1', k_1)\right]^2}{sn^2(C_1 z, k_1) - sn^2(K_1 + j\frac{K_1'}{2}, k_1)}$$

$$\times \frac{1}{sn^2(C_1 z, k_1) - sn^2(K_1 + j\frac{5K_1'}{6}, k_1)}$$

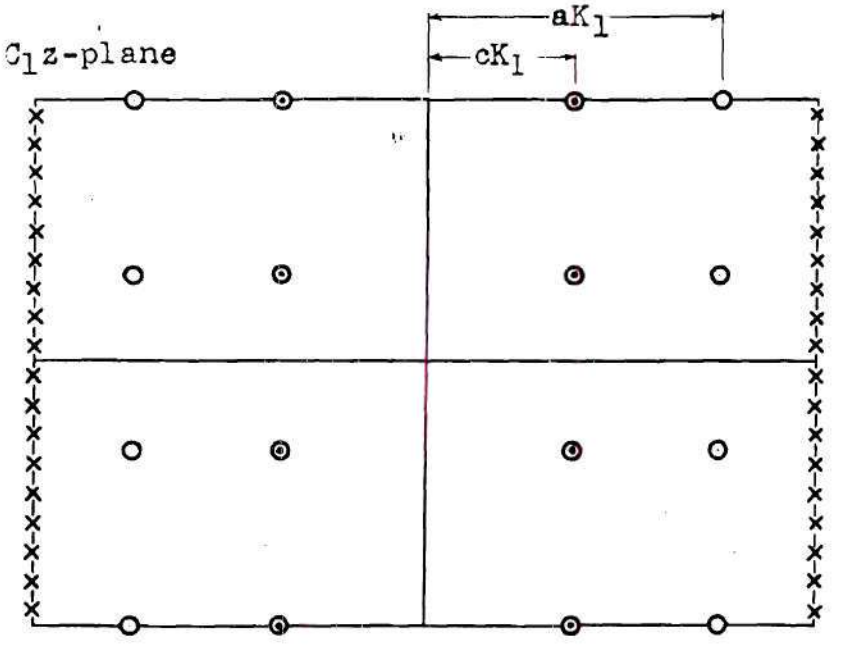

Fig. 64. Charges in the C_1z-plane.

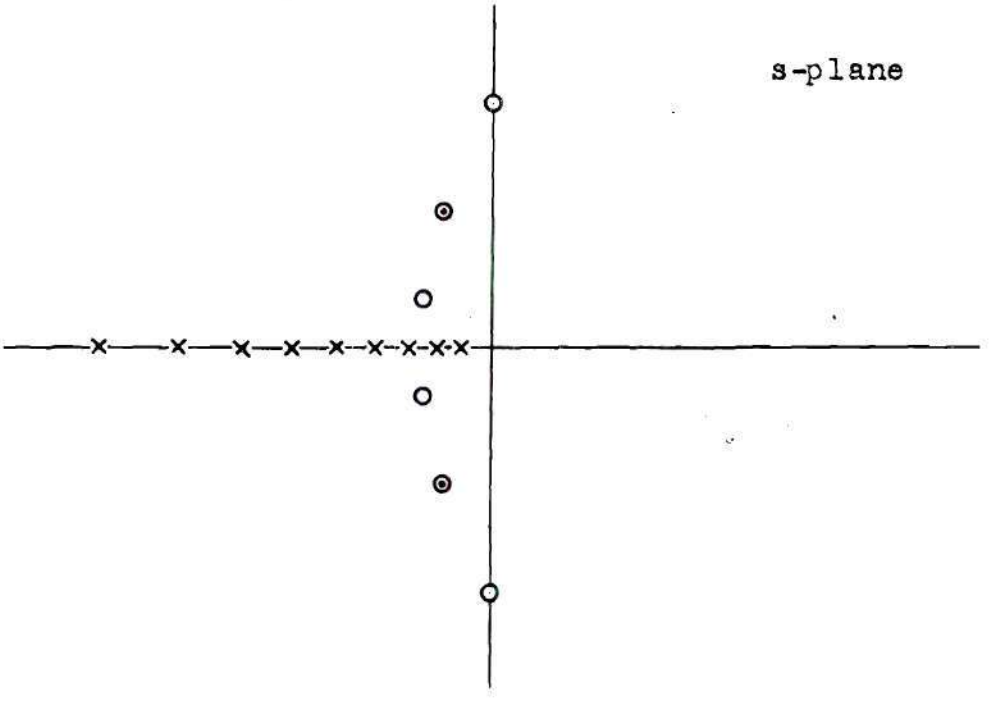

Fig. 65. Charges in the s-plane.

$$= \frac{sn^2(C_1 z, k_1) - \dfrac{1}{k_1^2\, sn^2(aK_1, k_1)}}{sn^2(C_1 z, k_1) - \dfrac{1}{dn^2(\frac{K_1'}{6}, k_1')}} \times \frac{\left[sn^2(C_1 z, k_1) - \dfrac{1}{k_1^2\, sn^2(cK_1, k_1)}\right]^2}{sn^2(C_1 z, k_1) - \dfrac{1}{dn^2(\frac{K_1'}{2}, k_1')}} \times \frac{1}{sn^2(C_1 z, k_1) - \dfrac{1}{dn^2(\frac{5K_1'}{6}, k_1')}} \qquad (113)$$

for odd $n/3$, and

$$T(s)T(-s) = \frac{sn^2(C_1 z, k_1) - sn^2(aK_1, k_1)}{sn^2(C_1 z, k_1) - sn^2(K_1 + j\frac{K_1'}{6}, k_1)} \times \frac{\left[sn^2(C_1 z, k_1) - sn^2(cK_1, k_1)\right]^2}{sn^2(C_1 z, k_1) - sn^2(K_1 + j\frac{K_1'}{2}, k_1)} \times \frac{1}{sn^2(C_1 z, k_1) - sn^2(K_1 + j\frac{5K_1'}{6}, k_1)}$$

$$= \frac{\left[sn^2(C_1 z, k_1) - sn^2(aK_1, k_1)\right]\left[sn^2(C_1 z, k_1) - sn^2(cK_1, k_1)\right]^2}{\left[sn^2(C_1 z, k_1) - \dfrac{61}{dn^2(\frac{K_1'}{6}, k_1')}\right]\left[sn^2(C_1 z, k_1) - \dfrac{1}{dn^2(\frac{K_1'}{2}, k_1')}\right]} \times \frac{1}{sn^2(C_1 z, k_1) - \dfrac{1}{dn^2(\frac{5K_1'}{6}, k_1')}} \qquad (114)$$

for even $n/3$.

The modulus k_1, whose quarter periods are K_1 and K_1', and C_1 must be so adjusted that

$$\frac{nK_1'}{3K_1} = \frac{K'}{K} \qquad \text{and} \qquad \frac{K_1}{C_1} = K. \tag{115}$$

Pass-band tolerance and stop-band attenuation.—One of the maxima of function (113) along the $j\omega$-axis occurs when $s = 0$, where $sn(C_1 z) = 0$. Hence

$$|T|^2_{max} = \frac{dn^2(\frac{K_1'}{6}, k_1')\ dn^2(\frac{K_1'}{2}, k_1')\ dn^2(\frac{5K_1'}{6}, k_1')}{k_1^6\ sn^2(aK_1, k_1)\ sn^4(cK_1, k_1)}. \tag{116}$$

Its minima occur when $C_1 z = jmK_1'$, where m is any odd integer, at which points $sn^2(C_1 z, k_1) = \infty$. Thus

$$|T|^2_{min} = 1. \tag{117}$$

Hence, when $n/3$ is odd

$$\text{Tolerance} = \varepsilon = 20 \log \left[\frac{|T|_{max}}{|T|_{min}} \right]$$

$$= 10 \log \left[\frac{dn^2(\frac{K_1'}{6}, k_1')\ dn^2(\frac{K_1'}{2}, k_1')\ dn^2(\frac{5K_1'}{6}, k_1')}{k_1^6\ sn^2(aK_1, k_1)\ sn^4(cK_1, k_1)} \right]. \tag{118}$$

A similar analysis from equation (114) will give, when $n/3$ is even,

$$\text{Tolerance} = \varepsilon$$

$$= 10 \log \left[\frac{1}{dn^2(\frac{K_1'}{6},k_1')dn^2(\frac{K_1'}{2},k_1')dn^2(\frac{5K_1'}{6},k_1')sn^2(aK_1,k_1)sn^4(cK_1,k_1)} \right]. \quad (119)$$

The potential at any point outside the pass band may be found by substituting $C_1 z = xK_1 + jK_1'$, where x has the same meaning as before, into equation (113). Thus

$$|T|^2 = \frac{dn^2(\frac{K_1'}{6}, k_1')\, dn^2(\frac{K_1'}{2}, k_1')\, dn^2(\frac{5K_1'}{6}, k_1')}{k_1^6\, sn^2(aK_1, k_1)\, sn^4(cK_1, k_1)}$$

$$\times \frac{sn^2(xK_1, k_1) - sn^2(aK_1, k_1)}{sn^2(xK_1, k_1) - \frac{1}{k_1^2}\, dn^2(\frac{K_1'}{6}, k_1')}$$

$$\times \frac{sn^2(xK_1, k_1) - sn^2(cK_1, k_1)}{sn^2(xK_1, k_1) - \frac{1}{k_1^2}\, dn^2(\frac{K_1'}{2}, k_1')}$$

$$\times \frac{1}{sn^2(xK_1, k_1) - \frac{1}{k_1^2} dn^2(\frac{5K_1'}{6}, k_1')}. \quad (120)$$

Hence,

$$\frac{|T|^2}{|T|^2_{max}} = \frac{1}{sn^2(xK_1, k_1) - \frac{1}{k_1^2} dn^2(\frac{K_1'}{6}, k_1')}$$

$$\times \frac{sn^2(xK_1, k_1) - sn^2(aK_1, k_1)}{sn^2(xK_1, k_1) - \frac{1}{k_1^2}\, dn^2(\frac{K_1'}{2}, k_1')}$$

$$\times \frac{\left[sn^2(xK_1, k_1) - sn^2(cK_1, k_1)\right]^2}{sn^2(xK_1, k_1) - \frac{1}{k_1^2} dn^2(\frac{5K_1'}{6}, k_1')}. \quad (121)$$

The point corresponding to $s = j\omega_a$ in the s-plane may be found either by setting the derivative of expression (121) with respect to $sn^2(xK_1, k_1)$, equal to zero and solving for $sn^2(xK_1, k_1)$, or by a cut-and-try method. After the potential at this point is found, the point corresponding to $s = j\omega_b$ in the s-plane, which has the same potential, can be located readily.

Design data.--The stop-band attenuation and the value of ω_b for different positions of the two rows of zeros when tolerances are held fixed at certain practical values are plotted in Figs. 66, 67 and 68. Sample computations for these curves are given in Appendix I. The value of n in these figures is taken as 9 and modulus k^2 again 0.1. Characteristics for n greater than 9 and other values of k do not differ materially from these. These curves can be used directly for design purposes.

Conclusions

The modified elliptic function transformation can be used to find R-C network functions with equal-ripple characteristics in both the pass band and the stop band. By properly arranging charge rows in the z-plane the potential can be written in closed form. Three cases have been investigated: one includes one row of zeros (equations (84) and (90)), one includes two rows of zeros (equation (104)) and one includes one row of simple zeros and one rows of double zeros (equations (113) and (114)) in the z-plane. From their potential expressions, tolerance and stop-band attenuation as well as stop-band angular frequency can be calculated for any values of k and n.

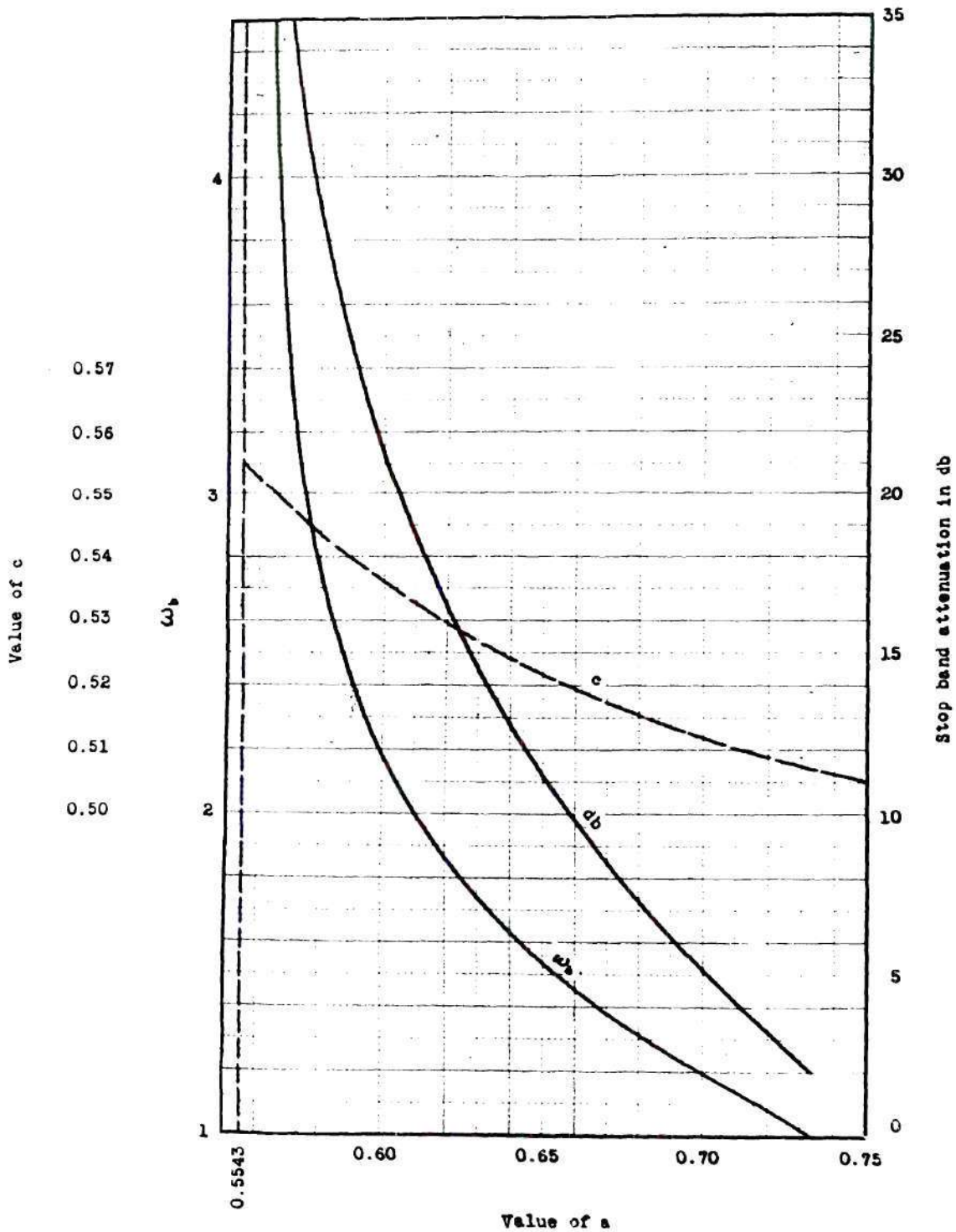

Fig. 66. Stop-band attenuation and ω_b for pass band tolerance of 2 db, n = 9, k^2 = 0.1.

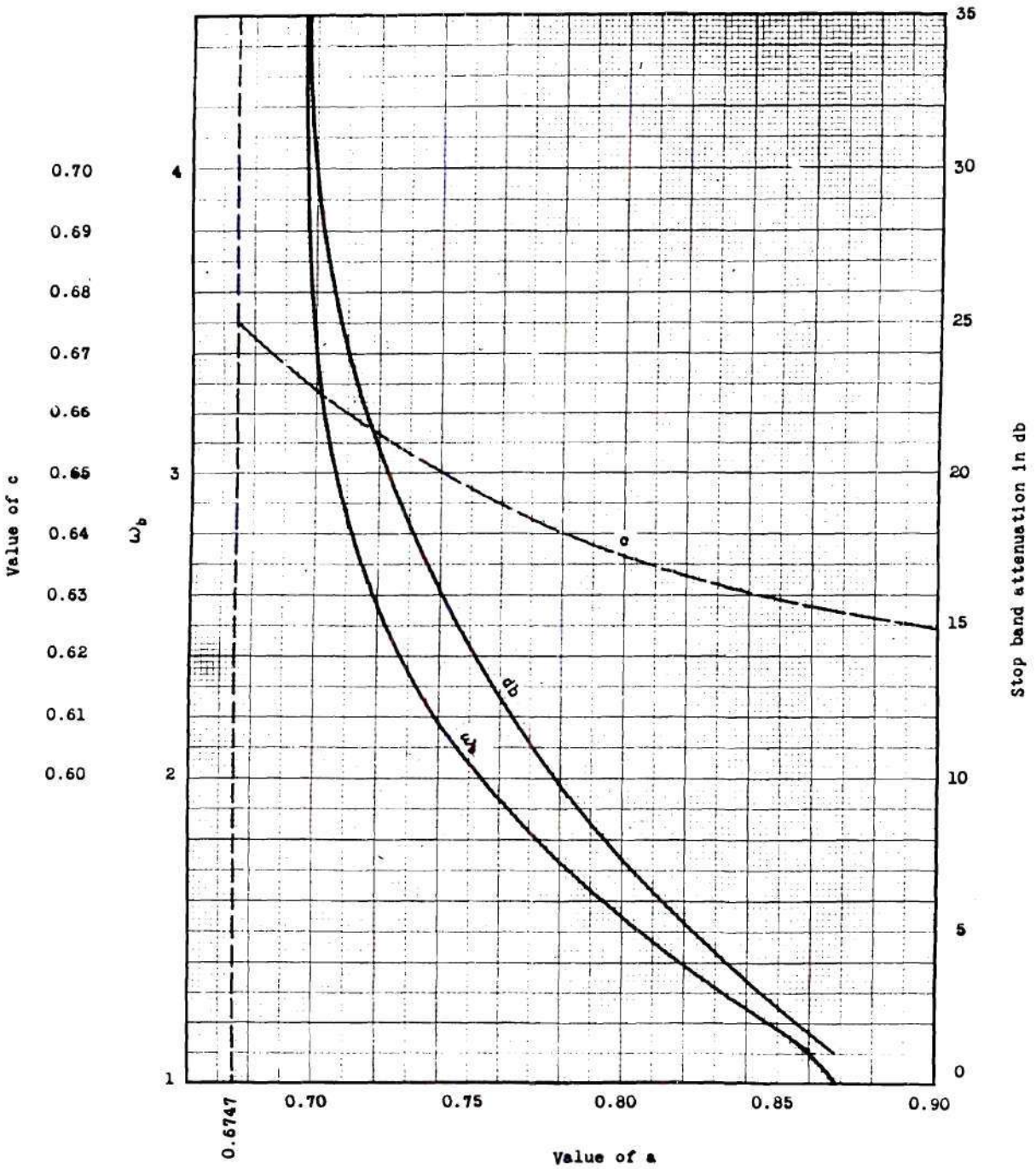

Fig. 67. Stop-band attenuation and ω_b for pass-band tolerance of 1 db, n = 9, k^2 = 0.1.

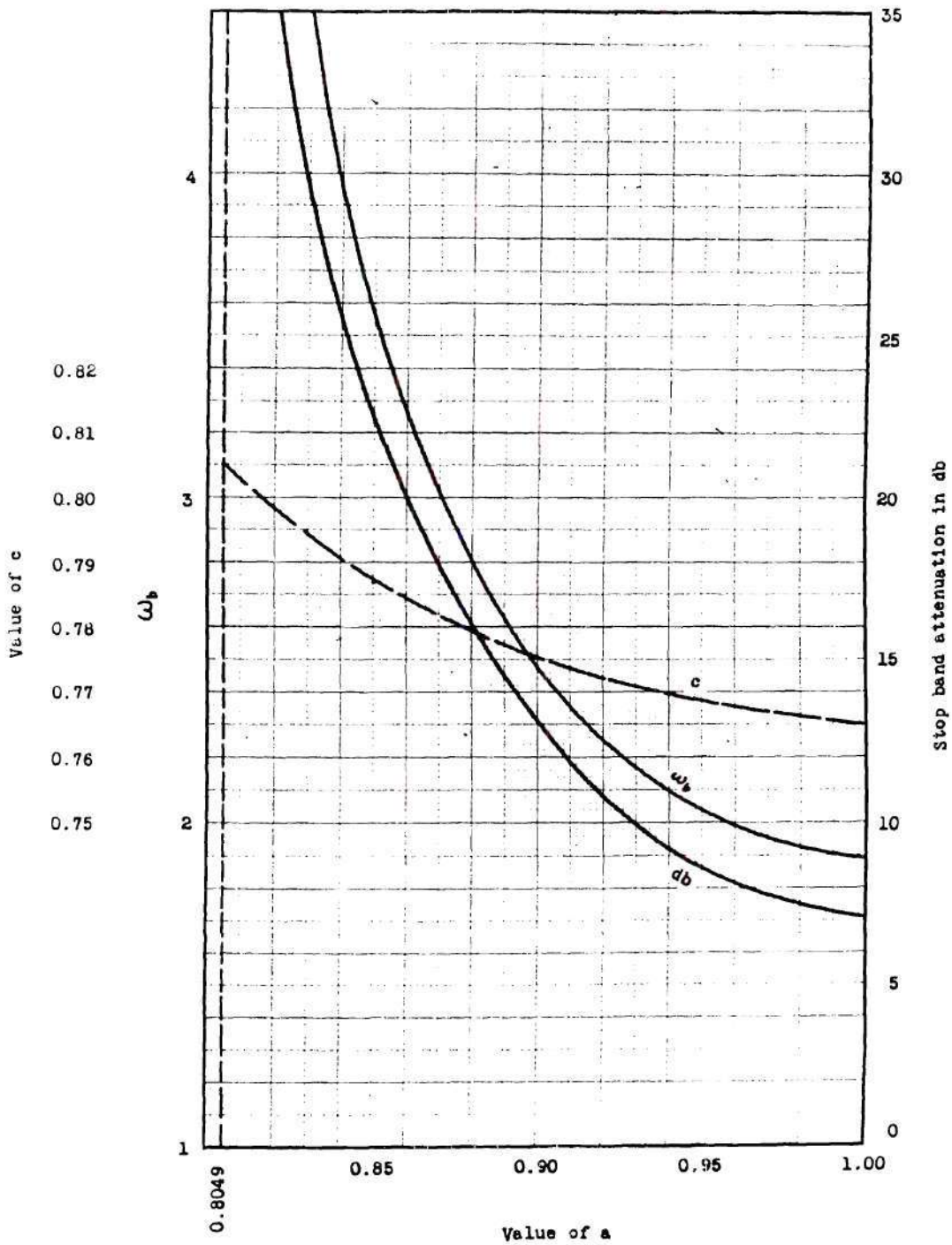

Fig. 68. Stop-band attenuation and ω_b for pass-band tolerance of 1/2 db, n = 9 and $k^2 = 0.1$.

For each case investigated the positioning of zero rows as well as their associated design parameters, viz. stop-band angular frequency and stop-band attenuation, are presented in the form of curves for some practical values of tolerance. They are shown in Figs. 50, 51, 57, 58, 59, 60, 66, 67 and 68. An example for the use of these curves are given in Appendix II.

It is found that the values of k and n have only slight effect on the low-pass characteristics. The choice of these values, therefore, depends on other practical considerations. Curves for other values of k and n may be computed and compared.

APPENDIX I

SAMPLE COMPUTATIONS

For networks of the type shown in Fig. 53.—A sample series of computations will be given here to illustrate how points in Fig. 57 to Fig. 60 are obtained. They correspond to those networks that have two rows of zeros in the z-plane, as shown in Fig. 53.

Since these curves are computed for the values

$$n = 6 \qquad \text{and} \qquad k^2 = 0.1,$$

corresponding to these values, one finds

$$K = 1.6124 \qquad \text{and} \qquad K' = 2.5781.$$

From equation (87), we have

$$q_1 = e^{-\frac{2K'}{2K}\pi} = 0.1874.$$

From the table, one finds

$$k_1 = 0.97815.$$

Suppose that it is desired to calculate all design parameters for a pass-band tolerance of 1 db and a value of a equal to 0.80. From equation (109), we have

$$10 \log \left[\frac{dn^2\left(\frac{K_1'}{4}, k_1'\right) dn^2\left(\frac{3K_1'}{4}, k_1'\right)}{k_1^4 \, sn^2(aK_1, k_1) \, sn^2(cK_1, k_1)} \right] = 0.5$$

or

$$\frac{\mathrm{dn}(\frac{K_1'}{4},\ k_1')\ \mathrm{dn}(\frac{3K_1'}{4},\ k_1')}{k_1^{\,2}\ \mathrm{sn}(aK_1,\ k_1)\ \mathrm{sn}(cK_1,\ k_1)} = 10^{0.025} = 1.059254.$$

After substituting the values

$$\mathrm{dn}\ (\frac{K_1'}{4},\ k_1') = 0.996769$$

$$\mathrm{dn}\ (\frac{3K_1'}{4},\ k_1') = 0.981318$$

$$\mathrm{sn}\ (0.80K_1,\ k_1) = 0.991437$$

$$k_1 = 0.978148$$

there is obtained

$$\mathrm{sn}\ (cK_1,\ k_1) = 0.991437,$$

which gives

$$\underline{c = 0.67677}$$

by the use of a table.

After substituting

$$\mathrm{sn}^2(aK_1,\ k_1) = 0.982947$$

$$\mathrm{sn}^2(cK_1,\ k_1) = 0.947673$$

$$\frac{1}{k_1^{\,2}}\ \mathrm{dn}^2(\frac{K_1'}{4},\ k_1') = 1.019037$$

$$\frac{1}{k_1^{\,2}}\ \mathrm{dn}^2(\frac{3K_1'}{4},\ k_1') = 1.003241$$

into equation (112) and setting

$$\frac{d}{d\ sn^2(xK_1,\ k_1)} \left[\frac{|T|^2_x}{|T|^2_{max}}\right]$$

equal to zero, it is found that the point corresponding to ω_a is

$$sn^2(xK_1,\ k_1) = 0.972386.$$

This, in turn, gives

$$\frac{|T|^2_a}{|T|^2_{max}} = 0.181319$$

which corresponds to a stop-band attenuation of

$$20 \log\left[\frac{1}{0.181319}\right] = \underline{14.828\ db}.$$

To find ω_b, from equation (112), we have

$$\frac{\left[sn^2(bK_1,\ k_1) - 0.982947\right]\left[sn^2(bK_1,\ k_1) - 0.947673\right]}{\left[sn^2(bK_1,\ k_1) - 1.019037\right]\left[sn^2(bK_1,\ k_1) - 1.003241\right]} = 0.181319$$

and

$$sn^2(bK_1,\ k_1) = 0.924572.$$

Thus

$$b = 0.62738$$

From a table. From equation (80), we have

$$j\omega_b = \frac{sn\,(bK + jK',\ k)}{\sqrt{\dfrac{1}{k^2\, sn^2(aK,\ k)} - sn^2(bK + jK',\ k)}}\ .$$

So

$$\omega_b = \frac{sn(aK,\ k)}{\sqrt{sn^2(\ aK,\ k) - sn^2(bK,\ k)}}\ .$$

Since

$$sn(aK,\ k) = 0.95342$$

and

$$sn(bK,\ k) = 0.84012,$$

there is obtained

$$\underline{\omega_b = 2.1150.}$$

For networks of the type shown in Fig. 64.--In this section, a sample series of computations will be given to illustrate how curves in Figs. 66, 67 and 68 are obtained. The singularities of these network functions are shown in Fig. 64 and Fig. 65 in the $C_1 z$-plane and the s-plane respectively.

Since these curves are computed for the values

$$n = 9 \qquad \text{and} \qquad k^2 = 0.1,$$

we have, again

$$k_1 = 0.97815$$

as in the preceeding section.

Again a sample set of values of design parameters for a pass-band tolerance of 1 db and a value of a equal to 0.80 will be calculated here. From equation (118), we have

$$10 \log \left[\frac{dn^2(\frac{K_1'}{6}, k_1') \, dn^2(\frac{K_1'}{2}, k_1') \, dn^2(\frac{5K_1'}{6}, k_1')}{k_1^6 \, sn^2(aK_1, k_1) \, sn^4(cK_1, k_1)} \right] = 1$$

or

$$\frac{dn\,(\frac{K_1'}{6}, k_1')\, dn\,(\frac{K_1'}{2}, k_1')\, dn\,(\frac{5K_1'}{6}, k_1')}{k_1^3\, sn\,(aK_1, k_1)\, sn^2(cK_1, k_1)} = 10^{0.05} = 1.12202.$$

Substitution of

$$dn\,(\frac{K_1'}{6}, k_1') = 0.998521$$

$$dn\,(\frac{K_1'}{2}, k_1') = 0.989013$$

$$dn\,(\frac{5K_1'}{6}, k_1') = 0.979596$$

$$sn\,(aK_1, k_1) = 0.991437$$

$$k_1^3 = 0.935866$$

into the equation above gives

$$sn^2(cK_1, k_1) = 0.929237$$

and

$$sn\,(cK_1, k_1) = 0.963969.$$

By interpolating values given by a table of elliptic functions, there is obtained

$$\underline{c = 0.636390}.$$

Substitution of

$$sn^2(aK_1,\ k_1) = 0.982947$$

$$sn^2(cK_1,\ k_1) = 0.929237$$

$$\frac{1}{k_1^2}dn^2\left(\frac{K_1'}{6},\ k_1'\right) = 1.042089$$

$$\frac{1}{k_1^2}dn^2\left(\frac{K_1'}{2},\ k_1'\right) = 1.022339$$

$$\frac{1}{k_1^2}dn^2\left(\frac{5K_1'}{6},\ k_1'\right) = 1.002962$$

into equation (121) gives the relative magnitude of $|T|^2$ outside the pass band

$$\frac{|T|^2}{|T|^2_{max}} = \frac{[sn^2(xK_1,\ k_1)-0.982947][sn^2(xK_1,k_1) - 0.929237]}{[sn^2(xK_1,\ k_1)-1.042089][sn^2(xK_1,\ k_1)-1.022339][sn^2(xK_1,k_1)-1.002962]}$$

This expression is found by cut-and-try to have a maximum at

$$sn^2(xK_1,\ k_1) = 0.97410$$

which corresponds to ω_a. This maximum is

$$\frac{|T|^2_a}{|T|^2_{max}} = 0.18850$$

which, in turn, gives

$$\text{Attenuation} = 10 \log \left|\frac{1}{0.18850}\right| = \underline{7.247 \text{ db}}.$$

Again by trial-and-error method it is found that $\frac{|T|^2}{|T|^2_{max}}$ also assumes a value of 0.18850 at

$$sn^2(xK_1, k_1) = 0.84056$$

which corresponds to ω_b, the stop-band. Thus

$$b = 0.51278.$$

Substituting

$$sn\ (aK, k) = 0.95342,$$

and

$$sn\ (bK, k) = 0.73021$$

into the equation

$$\omega_b = \frac{sn\ (aK, k)}{\sqrt{sn^2(aK, k) - sn^2(bK, k)}}$$

gives

$$\underline{\omega_b = 1.5554.}$$

APPENDIX II

NUMERICAL EXAMPLES

Example 1.—It is desired to design two identical interstage R-C networks to be used in the first two stages of the forward circuit of a feedback amplifier. The networks are to have a total insertion loss of not greater than 5 db below 440 cycles per second. The total loss at 4.4 kc, however, must be greater than 35 db.

Since the specifications of these interstage networks call for a low-pass R-C filter function with a drop of approximately 6 db per octave outside the pass band, it may be anticipated that the use of a network of the type shown in Fig. 20 may be attempted.

Choose the tolerance to be 1 db. From Fig. 22, it is found that

$$\sigma_1 = 0.275$$

and

$$\omega_p = 0.756.$$

Thus, we have, the network function for one single interstage

$$T(s) = \frac{E_2}{E_1} = \frac{s + 0.275}{(s + 0.924)(s + 0.383)}.$$

The insertion loss of this function at zero frequency is

$$20 \log \left[\frac{0.924 \times 0.383}{0.275} \right] = 20 \log (1.287) = 2.19 \text{ db.}$$

At a frequency one decade beyond the pass band, $\omega=7.56$,

$$T = \frac{E_2}{E_1} = \frac{0.275 + j7.56}{(0.924+j7.56)(0.383+j7.56)}$$

and

$$\left|\frac{E_2}{E_1}\right|^2 = \frac{57.229}{58.007 \times 57.300} = \frac{1}{58.079}.$$

This gives the insertion loss at $\omega=7.56$ to be 17.64 db. Therefore this function satisfies all requirements and may be used.

Finally, since the pass-band angular frequency must be $2\pi \times 440 = 2764$, the actual network function can be obtained by replacing s by $\frac{s}{2764}$. This yields

$$T(s) = \frac{2764(s + 760)}{(s + 2554)(s + 1059)}.$$

Example 2.--As an example for the application of data obtained in Chapter VI, a network function will be calculated based on the information contained therein.

From Fig. 58 it can be seen that if a value of a equal to 0.65 is chosen,

$$c = 0.5677.$$

The pass-band tolerance will be 2 db and the stop-band attenuation will be greater than 24.6 db for $\omega>2.15$.

For this network function, poles must be placed at

$$K + j\frac{K'}{12}, \qquad K + j\frac{K'}{4}, \qquad K + j\frac{5K'}{12},$$

$$K + j\frac{7K'}{12}, \qquad K + j\frac{3K'}{4}, \qquad K + j\frac{11K'}{12},$$

and zeros at

$$aK + j\frac{K'}{3}, \qquad cK + j\frac{K'}{3},$$

$$aK + jK', \qquad cK + jK'.$$

The position for these singularities in the w-plane will be

$$sn\ (K + j\frac{K'}{12}) = 1.0208 + j\ 0$$

$$sn\ (K + j\frac{K'}{4}) = 1.1899 + j\ 0$$

$$sn\ (K + j\frac{5K'}{12}) = 1.5375 + j\ 0$$

$$sn\ (K + j\frac{7K'}{12}) = 2.0568 + j\ 0$$

$$sn\ (K + j\frac{3K'}{4}) = 2.6575 + j\ 0$$

$$sn\ (K + j\frac{11K'}{12}) = 3.0979 + j\ 0$$

for the poles and

$$sn\ (aK + j\frac{K'}{3}) = 1.1789 + j\ 0.4539$$

$$sn\ (cK + j\frac{K'}{3}) = 1.0912 + j\ 0.5391$$

$$sn\ (aK + j\ K') = 3.6826 + j\ 0$$

$$sn\ (cK + j\ K') = 4.0224 + j\ 0$$

For the zeros.

In the s-plane, by the use of equation (80), poles are located at

0.2885,	0.3414,	0.4595,
0.6733,	1.0424,	1.5559,

and zeros at

$$0.3286 + j\,0.1431,$$

$$0.2986 + j\,0.1654,$$

$$0 + j\,2.4850,$$

$$\infty .$$

The singularities listed above are arranged in the same sequence as before. In all three planes only the singularities in the first quadrant are indicated since they are the easiest ones to handle. Other singularities can be located by symmetry.

By taking the singularities in the left half-plane only, the network function is formed; hence

$$T(s)=\frac{(s+0.329+j0.143)^2(s+0.329-j0.143)^2(s+0.299+j0.165)^2}{(s+0.299-j0.165)^2(s+j2.485)(s-j2.485)}$$

$$\frac{}{(s+0.288)^2(s+0.341)^2(s+0.459)^2(s+0.673)^2(s+1.042)^2(s+1.556)^2}$$

$$=\frac{(s^2+0.657\,s+0.129)^2(s^2+0.597\,s+0.117)^2(s^2+6.180)}{(s+0.288)^2(s+0.341)^2(s+0.459)^2(s+0.673)^2(s+1.042)^2(s+1.556)^2}.$$

This function has a value at $s=0$ equal to

$$T(0) = \frac{\overline{0.129}^2 \times \overline{0.117}^2 \times 6.180}{\overline{0.288}^2 \times \overline{0.341}^2 \times \overline{0.459}^2 \times \overline{0.673}^2 \times \overline{1.042}^2 \times \overline{1.556}^2} = 0.5814.$$

At $s = j1$, the band edge,

$$|T(j1)| = \frac{1.136 \times 1.190 \times 5.180}{1.083 \times 1.116 \times 1.210 \times 1.453 \times 2.086 \times 3.421} = 0.462.$$

Thus

$$\text{Tolerance} = 20 \log\left|\frac{T(0)}{T(j1)}\right| = 20 \log(1.259) = 2 \text{ db.}$$

At $s = j\ 2.15$

$$\left|T(j2.15)\right| = \frac{22.19 \times 21.95 \times 1.557}{4.705 \times 4.739 \times 4.833 \times 5.075 \times 5.708 \times 7.044} = 0.03449.$$

Therefore,

$$\text{Attenuation} = 20 \log\left|\frac{T(0)}{T(j2.15)}\right| = 20 \log 16.86 = 24.6 \text{ db.}$$

Both the tolerance and the stop band attenuation obtained here check with values given by Fig. 58.

APPENDIX III

LIST OF SYMBOLS

k, k'	Modulus and complementary modulus.
K, K'	Complete elliptic integral of the first kind of moduli k and k' respectively.
$s = \sigma + j\omega$	Complex-frequency variable.
$z = x + jy$	Complex variable.
$w = u + jv$	Complex variable.
ϵ	Tolerance.
ω_p	Pass-band angular frequency.
ω_b	Stop-band angular frequency.
$T(s)$	Transfer function.

BIBLIOGRAPHY

Literature Cited

1. Guillemin, E.A., Synthesis of R-C Networks, Journal of Mathematics and Physics, 28(1949), 22-42.

2. Patrick, K. W. and V. E. Thomas, A Design Procedure for Linear, Passive R-C Filter Networks, M. S. Thesis, Mass. Inst. of Tech., 1946.

3. Fialkow, A. and I. Gerst, The Transfer Function of an R-C Ladder Network, Jour. Math. Phys., 30(1951), 49-72.

4. Fialkow, A. and I. Gerst, The Transfer Function of General Two Terminal-Pair R-C Networks, Quart. Appl. Math., 10(1952), 113-127.

5. Guillemin, op. cit.

6. Patrick and Thomas, op. cit.

7. Ordung, P. F., G. S. Krauss, G. S. Axelby and W. P. Yetter, Synthesis of Paralleled Three-Terminal R-C Networks to Provide Complex Zeros in the Transfer Functions, Trans. A.I.E.E., 70(1951), 1861-1867.

8. Orchard, H. J., The Synthesis of R-C Networks to Have Prescribed Transfer Functions, Proc. I.R.E., 39(1951), 428-432.

9. Bower, J. L. and P. F. Ordung, The Synthesis of R-C Networks, Proc. I.R.E., 38(1950), 263-269.

10. Fleck, J. T. and P. F. Ordung, The Realization of a Transfer Ratio by Means of an R-C Ladder Network, Proc. I.R.E., 39(1951), 1069-1074.

11. Dasher, B. J., Synthesis of R-C Transfer Functions as Unbalanced Two Terminal-Pair Networks, Tech. Report No. 215, Research Lab. of Electronics, Mass. Inst. of Tech., 1951.

12. Fialkow, op. cit.

13. Guillemin, op. cit.

14. Hansen, W. W. and O. C. Lundstrum, Experimental Determination of Impedance Functions by the Use of Electrolytic Tank, Proc. I.R.E. 33(1945), 528-534.

15. Huggins, W. H., A Note on Frequency Transformations for Use with the Electrolytic Tank, Proc. I.R.E., 36(1948), 421-424.

16. Boothroyd, A. R., Design of Electric Wave Filter with the Aid of Electrolytic Tank, Proc. Instn. Elect. Engrs., 98(1951), Pt. III, 486-492.

17. Darlington, S., The Potential Analogue Method of Network Synthesis, B.S.T.J., 30(1951), 315-365.

18. Matthaei, G. L., A General Method for Synthesis of Filter Transfer Function as Applied to L-C and R-C Filter Examples, Technical Report No. 39(1951), Electronics Research Lab., Stanford University, Chap. 8.

19. Fano, R. M., A Note on the Solution of Certain Approximation Problems in Network Synthesis, Franklin Inst. Jour., 249(1950), 189-205.

20. Matthaei, op. cit.

21. Ibid.

Other References

Belove, C., A Note on the Synthesis of R-C Networks, Proc. I.R.E., 38 (1950), 1453.

Bode, H. W., Network Analysis and Feedback Amplifier Design, New York: D. Van Nostrand Co., 1945.

Butterworth, S., On the Theory of Filter Amplifier, Experimental Wireless, 7 (1930), 536.

Dixon, A. C., The Elementary Properties of the Elliptic Functions, London and New York: MacMillan and Co., 1894.

Fano, R. M. and A. W. Lawson, Jr., The Theory of Microwave Filters, New York: Radiation Laboratory Series, McGraw-Hill, Book Co., 1948.

Gewertz, C. M., Synthesis of a Finite Four-Terminal Network from Its Prescribed Driving-Point Functions and Transfer Functions, Jour. Math. Phys., 12 (1933), 1-257.

Guillemin, E. A., Communication Networks, New York: J. Wiley and Sons, Inc., 1931.

Guillemin, E. A., The Mathematics of Circuit Analysis, New York: J. Wiley and Sons, Inc., 1951.

Guillemin, E. A., A Note on the Ladder Development of R-C Networks, Proc. I. R. E., 40 (1952), 482-485.

Guillemin, E. A., A Summary of Modern Methods of Network Synthesis, Advances in Electronics, Vol. III, New York: Academic Press, 1951.

Hansen, W. W., On Maximum Gain-Bandwidth Product Amplifier, Jour. Appl. Phys., 16 (1945), 528-534.

Jahnke, E. and F. Emde, Tables of Functions with Formulae and Curves, New York: Dover Publications, 1943.

Kellogg, O. D., Fundations of Potential Theory, Berlin, Verlag von Julius, 1929, Chap. 12.

Kennelly, A. E., Tables of Complex Hyperbolic and Circular Functions, 2nd ed., Cambridge: Harvard University Press, 1927.

Klinkhamer, J. F., Empirical Determination of Wave-Filter Transfer Functions with Specified Properties, Philips Research Reports, 3 (1948), 60-80 and 378-400.

Kober, H., Dictionary of Conformal Representations, New York: Dover Publications, Inc., 1952.

Landon, V. D., The Low-Pass Band-Pass Analogy, Proc. I. R. E., 24 (1936), 1582-1584.

Matthaei, G. L., Filter Transfer Function Synthesis, Proc. I. R. E., 41 (1953), 337.

Milne-Thomson, L. M., Jacobian Elliptic Function Tables, New York: Dover Publications, Inc., 1950.

Neville, E. H., Jacobian Elliptic Functions, 2nd ed., Oxford at the Clarendon Press, 1951.

Ordung, P. F., F. Hopksin, H. L. Krauss and E. L. Sparrow, Synthesis of Cascaded Three-Terminal R-C Networks with Minimum-Phase Transfer Function, Proc. I. R. E., 40 (1952), 1717.

Scott, R. E., An Analog Device for Solving the Approximation Problem of Network Synthesis, Tech. Report No. 137, Research Lab. of Electronics, Mass. Inst. of Tech., 1951.

Scott, R. E., Network Synthesis by the Use of Potential Analogy, Proc. I. R. E., 40 (1952), 970-973.

Smythe, W. R., Static and Dynamic Electricity, New York and London, McGraw-Hill Book Co., Inc., 1939.

Spenceley, G. W. and R. M. Spenceley, Smithsonian Elliptic Functions Tables, Washington: Smithsonian Institution, 1947.

Stratton, J. A., Electromagnetic Theory, 1st ed., New York and London, McGraw-Hill Book Co., 1941.

Trautman, D. L., Maximally Flat Amplifier of Arbitrary Bandwidth and Coupling, Tech. Report No. 41, Electronics Research Lab., Stanford University, Calif., 1951.

VITA

Kendall Ling-chiao Su was born on July 10, 1926 in Nan-ping, Fukien, China. He is the son of Rev. and Mrs. Eu-chen Su.

He attended primary school in Nan-ping and graduated in 1937. After that he entered Chien Ching Middle School in Nan-ping and graduated in 1943. In the fall of 1943, he started his college education on the war-time campus of the National University of Amoy in Changting, Fukien, China. In the fall of 1946 the University moved back to Amoy, Fukien. Mr. Su spent his senior year in Amoy and graduated in July, 1947 with the B.S. in E.M.E. degree.

From August, 1947 to August, 1948 he was a junior engineer with the Taiwan Power Company, Taipeh, Taiwan, China, where he was engaged in substation work.

In the fall of 1948 he entered the Graduate School of the Georgia Institute of Technology. He received his M.S. in E.E. degree in June, 1949. He was a part-time research fellow with the Engineering Experiment Station of the University of Washington, Seattle, Washington, from September, 1949 to August, 1950, where he was engaged in a project dealing with the development of network analyzers. He returned to the Georgia Institute of Technology in the fall of 1950 and continued his graduate work.